LIVER-DIRECTED STRATEGIES AND IMMUNOLOGIC CONSEQUENCES OF RECOMBINANT AAV-MEDIATED CROSS-CORRECTION OF GLYCOGEN STORAGE DISEASE TYPE II

By

KERRY OWENS CRESAWN

A DISSERTATION PRESENTED TO THE GRADUATE SCHOOL
OF THE UNIVERSITY OF FLORIDA IN PARTIAL FULFILLMENT
OF THE REQUIREMENTS FOR THE DEGREE OF
DOCTOR OF PHILOSOPHY

UNIVERSITY OF FLORIDA

2004

Copyright 2004

by

Kerry Owens Cresawn

This work is dedicated to my mother, Mary Lea Lausch.

ACKNOWLEDGMENTS

There are many colleagues and friends whose technical support, advice, and encouragement have made this work possible. I would first like to express my gratitude to my mentor, Dr. Barry J. Byrne. Dr. Byrne's infectious enthusiasm for both patient care and the science behind it has provided our group with limitless innovative ideas and a better appreciation for our goals as scientists. I would also like to thank Dr. Byrne for his understanding and support of my commitments outside of the lab as a mother. I sincerely appreciate the guidance, insight, and patience of my friend and colleague, Dr. Cathryn Mah. I would also like to thank my committee members (Drs. Henry Baker, William Dunn, Alfred Lewin, and Gary Visner) as well as Dr. Mark Atkinson and Clive Wasserfall for their valuable advice and time.

I greatly appreciate the assistance and support of the many members of the Byrne Lab. Numerous friendly scientific discussions with my friend and colleague, Dr. Tom Fraites helped to broaden my knowledge of both gene therapy and Pompe disease, and provided helpful insight into experimental design and data analysis. I would like to express my appreciation for the dedication and commendable work ethic of our histologist, Melissa Lewis. I would also like to thank one of the most talented and skilled scientists I know, Irene Zolotukhin (whose meticulous technique I have always admired, although never mastered) for providing me with DNA, virus, and many other helpful reagents. I greatly appreciate the patience and excellent organizational skills of our laboratory manager, Denise Cloutier; and the countless hours Stacy Porvasnik has spent

with me, doing animal surgeries and necropsies. I thank all other members of the Byrne lab, past and present (especially Dr. Mary Rucker, Dr. Priscilla McAulliffe, Christina Pacak, Gregory Simon, Dr. Yoshihisa Sakai and Larysa Sautina). I would also like to thank the University of Florida's Powell Gene Therapy Vector Core, and Pathology Core (particularly Dr. Marth Campbell Thompson and Tina Yanchis) for their collaboration and technical expertise.

The tireless effort of Laura Miriel and Joyce Conners, who direct graduate students and faculty on a daily basis, has made the lives of all graduate students remarkably easier. Without them, this work would not be possible.

I would like to thank our collaborators, Drs. Nina Raben and Paul Plotz at the National Institutes of Health for developing and providing the animal model used in these studies (as well as two additional animal models that have been useful in answering important questions pertaining to this work). Additionally, the early work of Drs. Rochelle Hirschhorn and Arnold Reuser provided us and others in the field with an understanding of the molecular and cellular basis of GSDII, which has been necessary for the development of treatment modalities.

Special thanks go to my friend and mentor during my undergraduate studies at James Madison University, Dr. Douglas Dennis. It was in Dr. Dennis' lab that I first learned to think as a scientist and have a passion for the field. I would like to express my sincere gratitude to the patients and their families for sharing their stories of heartache and courage. They inspire us to continue our efforts.

Finally, I would like to thank my family for their encouragement and support during the difficult years of both undergraduate and graduate school. I especially thank my husband, Steve Cresawn (who has shared the graduate school journey with me) for his emotional support and continuous faith in my abilities as a wife, mother, and scientist. I lastly want to thank the person who has changed my life the most during the last 3 years of graduate school: my daughter, Abigail Cresawn. Her smile, laughter, and hugs have made every day a gift.

TABLE OF CONTENTS

Page

ACKNOWLEDGMENTS iv

LIST OF TABLES xii

LIST OF FIGURES xiii

ABSTRACT xvi

CHAPTER

I INTRODUCTION 1

Glycogen Storage Disease Type II 1
    Three Variants of GSDII 1
    Cardiac and Skeletal Muscle Involvement 3
Acid Alpha-Glucosidase 4
    Genotype-Phenotype Correlations 4
    Biochemistry and Cell Biology 6
Animal Models of GSDII 7
Therapeutic Strategies for GSDII 9
    Enzyme Replacement Therapy 9
    Gene Therapy 11
Recombinant Adeno-Associated Viral Vectors 13
    Recombinant AAV Serotypes 14
    Liver-Directed rAAV Delivery 16
Liver-Directed versus Muscle-Directed Gene Therapy 17
Immune Response to Vector-Derived Transgene Products 20

2 PRELIMINARY STUDIES TO EVALUATE LIVER-DIRECTED DELIVERY OF RECOMBINANT AAV VECTORS EXPRESSING HUMAN GAA TO GSDII MICE 25

Background 25
Materials and Methods 26
    Molecular Cloning of DNA Constructs 26
    DNA Sequencing of Cloned Constructs 27
    Packaging and Purification of rAAV Vectors 27
    In vitro Analysis of Liver Promoters Driving *LacZ* Expression 27

Animals ... 28
Intrahepatic Recombinant AAV Delivery Methods ... 29
Tissue Processing ... 29
GAA Enzymatic Activity Assay ... 29
ELISA Detection of Anti-GAA Antibodies ... 31
Histology ... 32
Statistical Analysis ... 32
Results ... 32
In Vitro Analysis of Four Liver-Specific Promoters ... 32
Superphysiologic Levels of Liver GAA Expression from the rAAV2-DHBV-*hGAA* Vector are not Sufficient to Restore Activity in Affected Tissues ... 34
Recombinant AAV Serotype 5 Vector Yields Higher Liver GAA Levels than Serotype 1 Vector ... 35
Gaa$^{-/-}$ Mice Elicit a Humoral Immune Response to Vector-Derived hGAA ... 36
Discussion ... 39

3 CHARACTERIZATION OF A NEONATALLY TOLERIZED GSDII MOUSE MODEL ... 42

Background ... 42
Materials and Methods ... 43
Pretreatment of *Gaa*$^{-/-}$ Mice ... 43
Intravenous Protein Delivery ... 43
ELISA for Detection of Anti-GAA Antibodies ... 44
ELISA for Detection of Distinct Isotypes ... 44
Competition ELISA to Determine Antibody Specificity ... 44
Lymphocyte Proliferation Assay ... 45
In vitro GAA Inhibition Assay ... 46
Results ... 47
Neonatal Pretreatment Results in Humoral Tolerance to Intravenous Protein Delivery ... 47
Antibodies are Specific to GAA ... 48
Recombinant Human GAA-Challenged Mice Show no Signs of Cell-Mediated Immunity ... 50
Susceptibility to Tolerization Decreases from 1 to 7 Days after Birth ... 53
Anti-GAA Antibodies in Treated Serum Inhibit GAA Activity *In Vitro* ... 54
Discussion ... 57

4 AAV5-MEDIATED CROSS-CORRECTION OF GSDII: EFFECTS OF INHIBITORY ANTIBODY FORMATION AND IMMUNOMODULATION ... 59

Background ... 59
Materials and Methods ... 60
Cloning and Packaging of rAAV Constructs ... 60
ELISA for Detection of Anti-GAA Antibodies ... 60
Animals ... 61
Tissue Processing ... 61

GAA Enzymatic Activity Assay 61
Histological Detection of Glycogen 62
Determination of Vector Genome Copy Number 63
RNA Isolation and Analysis of Human GAA Transcript 64
Immunoblot Detection of the Mannose 6-Phosphate Receptor 64
Statistical Analysis 65
Results 65
Liver GAA Activity and Antibody Formation after Intrahepatic Delivery of rAAV(5)-DHBV-*hGAA* to Naïve *Gaa*$^{-/-}$ Mice 65
Diaphragm GAA Levels are Dependent on Both Liver GAA Activity and Antibody Titer 68
Neonatally Pretreated *Gaa*$^{-/-}$ Mice do not Form Antibodies to rAAV-Derived hGAA after Low Dose Vector Delivery 69
Neonatal Tolerance is Broken after High Dose Delivery 71
Lack of Cell-Mediated Immune Response After rAAV(5)-DHBV-h*GAA* Treatment 75
Restoration of GAA Activity in Tolerized Mice Improves Glycogen Clearance 75
Human GAA Protein Observed in Corrected Tissues is Hepatic-Produced 78
Assessment of Hepatic Transduction Efficiency 79
Poor Correction of Quadriceps Correlates with Lower Levels of Mannose 6-Phosphate Receptor 81
Discussion 83
Impact of Immune Responses to Intrahepatic Delivery of rAAV- hGAA 83
Biochemical and Histological Assessment of Cross-Correction 85
Summary 87

5 DEVELOPMENT AND CHARACTERIZATION OF A GSDII MOUSE MODEL THAT CONDITIONALLY EXPRESSES HUMAN GAA 88

Background 88
Materials and Methods 89
Generation of the Transgenic Skin-*hGAA* / *Gaa*$^{-/-}$ Strain 89
Doxycycline Administration 90
Genotyping of Transgenic Lines by PCR 90
GAA Staining of Tail Snips and Skin 91
Tissue Processing 92
GAA Enzymatic Activity Assay 92
ELISA for Detection of Anti-GAA Antibodies 93
Results 93
Generation of Skin-*hGAA* / *Gaa*$^{-/-}$ Mice 93
Human GAA Transcript Detected in Skin, Spleen and Stomach 96
GAA Activity Detected in All Examined Tissues 97
Doxycycline-Mediated Repression of GAA Expression Leads to *Gaa*$^{-/-}$ Phenotype 99
Anti-GAA Humoral Response is Completely Inhibited in Skin-hGAA / *Gaa*$^{-/-}$ Mice 102

Unexpected Observations of the Skin-*hGAA* / *Gaa*$^{-/-}$ Phenotype 99
Conclusions 101

6 BIOCHEMICAL, HISTOLOGICAL, FUNCTIONAL, AND IMMUNOLOGIC ASSESEMENT OF RECOMBINANT AAV(8)-MEDIATED CROSS-CORRECTION IN TWO MURINE MODELS OF GSDII 105

Background 105
Materials and Methods 106
Cloning and Packaging of rAAV8 construct 106
Animals and Vector Delivery 107
Tissue Processing 107
GAA Enzymatic Activity Assay 108
ELISA Detection of Anti-GAA Antibodies and Isotypes 108
Histology 109
Western Blot Detection of GAA in Immunoprecipitated Serum 109
In Vitro Force Frequency Measurement 110
Results 111
Intrahepatic Delivery of rAAV8-DHBV-*hGAA* Vectors Leads to Higher Levels of Liver GAA expression than Previously Observed 111
Skin-hGAA/*Gaa*$^{-/-}$ Mice are Tolerant to rAAV8-Derived hGAA 112
Recombinant AAV8-DHBV-*hGAA* Delivery to Pretreated *Gaa*$^{-/-}$ Mice Results in Early Formation of High Titer Antibodies 112
Lack of Evidence For a Cell-Mediated Immune Response to rAAV8-Derived hGAA 114
Partial Restoration of Heart GAA Activity Observed after rAAV8-DHBV-*hGAA* Delivery 116
Superphysiologic Levels of Diaphragm GAA Result in Reversal of Glycogen Accumulation after rAAV8-DHBV-*hGAA* Delivery 117
Low Levels of GAA Activity Observed in Hind-Limb Skeletal Muscles Despite High Levels of Liver GAA in Tolerant Mice 118
110-kDa Circulating GAA Detected in rAAV8-Treated Mice 121
Partial Restoration of Soleus Muscle Function in rAAV8-DHBV-*hGAA*-Treated mice. 123
Human GAA RNA from the rAAV8-DHBV-*hGAA* Vector is Expressed in Multiple Tissues 124
Discussion 125
Relative Success of rAAV8-*hGAA* in the Liver 125
Immune Responses to rAAV8-Derived Human GAA 126
Cross-Correction of Affected Tissues 127
Correlation Between Human GAA Gene Expression and Cross-Correction ... 129
Summary 129

7 CONCLUSIONS AND FUTURE DIRECTIONS 130

APPENDIX 134

LIST OF REFERENCES..136

BIOGRAPHICAL SKETCH..150

LIST OF TABLES

Table page

4-1. Acid α-glucosidase activity and anti-GAA antibody titer 8 weeks after low dose vector delivery to naïve *Gaa*$^{-/-}$ mice. 67

4-2. Acid α-glucosidase activity and anti-GAA antibody titer 8 weeks after high dose vector delivery to naïve *Gaa*$^{-/-}$ mice. 67

4-3. Acid α-glucosidase activity and anti-GAA Ab titer 8 weeks after high dose vector delivery to pretreated *Gaa*$^{-/-}$ mice. 73

6-1. Acid α-glucosidase activity and anti-GAA antibody values after intrahepatic delivery of rAAV8-DHBV-*hGAA* to two *Gaa*$^{-/-}$ mouse models. 119

LIST OF FIGURES

Figure page

2-1. Cloned vector constructs 33

2-2. *In vitro* comparison of 4 liver promoters and the ubiquitous CMV promoter........ 34

2-3. Summary of *in vivo* studies comparing liver promoters by portal vein delivery of *human GAA*- expressing rAAV vectors in adult *Gaa*$^{-/-}$ mice 36

2-4. Weekly anti-GAA antibody formation in rAAV1- and rAAV5-hAAT-*hGAA*-treated *Gaa*$^{-/-}$ mice. 38

2-5. Exponential decay relationship between percent normal liver GAA activity versus terminal anti-GAA antibody titers in rAAV-hAAT-*hGAA* treated mice. 39

3-1. Anti-GAA antibody formation in pretreated and naïve *Gaa*$^{-/-}$ mice to rhGAA protein. 49

3-2. Competition ELISA of anti-GAA antibody-containing serum 50

3-3. Lymphocyte proliferation assay on splenocytes from pretreated and naïve *Gaa*$^{-/-}$ mice 52

3-4. Detection of anti-GAA isotype in naïve *Gaa*$^{-/-}$ mice after rhGAA delivery 52

3-5. Anti-GAA antibody titer in *Gaa*$^{-/-}$ mice after pretreatment at different ages followed by rhGAA challenge. 54

3-6. Diagram of *in vitro* GAA inhibition assay experimental design 56

3-7. Affects of anti-GAA antibody-containing serum on GAA activity *in vitro* 56

4-1. Exponential decay relationship between diaphragm activity normalized to liver activity versus anti-GAA antibody titer 69

4-2. Anti-GAA antibody formation in naïve and pretreated *Gaa*$^{-/-}$ mice over time after low dose vector delivery. 71

4-3. Anti-GAA antibody formation in naïve and pretreated *Gaa*$^{-/-}$ mice over time after high dose vector delivery 72

4-4. Summary of percent normal GAA activity 8 wk post-delivery of rAAV5-DHBV-*hGAA*. 74

4-5. Isotype analysis of anti-GAA antibodies formed against rAAV5-derived hGAA.. 76

4-6. Semi-quantitative analysis of rAAV5-*hGAA* vector genome copies 77

4-7. Detection of glycogen by PAS staining on longitudinal sections of cardiac and skeletal muscle 78

4-8. RT-PCR detection of rAAV5-delivered hGAA RNA. 79

4-9. Immunhistochemical detection of human GAA-expressing hepatocytes 81

4-10. Immunodetection of the 220-kDA mannose 6-phosphate receptor. 82

5-1. Schematics of the tetracycline-mediated gene regulation system (tet-off) and breeding strategy 95

5-2. X-Gluc detection of GAA on tails of mice after PCR determination of genotype.. 96

5-3. Genetic and biochemical characterization of skin-*hGAA* / *Gaa*$^{-/-}$ mice and their single transgenic littermates. 98

5-4. Biochemical and genetic affects of Dox-mediated repression 101

5-5. Anti-GAA antibody formation in skin-*hGAA*/*Gaa*$^{-/-}$, naïve *Gaa*$^{-/-}$ and neonatally pretreated *Gaa*$^{-/-}$ mice 103

5-6. Photograph of skin-*hGAA*/*Gaa*$^{-/-}$ mice with single transgenic littermates. 105

6-1. Anti-GAA antibody formation in pretreated *Gaa*$^{-/-}$ mice (1-10) and skin-*hGAA*/*Gaa*$^{-/-}$ mice (S1-S6) 112

6-2. Hematoxylin and Eosin-stained section of liver 16 wk after rAAV8-DHBV-*hGAA*-treatement. 113

6-3. Relative levels of IgG1, IgG2b, IgG2a and IgE in pretreated *Gaa*$^{-/-}$ mice 12 wk post injection of rAAV8-DHBV-*hGAA* 114

6-4. Acid α-glucosidase activity values in the 6 distal tissues of tolerant (Ab-) versus immune-responsive (Ab+) mice 118

6-5. Detection of glycogen by PAS staining of diaphragm sections 119

6-6. Western blot analysis of hGAA in the serum of rAAV8-DHBV-*hGAA*-treated mice 16 wk post injection 121

6-7. Force-frequency relationship of intact soleus muscle 16 wk after intraheptic delivery of 1 x 10^{12} vg rAAV8-DHBV-*hGAA*. 122

6-8. RT-PCR of rAAV8-delivered *hGAA* 123

Abstract of Dissertation Presented to the Graduate School
of the University of Florida in Partial Fulfillment of the
Requirements for the Degree of Doctor of Philosophy

LIVER-DIRECTED STRATEGIES AND IMMUNOLOGIC CONSEQUENCES OF RECOMBINANT AAV-MEDIATED CROSS-CORRECTION OF GLYCOGEN STORAGE DISEASE TYPE II

By

Kerry Owens Cresawn

May 2004

Chair: Barry J. Byrne
Major Department: Molecular Genetics and Microbiology

Glycogen Storage Disease Type II (GSDII) is a lysosomal storage disease caused by a deficiency in the lysosomal enzyme acid α-glucosidase (GAA). The disorder causes cardiac and skeletal myopathy in infants and is fatal within 2 years of life. Currently, there are no effective treatments for GSDII patients. The ultimate goal of viral vector-mediated correction includes transduction of a repository of producer cells, such as hepatocytes, with secretion and re-uptake of GAA by the affected muscles (in particular the heart, skeletal, and respiratory muscles) *via* the mannose 6-phosphate receptor (M6PR) pathway. Our initial studies using rAAV serotype 2 vectors in a null mouse model of GSDII ($Gaa^{-/-}$) demonstrated superphysiologic levels of hepatic GAA without correction of affected tissues. After observing anti-GAA antibody formation in rAAV2-treated $Gaa^{-/-}$ mice, we generated two models of tolerance in $Gaa^{-/-}$ mice. The first involved low-dose subcutaneous delivery of recombinant hGAA (rhGAA) to 1 day-old *Gaa*$^{-/-}$ mice. The second involved generating a *Gaa*$^{-/-}$ mouse model that expresses skin-restricted *human GAA* under control of the tetracycline response element.

Both of these models were shown to be completely tolerant to repeated intravenous injections of rhGAA at a dose that resulted in 100-fold elevation of anti-GAA antibody titers in naïve *Gaa*$^{-/-}$ mice. While neonatally-induced tolerance was broken in 66% of mice after challenge with liver-directed delivery of 1×10^{12} particles of rAAV(5)-*hGAA* or rAAV(8)-*hGAA* , tolerance was sustained in 100% of the skin-hGAA-tolerized mice. Results from these combined studies demonstrate the inhibitory affect of the anti-GAA humoral response; as significantly higher levels of GAA activity were observed in the heart, hindlimb muscles, and diaphragm of tolerant mice than of immune-responsive mice. We also noted that the ability to correct the affected muscles is dependent on both anti-GAA antibody titer and the level of liver-GAA expression, and that the degree of impact of these two parameters varies among the different muscle types examined. Overall, these results demonstrate the feasibility of liver-directed cross-correction of GSDII using rAAV-mediated gene delivery in the presence of high-expressing vectors and immunosuppression.

CHAPTER 1
INTRODUCTION

Glycogen Storage Disease Type II

Glycogen storage disease type II (glycogenosis type II, acid maltase deficiency, Pompe disease) was first described in 1932 by J.C. Pompe after examining the heart of a 7-month-old girl who died suddenly 2 days after admission to the hospital. While examining the girl's enlarged heart, Pompe noted massive accumulation of glycogen within vacuoles of the heart as well as other tissues (97). Within the next 2 decades, additional reports emerged on the association of glycogen storage with muscular weakness, hypotonia, and cardiomegaly, with death by the age of 1. The biochemical link in these observations was not understood until 2 landmark discoveries in the 1960s. With De Duve's (24) identification and characterization of the lysosome as a membrane-bound vacuole containing pH-active, hydrolytic enzymes, Hers *et al.* (47,67) were able to identify the lysosomal acid α-glucosidase that can release glucose from glycogen; and recognized that Pompe disease was due to the absence of this enzyme. Since these findings, over 40 lysosomal storage disorders have been discovered.

Variants of GSDII

Glycogen storage disease type II (GSDII) is inherited as an autosomal recessive trait. The frequency of GSDII varies among ethnic groups; and while the frequency in the general population is still debated, estimates range between 1 in 300,000 and 1 in 40,000 live births (52). The clinical presentation of GSDII represents a continuum of phenotypes that is, for the most part, correlated with age of onset, organ involvement and degree of residual enzyme activity. The clinical phenotypes have traditionally been divided into 3 groups.

Adult-onset GSDII is characterized by onset between the third and seventh decade of life with residual enzyme activity levels around 15 to 20% of normal. These patients present predominantly with progressive proximal muscle weakness, with truncal and lower limb involvement. Respiratory insufficiency (which is ultimately the cause of death) is apparent at the time of presentation in approximately 30% of patients and does not develop until years later in others (52,109). The juvenile-onset form is characterized by onset in the first to second decade, with residual enzyme activity levels around 3 to 10% of normal. Juvenile-onset patients present with progressive proximal muscle weakness, respiratory muscle involvement, mild hepatomegaly and absent or mild cardiomegaly. The course of juvenile-onset GSDII is more rapidly progressive than the adult onset form. Death usually occurs before the end of the third decade, and (as in the adult-onset patients) usually results from respiratory insufficiency. However, age of death in juvenile-onset patients does not always correlate with age on onset (52,109).

The term Pompe disease generally refers to the third clinical phenotype of GSDII, infantile-onset. Infantile-onset patients have complete or near complete enzyme deficiency, and present from birth to 7 months of age (109). The clinical presentation is that of a floppy baby with rapidly progressive skeletal muscle weakness, cardiomegaly, respiratory muscle weakness, severe hypotonia, mild hepatomegaly, and macroglossia. The progressive cardiomegaly involves left ventricular wall thickening, with obstruction of left ventricular outflow (which can lead to further signals of hypertrophy). Electrocardiograms reveal a shortened PR interval and large QRS complex (112,118).

The respiratory insufficiency caused by the weakened diaphragm is further complicated by bronchial compression (caused by the enlarged heart). Pompe patients usually die within the first 2 years of life of cardio-respiratory failure (52,106,109). Mental development is normal, despite glycogen accumulation in the central nervous system. Intellectual decline is not characteristic of the juvenile or adult-onset patients either (106).

This continuum of diseases has leads to the observation that some patients may present within the first 6 months of life with symptoms that are similar to traditional early onset patients, but with less severe cardiomegaly (29,119). Within the group of patients presenting in the first 6 months of life, there is an overall correlation of increasing age of onset and absence of cardiomegaly. The less severe cardiac disease has allowed this group of patients to survive past infancy with assisted ventilation.

Cardiac and Skeletal Muscle Involvement

Acid α-glucosidase (GAA) is the only enzyme capable of hydrolyzing lysosomal glycogen. Consequently, GAA deficiency results in lysosomal glycogen accumulation in all tissues including liver, cardiac, skeletal and smooth muscle, kidney, skin, endothelial cells, lymphocytes and in the peripheral and central nervous system (52,109). Despite the global tissue involvement, the cardiac and skeletal muscles are the most susceptible to the effects of glycogen accumulation. Several theories have been proposed to explain the severe phenotype specific to these tissues, including the following:

- Lysosomes in the intrafibrillar spaces rupture due to spatial constraints, mechanical effects of muscle contraction, or osmotic and/or destabilizing effects of glycogen accumulation. Additionally, the upregulation of other lysosomal hydrolases, some of which remain active at neutral pH, can exacerbate the effects of lysosomal rupture by continuing the breakdown of the contractile apparatus (47).

- As the lysosomal membrane is forced to expand, the sarcoplasmic reticulum membrane is recruited to form the expanding membrane; and its depletion from its normal function results in abnormal calcium regulation.
- The pathway of some unidentified cellular protein is altered leading to the accumulation of a toxic metabolite (106).

Acid Alpha-Glucosidase

Genotype-Phenotype Correlations

The gene encoding acid α-glucosidase is 28 kb long, contains 20 exons, and is localized to the long arm of chromosome 17 (17q25.2-q25.3) distal to the thymidine kinase gene at the same localization (44,66). The GAA promoter has characteristic "house-keeping" features contributing to the ubiquitous gene expression observed (98), however, there is also evidence from *in vitro* studies of tissue-specific gene regulation (56,92,105,139-141). The cDNA (Genbank accession numbers M34424 and Y00839) is approximately 3.6 kb with 2859 coding nucleotides encoding a protein of 952 amino acids (53,79). The amino acid sequence shares considerable homology with the amino acid sequence of the sucrose-degrading enzymes human isomaltase and rabbit sucrase isomaltase. This similarity includes identical sequence homology around the catalytic sites, suggesting a common ancestral gene among these 3 enzymes (53,77).

Over 70 different mutations have been identified in the GAA gene. While most mutations have been reported only in 1 or 2 patients, there is some association between mutation and ethnicity (106). In general, the genotype is an accurate predictor of the clinical phenotype. In the early-onset patients all mutations (nonsense, frameshift and missense) result in lack of GAA transcription or transcription of unstable mRNA with no detectable protein. It is rare that a mutation results in normal amounts of protein that are catalytically inactive. Later-onset mutations involve homozygosity of a less deleterious mutation; or heterozygosity for a fully deleterious mutation in combination with a milder one (109). For example, the most common mutation in the late-onset Caucasian group is a **t** to **g** transition in intron 1 (IVS1 t-13g) that has an allele frequency of 0.46 to 0.67 (54). This mutation results in the generation of several splice variants (including one in which exon 2 is partially or completely deleted) that leads to complete loss of GAA activity. However, this mutation is restricted to the later-onset phenotype due to the presence of low levels of correctly spliced exon 2-containing mRNAs that allow for the production of low levels of functional protein (106). Alternatively, the Δ exon 18 mutation results in deletion of the region crucial for maturation and processing of the enzyme, leading to no residual enzyme activity. As a result, patients homozygous for the Δ exon 18 mutation fall into the severe early-onset group. However, patients heterozygous for IVS1 t-13g and Δ exon 18 have the less severe, later-onset phenotype (106).

Recently, more cases have been reported of patients with a more severe genotype, presenting with less severe, later-onset symptoms (such as a group of German adult-onset patients homozygous for the Δ exon 18 mutation associated with the infantile-onset phenotype) (130). The lack of correlation observed among genotype, degree of residual activity, and severity of phenotype in some patients (45) suggests that genetic factors such as genetic background, somatic mosaicism, presence of a second mutation or polymorphism at the same allele, differential leakage of splice site mutations and/or environmental factors (such as diet and exercise) could influence the time course and severity of the disease (106,109).

Biochemistry and Cell Biology

Acid α-glucosidase catalyzes the hydrolysis of alpha 1, 4- and alpha 1,6-glucosidic linkages of glycogen at an optimal pH of 4.3, resulting in the complete hydrolysis of lysosomal glycogen to glucose. Muscle glycogen contains about 60,000 glucose residues per glycogen molecule, with alpha 1,4 linkages every 4-10 residues and alpha 1,6-branches every 10 residues (145). The role of glycogen storage varies depending on the tissue. Conversion of glycogen (stored in the brain) to glucose provides emergency supplies during times of hypoglycemia or hypoxia. In the muscle (which contains 3/4 of the total glycogen in the body), breakdown of glycogen to glucose is necessary for short-term energy consumption (such as muscle contraction) (145). Glycogen enters the lysosome either by fusion of glycogen-containing autophagic vacuoles with the lysosome, to form secondary lysosomes (43); or by direct invagination of the membrane. The signals responsible for entry of glycogen into the lysosome are not known.

The GAA precursor is translated as a 110 kDa product, and further undergoes extensive modifications that are characteristic of lysosomal enzymes. In the endoplasmic reticulum, GAA is glycosylated at 7 potential sites, at least 2 containing high-mannose chains (46). In the *cis* golgi, N-acetylglucosamine (GlcNAc)-1-phosphate is transported to the high-mannose residues. The GlcNAc group is then removed by the enzyme, N-acetylglucosamine-1-phosphodiester alpha-N-acetylglucoasminidase resulting in exposure of the mannose 6-phosphate (M6P) groups (108). The precursor GAA protein can subsequently be transported to the *trans* golgi, by binding of the M6P groups to one of two distinct M6P receptors present on the *trans* golgi membrane. The M6PR-GAA complex pinches off *via* clathrin coating on the external membrane to create clathrin-coated vesicles containing the M6PR-bound 110 kDa precursor. As the clathrin disassociates, the uncoated vesicle fuses with a low-pH sorting vesicle (called an endosome). The low pH of the endosome causes the M6P receptor to dissociate from the enzyme, allowing the receptor to be recycled either back to the *trans* golgi or to the cell surface where it can bind and internalize exogenous GAA. The early endosome containing the phosphorylated GAA finally fuses with the lysosome *via* an intermediate compartment where the phosphate groups are removed. The 110 kDa precursor protein is processed in the lysosomal compartments to yield an intermediate 95 kDa form and the two mature, fully active, 76 and 70 kDa, forms of GAA (109).

While 80-90% of GAA in the *trans* golgi is directed toward this lysosomal targeting pathway, 10-20% of the 110 kDa form is secreted from the cell (132). This secreted, M6P-containing GAA can subsequently bind to the M6P receptor on the cell membrane of the same cell or neighboring cells; and re-traffic to the lysosomes to produce catalytically active protein. This 10-20% of GAA that enters the secretory pathway provides the rationale for both enzyme and gene replacement therapies where GAA-deficient cells can be corrected by uptake of phosphorylated GAA supplied exogenously (*via* either intravenous delivery of the enzyme or from a repository of producer cells).

Animal Models of GSDII

Animal models are valuable tools for studying disease pathophysiology, as well as treatment modalities. Several naturally occurring animal models of GSDII have been reported, including cat, Brahman and Shorthorn cattle, Correidale sheep, Lapland dog, and Nicholas turkey (131). The cat, sheep and dog strains have not been maintained.

The Japanese quail model resembles the adult human form of the disease, and has been the most extensively used (of the naturally occurring models) to study the efficacy of various therapies (19). While the small size and obvious clinical phenotype make the quail a relatively easy disease model, quails are evolutionarily too far distant from humans; and their usefulness as an accurate disease model is limited by the existence of two separate GAA-encoding genes (65).

As an alternative, 3 different genetically engineered GSDII mouse models have been created by targeted disruption of the GAA gene. The two most-extensively used to study gene or enzyme replacement therapies are the exon 13 knockout ($13^{-/-}$), created by a targeted disruption with a Neomycin gene (*neo*) cassette in exon 13 (7), and the exon 6 knockout ($6^{neo}/6^{neo}$), generated by insertion of the neogene cassette into exon 6 (103). Both of these knockout strategies result in no detectable protein and low levels of detectable mutant GAA-neo transcript by RT-PCR. After observation of these two strains for up to 7-9 months of age, both strains showed complete absence of GAA enzyme activity, and marked glycogen accumulation. However, only the exon 6 knockout showed reduced mobility and muscle strength along with signs of muscle weakness (104). One likely explanation for the varying phenotypes in these two models is the different targeting exon suggesting that the targeted allele may be differentially inactivated. Alternatively, the difference could be due to the backgrounds. While the exon 6 knockout model is maintained on a 129SvJ x C57BL/6 background, the exon 13 knockout has been maintained on 129SvJ x C57BL/6 or 129SvJ x FVB background. Raben *et al.*(104) noted that the same knockout generated on a 129SvJ x C57BL/6 background, backcrossed to the C57BL/6 strain, developed a more-progressive cardiomyopathy with earlier-onset symptoms than when knockouts on the same background were backcrossed to the FVB strain. While the heterozygosity in phenotype (due to mixed genetic background) complicates characterization of the disease pathophysiology, it does recapitulate the heterozygosity of the patient population, allowing investigators to better anticipate the variegated responses to therapy. Because the exon 6 knockout model has the more severe phenotype, it is the chosen model for our studies. The biochemical phenotype of these mice recapitulates the infantile form of the disease, allowing investigators to test both enzyme and gene replacement therapies for restoring GAA activity. Additionally, our group demonstrated the ability to detect glycogen accumulation from as early as 1 month of age (117); as well loss in skeletal muscle function evident at 3 months of age (38). These functional phenotypes provide appropriate outcome measurements for determining the therapeutic efficacy of enzyme restoration.

Therapeutic Strategies for GSDII

Enzyme Replacement Therapy

Early attempts at enzyme replacement therapy (ERT) in the 1960s-1970s involved administering unphosphorylated GAA from *Aspergillus niger* (5) or human placenta (23) to infantile-onset patients. In both studies, an increase in enzyme activity was observed in the liver, but there was no reduction in stored glycogen. Additionally, the protein derived from *Aspergillus niger* was highly immunogenic, causing the study to be terminated. In 1984, Reuser and co-workers (110) demonstrated that uptake by fibroblasts of phosphorylated GAA from bovine testis and unphosphorylated GAA from human placenta occurred *via* M6PR-mediated endocytosis. However, uptake of the bovine testis GAA was 200-fold more efficient. These studies also showed that skeletal muscle cells isolated from GSDII patients do express M6PR on the surface and can be completely corrected by uptake of phosphorylated GAA. A later study showed that uptake of dephosphorylated bovine testis GAA was not detectable (110,127). These findings demonstrated that the extent of phosphorylation of mannose groups directly correlates with uptake efficiency and paved the way for developing more-effective recombinant enzyme for enzyme replacement therapy. Since these findings, recombinant enzyme has been produced in Chinese hamster ovary (CHO) cell lines (62,129); the milk of transgenic rabbits (8); and milk from transgenic mice (7). Transfer of enzyme activity and glycogen clearance was observed in transgenic mice after administering purified GAA from the milk of rabbits and mice. Similar results were also observed after administration of CHO cell-derived GAA in the Japanese quail model (62).

These promising results led to several clinical trials around the world, including two ongoing trials initiated by Genzyme Corporation (Cambridge, MA): One Phase II trial for subjects less than 6 months of age, and one Phase I/II trial for subjects between 6 and 36 months of age (89). These trials are currently evaluating the efficacy of a recombinant human GAA (rhGAA), isolated from CHO cell-lines and subsequently modified *in vitro* to manipulate the degree of phosphorylation. While no data are available on these patients (to date), results from preclinical studies in an immune-tolerant tolerant GSDII mouse model show 75% clearance of skeletal muscle glycogen and complete clearance of cardiac muscle glycogen at a dose of 100 mg/kg. However, at a dose of 20 mg/kg, there was only partial cardiac muscle correction and no skeletal muscle correction. When naïve GSDII mice were given the 20 mg/kg dose, 100% of the mice died from anaphylaxis after the seventh injection, demonstrating the potential need for immunosuppression in the null patient population (101).

Gene Therapy

Gene therapy strategies offer the potential for providing a permanent, endogenous source of a therapeutic protein both by direct correction of transduced cells and cross-correction of distal cells, *via* uptake of the secreted protein after single administration of vector. Many obstacles have thwarted progress toward clinical application of gene therapy, including low and/or transient levels of gene expression; immunogenicity of viral vectors (particularly the adenoviral-based vectors); germ-line transmission of the vector; and the potential for vector integration into regions of the genome crucial to homeostasis (resulting in events such as activation of oncogenes). Recent advances in vector development and an understanding of the immune response to vector and transgene have made gene therapy for GSDII a realistic goal for the future.

The first study to demonstrate correction of GAA-deficient cells from a viral vector involved *in vitro* transduction of myoblasts and fibroblasts isolated from a Pompe patient (146). Using a retroviral vector carrying the *GAA* cDNA, there was an increase in GAA activity and a decrease in glycogen content in both of these cell types. More importantly, the transduced cells were able to cross-correct GAA-deficient myoblasts by secretion of GAA.

The first adenovirus studies for correction of GSDII performed by our group and others (2,91,94,95) demonstrated the ability of recombinant E1-deleted adenovirus carrying the *human GAA* (*hGAA*) cDNA (rAd-*hGAA*) to yield expression of GAA in deficient fibroblasts. It was also demonstrated that these cells could then serve as producer cells of human GAA that could subsequently be recaptured by untransduced acceptor cells *via* M6PR-mediated endocytosis (94). Furthermore, intrahepatic administration of the same adenoviral vector carrying the *murine GAA* (*mGAA*) cDNA (94)or *hGAA* cDNA to mice resulted in enzyme secretion and increase in enzyme activity in cardiac and skeletal muscle (27). While these studies demonstrated the feasibility of recombinant viral vector delivery of *GAA*, adenoviral-mediated gene delivery has been shown to be highly immunogenic. Problems arising from adenoviral delivery consist of a humoral response to both the transgene product and vector, and potentially a cell-mediated response to the vector. Such a response was shown to be fatal in one adenovirus-mediated gene therapy trial conducted at the University of Pennsylvania in 1999 (36,58,107).

Non-viral gene delivery systems are being evaluated for treatment of genetic disorders in hopes of avoiding the safety issues presented by viral vectors. Martinuik and co-workers (78) have reported success using “gene gun” delivery of human GAA plasmid DNA to *Gaa*$^{-/-}$ mice. Although results were somewhat promising, expression was transient, as is common with plasmid-based delivery methods; and repeated dosing was required.

As safety is becoming the primary concern of viral-mediated gene delivery, recombinant adeno-associated viral vectors (rAAV) are emerging as a favorable gene delivery system. Fraites *et al.* (39) demonstrated that intramyocardial or intramuscular injection of rAAV serotype 2 vectors carrying the murine *GAA* cDNA results in restoration of GAA activity levels to near normal in the injected tissues, with partial restoration of skeletal muscle function after intramuscular delivery. These studies are the first and only (to date) to show GAA expression from a rAAV vector in GSDII mice.

However, it appears that higher levels of expression (requiring higher doses, stronger promoters, and/or alternative serotypes) will be needed for successful cross-correction in GSDII mice from a rAAV vector.

Recombinant Adeno-Associated Viral Vectors

Adeno-associated virus (AAV) is a member of the *dependovirus* genus of the *Parvoviridae* family of small DNA animal viruses. As a dependovirus, AAV requires helper virus (such as adenovirus or herpes virus) for a productive viral infection. In the absence of a helper virus, AAV establishes a latent infection (6). AAV was first discovered as a satellite contaminant in human and simian cell cultures infected with adenovirus (6); and subsequently found as human, simian and avian isolates causing no apparent disease (10). This lack of association with human disease makes AAV an attractive vector for gene delivery. Other favorable characteristics include the following:

- Recombinant AAV particles can be produced that completely lack AAV-encoding sequences, contributing to the ability of these vectors to escape host-defense mechanisms.
- AAV can infect both dividing and quiescent cells.
- AAV has a broad host and tissue tropism.
- AAV particles are relatively stable (resistant to chemical and physical treatment), which is important for vector production and commercialization (51,135).

AAV serotype 2 has been the most-extensively studied serotype; and the isolation of a molecular clone for AAV2 by Samulski *et al.* in 1983 (113) allowed for the development of recombinant AAV (rAAV) serotype 2 vectors for gene transfer. The AAV2 genome consists of an approximate 4.7 kb of single-stranded DNA of plus or minus polarity, including two 145 bp inverted terminal repeats (ITRs) located at the 5' and 3' ends. The palindromic regions of the ITRs can form hairpin structures in the single-stranded DNA, with the 3' hairpin acting as a primer for DNA replication as well as a binding site for the Rep protein. This special structural feature of the AAV ITRs makes them the only *cis*-acting viral sequences necessary for replication, packaging and rescue (135). Therefore, recombinant AAV vectors can be produced by deleting viral gene sequences and adding a therapeutic gene expression cassette. The wild-type AAV viral proteins (3 structural Cap proteins and 4 nonstructural Rep proteins) must be supplied in *trans* in order to make recombinant AAV virions (136).

Wild-type AAV2 has been shown to preferentially integrate into a region of the q arm of human chromosome 19 (AAVS1) (63,86,114,136). This site-specific integration is restricted to wild-type AAV2 as it is catalyzed by Rep proteins, which are absent in an infection with recombinant AAV. The extent to which rAAV integrates into the host genome is still under debate (85). The ubiquitously expressed heparin sulfate proteoglycan receptor was shown to be the primary receptor for AAV2 (124), with the fibroblast growth factor and $\alpha_v\beta_5$ integrin acting as co-receptors (100,124). The use of rAAV2 as a gene delivery vector for some diseases is limited by the delayed onset of gene expression compared to other vector systems. While adenoviral gene expression is detected within 1 week after delivery, gene expression from rAAV2 vectors takes approximately 4 weeks. The primary rate-limiting step remains in discussion, with evidence suggesting roles of conversion of the single-stranded genome to double-stranded DNA (35) as well as the nuclear entry process (4).

Recombinant AAV Serotypes

As the gene therapy field advances and the number of disease applications for rAAV-mediated gene delivery increases, interest in achieving higher levels of tissue-enhanced transgene expression and earlier gene expression has become a focus of AAV biologists, who have set out to isolate new AAV serotypes that can be developed for gene therapy. As of March 2004, eight distinct AAV serotypes have been isolated from primates, with 7 being distinct serotypes based on antibody cross-reactivity studies (40). The standard approach to generating rAAV viruses of alternative serotypes is pseudotyping, which involves packaging the gene expression cassette with AAV2 ITRs in the capsid of the alternative serotype. Pseudotyping is a favorable approach to creating recombinant AAV as there is more experience and information concerning the safety, chromosomal integration efficiency, and specificity with AAV2 ITRs in animal models and humans (150). Numerous studies have been performed to compare transgene expression levels in specific tissues from different serotypes cross-packaged with AAV2 ITRs. Serotype 6 (which appears to be a recombinant of serotypes 1 and 2) and serotype 1 have both been shown to be far more efficient at muscle transduction than serotype 2 (15,111,134,135). Additionally, Fraites *et al.* (39) observed transgene expression from an rAAV1 vector at 1 week post injection (3 weeks earlier than observed for rAAV2). Serotype 5, isolated from a human condylmatous wart, improved transgene expression in the liver by 3 to 10-fold compared to serotype 2 vectors (40,82). Serotypes 7 and 8, recently isolated by Gao *et al.* (40) from monkey tissue, appear to have the greatest divergence in capsid proteins; and are not neutralized by heterologous anti-AAV sera raised against any other serotype. Serotype 7 (compared with serotypes 1 and 6) was shown to have similarly high levels of expression in muscle. Serotype 8 (compared with serotype 5) was shown to yield up to 15-fold higher transgene levels in the liver.

Liver-Directed rAAV Delivery

The liver is the largest gland in the body, comprising 2% of the total body weight. Additionally, 1/5 of the total cardiac output passes through the liver each minute. The large mass, high vascularity, and protein production and secretion efficiency make the liver an ideal target organ for correction of multiple tissue beds after single-vector delivery.

Delivery of rAAV vectors to the liver *via* intraportal or intravenous injection in experimental animals has resulted in stable hepatocyte transduction, with therapeutic levels of transgene expression in the circulation and/or target tissue (14,16,22,48,59,60,84,120-122,133,138). Additionally, liver-directed delivery of rAAV vectors is being evaluated in clinical trials for the treatment of hemophilia B (60). Numerous studies over the past 10 years have answered important questions concerning the potential for liver-directed, rAAV-mediated gene therapy. In 1997, Snyder *et al.* (121) noted that only 2 to 5% of hepatocytes were successfully transduced 11 weeks post portal vein injection; and that this number was sufficient to supply therapeutic concentrations of transgene product. In 1999, Nakai *et al.* (85) observed (after portal vein delivery of rAAV vectors) episomal forms of head-to-tail circular intermediates as well as host-hepatocyte genome integration of head-to-tail high-molecular weight concatemers at two different locations. In 2000, Miao *et al.* (80) demonstrated that while only approximately 5% of hepatocytes express the rAAV-delivered transgene, the rAAV genome is taken up by most hepatocytes. The authors also noted that the small population of hepatocytes permissive to transduction is a changing population and that cell cycling did not influence the cell's ability to undergo stable transduction.

Despite this small percentage of hepatocytes permissive to transduction by rAAV vectors, high levels of transgene expression can be produced from the liver in a dose-responsive manner. In 2002, Nakai *et al.* (88) reported that a 2-log range linear dose-response curve of transgene expression was obtained from 3.7×10^9 to 3.0 to 10^{11} vector genome (vg) per mouse. Above 3.0×10^{11} vg/mouse there was a disproportionally smaller increase in both the level of transgene expression and number of hepatocytes transduced, with saturation at doses above 1.8×10^{12} vg/mouse. However, there was a linear increase in the number of vector genomes per cell (up to 1.8×10^{12} vg/mouse). These findings overall are important for understanding the feasibility of liver-targeted rAAV transduction. The low percentage of hepatocytes susceptible to successful rAAV transduction and loss of dose-response at higher doses may present obstacles for achieving superphysiologic levels of hepatic transgene expression.

Liver-Directed versus Muscle-Directed Gene Therapy

An alternative target organ for cross-correction from a gene delivery vector is skeletal muscle which is also highly vascularized and efficient at protein production and secretion. Phase I clinical trials of liver- or muscle-directed gene transfer with human factor IX-expressing AAV-2 vectors are currently ongoing (50,60). The liver-directed trials for hemophilia B were halted for 3 months because of detection of AAV in the gonads of treated patients (49). The increased risk of germline transmission of vector after intrahepatic delivery versus intramuscular delivery was also demonstrated in mice and rabbit studies (3). Along with this increased risk of germline transmission, another potential disadvantage of the liver-directed approach is the invasive nature of portal vein or hepatic artery delivery.

Despite these issues, there are two important advantages of intrahepatic delivery versus intramuscular delivery: higher transgene expression levels and decreased immunogenicity. Because the liver is naturally more efficient at protein production and secretion, lower doses may achieve the same therapeutic effect in the liver as those seen in the muscle after significantly higher doses (75). The only direct comparison of intrahepatic versus intramuscular delivery in humans is a clinical trial that began in 2000, evaluating delivery of rAAV-human *factor IX* (*hFIX)* by either direct muscle or portal vein injection in hemophilia patients. At a dose of 2 x 10^{12} vg, patients receiving intramuscular delivery failed to show any significant elevation in serum hFIX levels, despite having tolerated the vector; while one intrahepatic patient had therapeutic levels of serum hFIX. Unfortunately, these levels dropped within 1 week to sub-therapeutic levels (51,76).

The lack of consistent and significant differences in the level of secreted transgene product observed in liver versus muscle-directed rAAV gene therapy in mice and/or humans encouraged Raben *et al.* (102) to generate two alternative *Gaa*$^{-/-}$ mouse models to compare the two approaches. In their study, two mouse models were generated using the *Gaa*$^{-/-}$ background: one expressing *hGAA* from the liver, and one expressing *hGAA* from the muscle. In both cases, the *hGAA* gene was under control of the tetracycline response element (TRE) promoter and could therefore be regulated in response to administration of tetracycline in the food, water, or subcutaneous pellets. Tissue-specific expression was conferred by the promoter used to drive expression of the tetracycline transactivator (*tTA*) (the element that binds the TRE promoter to initiate expression of *hGAA*). Therefore, these mice were transgenic for 3 genotypes: the *Gaa*$^{-/-}$

genotype (as previously described); the *hGAA* gene, under control of the ubiquitously expressed TRE promoter; and the *tTA* gene, under control of either the albumin or muscle creatine kinase promoter. Raben *et al.* showed that cross-correction from liver-produced hGAA required 12-fold normal liver GAA enzyme activity levels; whereas cross-correction from muscle-produced hGAA required 100-fold normal muscle GAA activity levels. While these data suggest that the liver is a more optimal target organ for achieving cross-correction in GSDII mice, it should be noted that different tissues were analyzed for comparing cross-correction outcome. Additionally, the different promoters driving tissue-specific expression of the transactivator may have resulted in significantly higher levels of transactivator, and potentially higher levels of hGAA in the liver, although there is no evidence to support this.

The second potential advantage of intrahepatic delivery versus intramuscular delivery is decreased immunogenicity of the transgene product as demonstrated by two groups, both using rAAV-*hFIX*. In the first study by Ge *et al.* (42), rAAV vectors expressing *hFIX* were delivered to the liver or muscle of immunocompetent mice at identical doses. While all of the intramuscular-treated mice developed a robust humoral immune response blocking hFIX expression in the serum, none of the intrahepatic-treated mice elicited an immune response coinciding with significant levels of serum hFIX. Results from this study suggest that the likelihood of an immune response was directly related to the target tissues, rather than the level of protein expression. The reason for increased immunogenicity observed after intramuscular delivery is not fully elucidated. However, naked DNA delivery studies have demonstrated that expression of transgene product from muscle leads to binding of the protein to the extracellular matrix. This results in high levels of locally concentrated protein which may lead to more efficient cross-presentation of antigen to antigen-presenting cells (21,28,126). Because more of the total transgene product is secreted from the liver than from the muscle, the liver-produced transgene product may not reach high enough local levels of antigen, and may therefore remain undetectable by the immune system (57).

In the second study by Mingozzi *et al.* (81), immune tolerance was induced in immunocompetent mice by intrahepatic administration of rAAV-delivered *hFIX*. Tolerance of hFIX was challenged by administration of recombinant hFIX protein in adjuvant after pretreatment with intrahepatic delivery of either rAAV-*hFIX* or rAAV-*GFP*. Mice pretreated with rAAV-*hFIX* developed no anti-hFIX antibodies and had reduced *in vitro* T cell responses. However, mice pretreated with rAAV-*GFP* developed anti-FIX antibodies 14 days after injection of rhFIX along with significantly higher *in vitro* T cell responses. Results from their study and others (16) suggest that the combination of intrahepatic delivery of high levels of sustained expression of a rAAV-expressed foreign transgene is sufficient to evade the immune response; and also induce tolerance to subsequent challenge by recombinant protein. The advantages and disadvantages of intrahepatic versus intramuscular delivery will have to be weighed for each disease, and will likely depend on factors such as immunologic background, minimal level of expression required for correction, and any associated diseases that may complicate targeting of a specific tissue (such as the increased incidence of hepatitis observed in hemophilia patients) (51).

Immune Response to Vector-Derived Transgene Products

Gene transfer, in general, has been shown to be an efficient way to elicit humoral and cellular immune responses to foreign proteins in the development of vaccines for diseases such as cancer (25,69,83), HIV (137), and HSV (74). While this immunologic property is an attractive feature for vaccine development, it limits the application of gene transfer for the treatment of diseases where prolonged transgene expression is necessary. Immune responses to recombinant adenoviral-derived transgene products have been the most extensively studied. Vigorous cellular and humoral immune responses to recombinant adenoviral-derived cytosolic beta galactosidase (β-gal) was observed following delivery to the liver, lung, and muscle and (in many cases) led to the destruction of transduced cells, inflammation, and loss of the *lacZ* transgene expression. (41,128,142-144).

In effort to understand earlier studies demonstrating that rAAV vectors did not elicit immune responses to foreign transgene products (while delivery of the same protein by recombinant adenovirus and naked DNA did), Jooss *et al.* (58) evaluated the mechanisms by which rAAV evades immunologic response. These studies found that adoptive transfer of dendritic cells isolated from murine spleen (and transduced by rAAV-*lacZ*) did not elicit transgene-specific immune responses *in vivo*. Transduction of the same cell type by adenoviral-*lacZ* vectors, followed by adoptive transfer, did lead to immune-mediated elimination of transduced cells. These results were explained by the fluorescent *in situ* hybridization experiments showing rAAV genomes in the perinuclear space of dendritic cells (compared to the intranuclear localization of adenoviral vectors). The conclusions from this important study were that AAV can enter dendritic cells, but post-entry blocks interfere with efficient transduction and antigen presentation. Later studies suggested that the efficiency of dendritic cell transduction, by rAAV, depends heavily on the number of dendritic cells and maturation state of the dendritic cell population at the time of rAAV encounter (147). It is not known whether the number of immature dendritic cells required to elicit a cell-mediated response after rAAV-*LacZ* transduction *in vitro* is realistic *in vivo.* The general consensus (to date) concerning rAAV and immunity is that rAAV vectors are incapable of recruiting enough immature antigen presenting cells to the site of vector administration to lead to T cell activation (57). These important studies were all performed using rAAV serotype 2 vectors, and similar studies will need to be done with alternative serotypes.

While the studies described above suggest that rAAV-mediated gene delivery is not likely to result in cell-mediated immunity to transgene products, the potential for a humoral immune response to rAAV-derived and secreted transgene products remains a considerable concern for many investigators. The likelihood of rAAV-derived transgene products eliciting a humoral immune response depends on several factors, including the genetic background of the host; amount of foreign protein secreted by transduced cells; presence or absence of residual mutant protein (13); structural differences between the replacement and mutant protein; and the route of vector administration (12,20,81).

While delineation of the immune response to secreted transgene products is complicated by the presence of both the vector and therapeutic protein as potential antigens, several in depth studies have been able to elucidate the mechanisms of immune activation of rAAV-derived foreign proteins (33,34,42). Quantitative assays for detecting various cytokines, isotypes of B-cell secreted antibodies and cytolytic activity, along with histological detection of lymphocyte infiltration can all be used to further understand the immunologic consequences of any treatment. T lymphocytes consist of both T helper (Th) lymphocytes and cytotoxic T lymphocytes (CTLs). Within the Th class exist Th1 and Th2 cells. The Th1 subset characteristically secretes IL-2 and IFN-γ and is capable of stimulating both proliferation of cytotoxic T lymphocytes (leading to destruction of antigen-expressing tissues) as well as proliferation of B cells secreting antibodies of the IgG2a isotype. The Th2 subset characteristically secrete IL-4 and IL-10 and can activate B cells leading to production of antibodies of the IgG1 and IgG2b, and IgE isotype. In the context of rAAV-mediated delivery of therapeutic transgenes, Fields *et al.* (34) found that the immune response to secreted factor IX after rAAV-mediated delivery was characterized by activation of the Th2 subset of T helper cells (determined by cytokine profile). This resulted in the production of predominately IgG1 antibodies and absence of Th1 subset activation coinciding with lack of both CTL stimulation and inflammatory cell infiltrates. In contrast, factor IX delivery by recombinant adenoviral vectors resulted in activation of both Th2 and Th1 cells. This resulted in IgG2a antibody formation, CTL stimulation, inflammation and rejection of transduced muscle fibers. In a later study, Sarukhan *et al.* (34,116) demonstrated that rAAV-derived transgene products can elicit a cell-mediated immune response leading to destruction of transduced cells provided the foreign gene product is highly immunogenic (such as the influenza virus hemagglutinin (HA) protein). Consistent with the previous study, these authors found that while the immune response to rAd-HA resulted from direct transduction of dendritic cells as well as cross-presentation of transgene product, the immune response to rAAV-HA delivery was only activated by the latter mechanism.

Summary

Clinical evaluation of enzyme replacement therapy for the treatment of GSDII is underway. However, long-term goals for GSDII treatment involve gene replacement therapy using rAAV-mediated delivery of GAA. To understand the full potential of this therapy, we evaluated one of the proposed gene therapy approaches: rAAV-mediated delivery of GAA to the liver to achieve cross-correction of a mouse model of GSDII. Preliminary results from this proposal led us to investigate the potential for and consequences of an immune response to rAAV-derived GAA and determine the necessary elements for achieving varying levels of correction in GSDII mice. These findings provide us with both a new appreciation for the potential pitfalls of gene replacement therapy for GSDII (as well as other similar diseases) and an understanding of how these obstacles can be overcome.

CHAPTER 2
PRELIMINARY STUDIES TO EVALUATE LIVER-DIRECTED DELIVERY OF RECOMBINANT AAV VECTORS EXPRESSING HUMAN GAA TO GSDII MICE

Background

Achieving high levels of sustained transgene expression is a critical component for the success of gene therapy. The level of transgene expression necessary to reverse the disease pathophysiolgy varies for each disease. In the case of GSDII, adult-onset patients have approximately 20% of normal GAA activity. With this level of GAA, these patients have a relatively mild presentation with no cardiac involvement. It has therefore generally been accepted in the field that restoring at least 20% of normal enzyme activity to infantile-onset (Pompe) patients would likely ameliorate most of the symptoms associated with the Pompe patients, particularly those associated with cardio-respiratory failure (109). However, the ability to restore cardiac and respiratory function with this percentage of normal enzyme activity will depend on the age at treatment and severity of phenotype and may be different between the GSDII mouse model and human patients.

While this level of enzyme restoration (20%) is relatively low, achieving this in non-transduced tissue will require high, yet undefined, levels of GAA expression in the transduced tissue (particularly because only 10-20% of GAA in transduced cells is secreted for uptake by distal cells). The aim of the following studies was to optimize hepatic GAA expression by the use of high-expressing, liver-specific promoters. After confirming hepatocyte-specific activity *in vitro* from four promoters using the β-galactosidase (β-*gal)* reporter gene, 3 promoters were chosen for evaluating the ability to drive high levels of hepatic GAA expression after intrahepatic delivery of recombinant AAV (rAAV) vectors in *Gaa*$^{-/-}$ mice. Candidate promoters were restricted to a size of no greater than 1.0 kb in order to produce a final plasmid of less than 4.9 kb, the upper limit for packaging of rAAV vectors.

Materials and Methods

Molecular Cloning of DNA Constructs

The 3.1 kb human *GAA* (*hGAA*) cDNA was constructed as described (95). The full-length cDNA was first subcloned under the transcriptional control of the cytomegalovirus (CMV) immediate early promoter in the mammalian expression plasmid, pCI (Clonetch, Palo Alto, CA), to yield pCI-*hGAA*. The expression cassette was subcloned in the p43.2 plasmid containing the two rAAV serotype 2 inverted terminal repeats (ITRs) *via* *Eco*RI-*Xba*I digestion to yield p43.2-*hGAA*. The pGHP3 plasmid containing 350 bp of the Duck Hepatitis B Virus (DHBV) core promoter was constructed as described (68) and received as a gift from C. Liu (University of Florida, Gainesville, FL). The pAT2 plasmid containing the 950 bp albumin promoter and 3 upstream hepatocyte nuclear factor-1 enhancer (HNF-1) elements was constructed as described (70) and received as a gift by K. Zarret (Fox Chase Cancer Center, Philadelphia, PA). The phAAT-*hAAT* del IRES (p547) containing the 400 bp human alpha-1-antitrypsin (hAAT) promoter and the pTTR-*CAT* (p481) construct containing the 300 bp human transthyretin (TTR) promoter and enhancer were received as gifts from K. Ponder (Washington University, St Louis, MO). The DHBV, albumin, hAAT and TTR promoters were all subcloned from the parent vector into the p43.2*hGAA* plasmid by the following methods: 5' *Bgl*II and 3'*Hind*III sites were added to the promoter sequence by PCR and the amplified product was subcloned into the PCR2.1 Topo Cloning vector

(Invtirogen, Carlsbad, CA). The *Bgl*II-*Hind*III-flanked promoters were subsequently subcloned in the p43.2-*GAA* plasmid *via Bgl*II-*Hind*III digestion to yield the following pTR-Liverp-*hGAA* constructs: pTR-DHBV-*hGAA*, pTR-hAAT-*hGAA* and pTR-Alb-*hGAA*. A schematic of the constructs is shown in Figure 2-1. The pTR-*LacZ* plasmids (pTR-DHBV *LacZ*, pTR-hAAT *LacZ*, pTR-Alb *LacZ*, pTR-TTR *LacZ*) were constructed by replacing the *hGAA* cDNA in the pTR-Liverp-*hGAA* plasmids with the *LacZ* cDNA from the pAAV-*LacZ* plasmid described previously (61) via *Nhe*I-*Not*I digestion.

DNA Sequencing of Cloned Constructs

DNA samples of cloned constructs along with sequencing primers flanking the promoter regions were sequenced using the fluorescent dideoxy terminator method of automates sequencing by to the Interdisciplinary Center for Biotechnology Research DNA Sequencing Core at University of Florida.

Packaging and Purification of rAAV Vectors

Recombinant AAV2 vectors and rAAV pseudotype vectors (rAAV2 *rep* / 5 *cap* and rAAV2 *rep* / 1 *cap*) were packaged by the University of Florida Powell Gene Therapy Vector Core as previously described (136,149,150). Purified rAAV stocks were characterized by SDS/polyacrylamide gel electrophoreses with silver-stain and particle count. Total particle titer was determined by dot blot method as previously described (149). The infectious titer of rAAV2 serotype vectors was determined by infectious center assay (149).

In vitro Analysis of Liver Promoters Driving *LacZ* Expression

Cultured cells were maintained in humidified air, 5% CO_2 at 37°C. HepG2 (ATCC #HB-8065) or HEK 293 (ATCC #CRL-1573) cells plated at 80% confluency in 12-well plates were transfected with 2 μg pTR-Liverp-*LacZ* or p43.2-CMV-*LacZ* plasmids using Lipofectamine PLUS Transfection Reagent (Invitrogen, Carlsbad, CA) according to the manufacturer's instructions. Mock-treated wells were transfected with lipofectamine reagent alone. Cells were harvested from the dish in 500 μL of 1x phosphate buffered salt solution (PBS) at 48 hrs post-transfection. The cells were centrifuged and the cell pellet was resuspended in 1X PBS. Cell lysates were subjected to three freeze-thaw cycles and centrifuged. Clarified lysate (10 μL) was used in the Galacto-Star chemiluminescent reporter gene assay system for detection of β-galactosidase activity (Tropix Inc., Bedford, MA.). Protein concentrations of cell lysates were determined using a standard Bradford assay (11) based the binding properties detection of Coosmassie Brilliant Blue G-250 dye reagent (Bio-Rad, Hercules, CA). The Coomassie dye allows for an increasingly intense blue color to be detected at 620 nm wavelength with increasing amounts of total protein in the well. A standard curve was generated using seven concentrations of bovine serum albumin and corresponding A620 values.

Animals

The *Gaa*$^{-/-}$ mouse model used in these studies was generated from a targeted disruption of exon 6 and is maintained on a mixed C57BL/6 x 129X1/Svj background, as described previously (103). Age-matched C57B6/129 were used as controls. All mice were housed in the University of Florida SPF animal facility and all animal procedures were done in accordance with the University of Florida's Institutional Animal Care and Use Committee approval guidelines

Intrahepatic Recombinant AAV Delivery Methods

Animals were anesthetized with 2% isoflurane and restrained supine on a warmed operating surface. A midline incision was made and the abdominal skin and muscles were retracted. To expose the portal vein, the intestines were moved out of the abdominal cavity, covered with sterile gauze sponge and irrigated with warm saline (0.9%). Using a 29-gauged tuberculin syringe, 100-200 μL rAAV-*hGAA* diluted in Lactated Ringer's Saline (Baxter Healthcare Corporation, Deerfield, IL) was injected into the portal vein. Pressure was applied to the portal vein using a cotton applicator to prevent bleeding. The intestines were placed back into the abdominal cavity. The abdominal muscles were sutured using 5-0 prolene. The skin was closed using 5-0 vicryl. Prior to awakening from the anesthetic, the animal received 500 μL subcutaneous fluids consisting of 0.9% sodium chloride, ampicillin (50 mg/kg) and buprenorphine (0.1 mg/kg).

Tissue Processing

Eight weeks post injection, animals were euthanized by intraperitoneal injection of pentobarbital sodium solution (150 mg/kg) and extracted tissues (liver, heart, quadriceps, and diaphragm) were immediately cut and frozen in liquid nitrogen. Quadriceps muscle was first crushed to a powder using a hemostat in liquid nitrogen prior to homogenization. Tissues were homogenized in sterile water on ice using a PowerGen 35 Homogenizer (Fisher Scientific, Pittsburg, PA) and centrifuged. Homogenized supernatants were subjected to three freeze-thaw cycles and centrifugation.

GAA Enzymatic Activity Assay

Enzymatic activity assay for GAA was determined by measuring cleavage of the synthetic substrate 4-methylumbelliferyl-α-D-glucoside (4-MUG) (Sigma M9766, Sigma-Aldrich, St Louis, MO). Cleavage of 4-MUG by active GAA results in a fluorescent product, 4-methylumbelliferone (4-MU), that emits a fluorescent signal at 448 nm when excited at 360 nm. A 75 mM 4-MUG stock solution is prepared with dimethyl sulfoxide (DMSO). Twenty µL of clarified cell lysate was added to one well of a black 96-well plate. To each well, 1.6 µL of 75mM 4-MUG diluted in 38.4 µL of 200 mM sodium acetate (pH 3.6) was added. The plate was then incubated at 37°C for 1 h. The enzyme reaction was stopped by adding 200 µL of 0.5 M sodium carbonate (pH 10.7). Six standards of 4-MU (Sigma-Aldrich) were prepared from a 1 mM stock of 4-MU diluted in sterile water. Twenty µL of each standard were added to individual wells along with 40 µl sodium acetate and 200 µL sodium carbonate. Fluorescence was measured at 460 nm using the Flx800 microplate fluorescence reader (Bio-Tek Instruments, Winooski, VT). A standard curve was generated using a linear regression of the 4-MU standards ranging from 0 µm to 500 µm.

Protein concentrations were determined using the Bio-Rad *DC* Protein Assay kit (Bio-Rad, Hercules, CA). Clarified lysate was diluted 1:5 or 1:20 depending on the tissue type. Standards ranging from 0 to 5 µg of bovine serum albumin (BSA) were prepared in sterile water. Five µl of diluted lysate or standard were added to individual wells of a 96-well plate along with 225 µL total volume of Bio-Rad Coomassie Brilliant Blue dye reagents. After 15-minute incubation, the plate was read at 750 nm. A standard curve was generated using a linear regression of the BSA standards. For both the activity and protein assays, samples that generated fluorescence or absorbance values outside of the linear range were subsequently diluted and re-calculated. GAA activity was calculated as nmol 4-MUG cleaved per hour per milligram of total protein in the lysate.

Data are represented as the percent of normal GAA activity observed in tissues from age-matched and sex-matched normal (C57BL/6/129) mice processed and assayed side-by-side with treated mice.

ELISA Detection of Anti-GAA Antibodies

Serum samples were obtained weekly by tail vein bleeds of anesthetized animals. Whole blood was collected in Microtainer tubes (Becton Dickinson, Franklin Lanes, NJ), spun at 5500 rpm for 10 min and serum was removed and stored at –20°C. Immulon microtiter plates (Thermo Labsystems, Franklin, MA) were coated overnight at 4°C with 200 µl of 0.5 mg/mL human GAA in 0.1M $NaHCO_3$ (pH 8.2). Wells were washed 3 times with 300 µL PBS containing 1% Tween20 (PBS/T) and blocked with 300 µL 10% fetal bovine serum (FBS) in PBS/T for 2 h at room temperature. Wells were washed 3 times and serum samples (diluted 1:80 in the blocking reagent) were added to the wells in a total volume of 100 µl. Serial dilutions of rabbit-anti-human GAA antibody (from 1:500 to 1: 5 x 10^6) were used to derive the standard curve. Samples and standards were incubated for 1h at room temperature. Washing was repeated and 100 µL sheep of anti-mouse IgG-HRP linked antibody or donkey-anti-rabbit-IgG-HRP-linked antibody (Amersham Pharamcia Biotech, Piscataway, NJ) diluted 1:10,000 was added to the sample wells or standard wells respectively and incubated for 30 min at room temperature. After incubation, washing was repeated and 100 µl of Tetramethyl benzidine (Sigma-Aldrich) was added to the wells for 1-3 minutes. The reaction was stopped with 100 µl of 1N H_2SO_4 and absorbance was measured at 450 nm. A standard curve was generated (to control for assay variability) with the dilution of rabbit anti-human GAA antibody as the abscissa and the corresponding A450 values as the ordinate (R^2=0.95-0.98). Standardized values for serum of treated mice were divided by mean standardized values for serum from untreated *Gaa*$^{-/-}$ mice (n=3). Final values were reported as fold over background anti-GAA antibody titer.

Histology

Tissues were fixed in 10% buffered formalin and embedded in paraffin and sectioned. Sections were stained with hematoxylin and counterstained with eosin (H&E). H&E-stained liver sections were examined for histopathology by a veterinary pathologist at the University of Florida Pathology Core Lab.

Statistical Analysis

Unpaired Student's *t*-test (Sigma Plot 2001, SPSS Inc, Chicago Illinois) was used for statistical analysis comparing treatment groups with statistical significance considered if $P<0.05$.

Results

In Vitro Analysis of Four Liver-Specific Promoters

The relative strengths and hepatic-specificities of four liver-specific promoters (albumin, hAAT, DHBV, and TTR) were evaluated *in vitro* by transient transfection of β-galactosidase expressing plasmids (Figure. 2-1). The *LacZ* reporter cDNA was used in place of the *hGAA* cDNA for these studies due to the high background levels of GAA activity in hepatocyte cell lines. The p43.2-CMV- *LacZ* plasmid was used as a positive control as the CMV promoter is known to yield high levels of expression in most cell types *in vitro*.

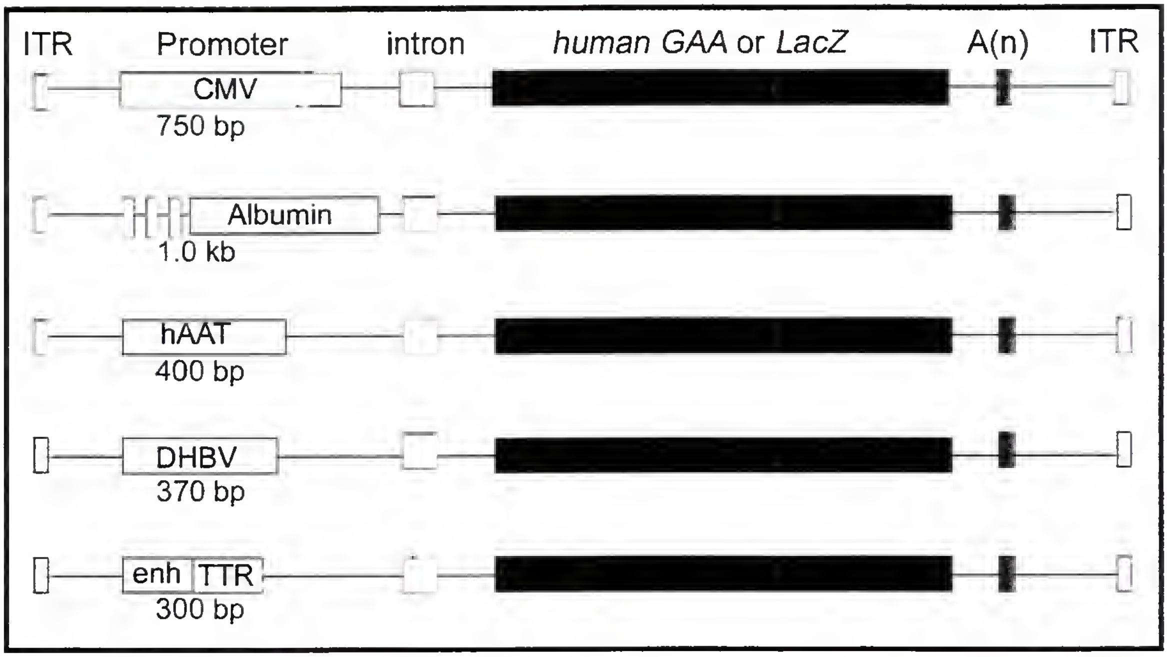

Figure 2-1. Cloned vector constructs. All constructs contain the 5' and 3' rAAV2 ITRs, promoter (with size designated below), chimeric intron, the human *GAA* cDNA (used for *in vivo* studies) or *LacZ* cDNA (used for *in vitro* studies) and a poly A tail. Drawings are not to scale.

After transfection of the human hepatoma cell line, HepG2, the TTR (transthyretin) promoter yielded the highest levels of β–galactosidase activity followed by the hAAT (human α-1-antitrypsin) promoter (Figure 2-2). Additionally, all four liver promoters yielded undetectable or very low levels of β–galactosidase activity in the HeLa cell line (a cervical cancer cell line consisting predominately of epithelial cells). While these results were valuable in confirming hepatocyte-enhanced activity from all four promoters, it has become apparent, based on work from our laboratory and others (unpublished) that accurate predictions of transgene expression from various gene regulatory elements in animals cannot be made based on *in vitro* transfection data. Three promoters, DHBV, albumin and hAAT were chosen for *in vivo* analysis of hGAA activity. The TTR promoter, which yielded the highest transgene levels *in vitro* was not evaluated for *in vivo* studies at this time based on consistent results from other (obtained after our *in vitro* studies were performed) demonstrating poor activity *in vivo* (99).

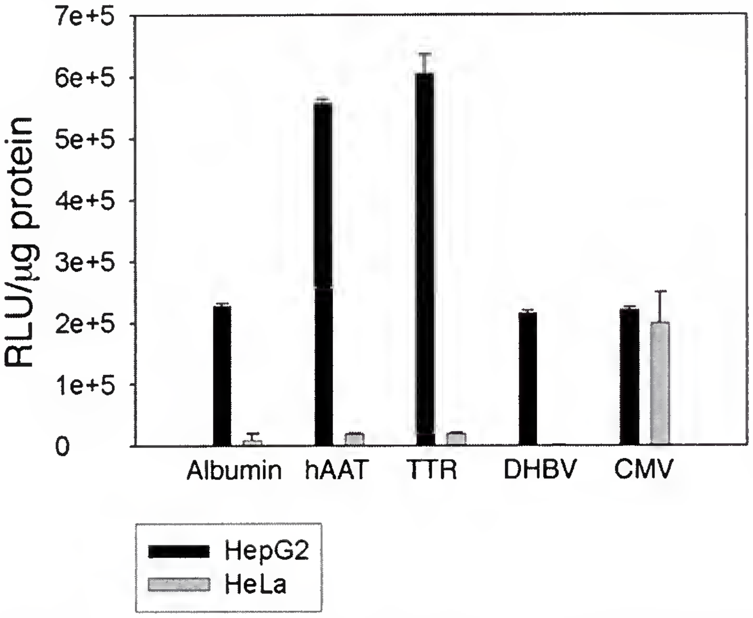

Figure 2-2. *In vitro* comparison of 4 liver promoters and the ubiquitous CMV promoter by transient transfection of *LacZ* expressing constructs in HepG2 and HeLa cell lines. Background luminescence in mock-transfected wells was subtracted from all values. Bars represent mean ± standard error of the mean (n=3 wells per plasmid).

Superphysiologic Levels of Liver GAA Expression from the rAAV2-DHBV-*hGAA* Vector are not Sufficient to Restore Activity in Affected Tissues of *Gaa*$^{-/-}$ Mice

The albumin promoter has been one of the most well characterized liver-specific promoters and numerous studies have reported high levels of transgene expression under the control of this promoter (64,73,115,133). While the DHBV promoter was also shown to have strong hepatic cell type specificity in tissue culture (68), it had not been previously tested as a candidate promoter for gene delivery studies. In effort to determine whether the DHBV promoter could yield higher levels of hepatic transgene expression *in vivo* than the well-studied albumin promoter, the pTR-Alb-*hGAA* and pTR-DHBV-*hGAA* constructs were packaged in rAAV serotype 2 viruses and administered *via* intrahepatic delivery to 8 wk-old *Gaa*$^{-/-}$ mice. Eight weeks after portal vein delivery of

3×10^{12} vector genomes (vg) of rAAV2- *hGAA*, liver GAA expression was 6-fold greater from the DHBV promoter than from the albumin promoter (180 ± 21.7% versus 30 ± 3.4% of normal; P=0.003) (Figure 2-3). Despite these superphysiological levels of GAA observed in the livers of mice receiving the rAAV-DHBV-*hGAA* vector, we observed no increase in GAA enzyme activity levels in the cardiac or skeletal muscle (not shown).

At this time, the use of alternative rAAV serotypes was reported and results consistently demonstrated that rAAV serotype 5 yielded significantly higher transgene levels in the liver than serotype 2 (82). However, results comparing the relative strength of serotype 1 versus serotype 2 in the liver were not consistent. The second *in vivo* study was designed to evaluate rAAV-mediated delivery of human GAA, under control of the hAAT promoter in *Gaa*$^{-/-}$ mice using serotypes 1 and 5.

Recombinant AAV Serotype 5 Vector Yields Higher Liver GAA Levels than Serotype 1 Vector

After portal vein delivery of 5×10^{11} vg of rAAV1-hAAT-*hGAA* or rAAV5-hAAT-*hGAA* to 8 wk old *Gaa*$^{-/-}$ mice, liver GAA activity levels were 2-fold higher with rAAV5 (P=n.s.) (Figure 2-3). However, these levels (30.9 ± 11.0% of normal) were again insufficient to restore GAA activity in cardiac or skeletal muscle. Although comparison of the DHBV promoter used in the serotype 2 study and the hAAT promoter used in this study is complicated by both the dose and serotype variables, if the doses are accounted for (3×10^{12} vg and 5×10^{11} vg respectively), expression from the hAAT promoter appears to be equal to expression from the DHBV promoter. That is, both the dose and liver GAA levels from rAAV2-DHBV-*hGAA* vector are 6-fold greater than from the rAAV5-hAAT-*hGAA* vector. However, data from numerous groups reporting that liver transgene levels from rAAV5 vectors are consistently 5 to 10-fold greater than from rAAV2 vectors (40,82) suggests that the promoter strengths may not be equal. Future studies would benefit from evaluating the DHBV promoter using the rAAV5 vector.

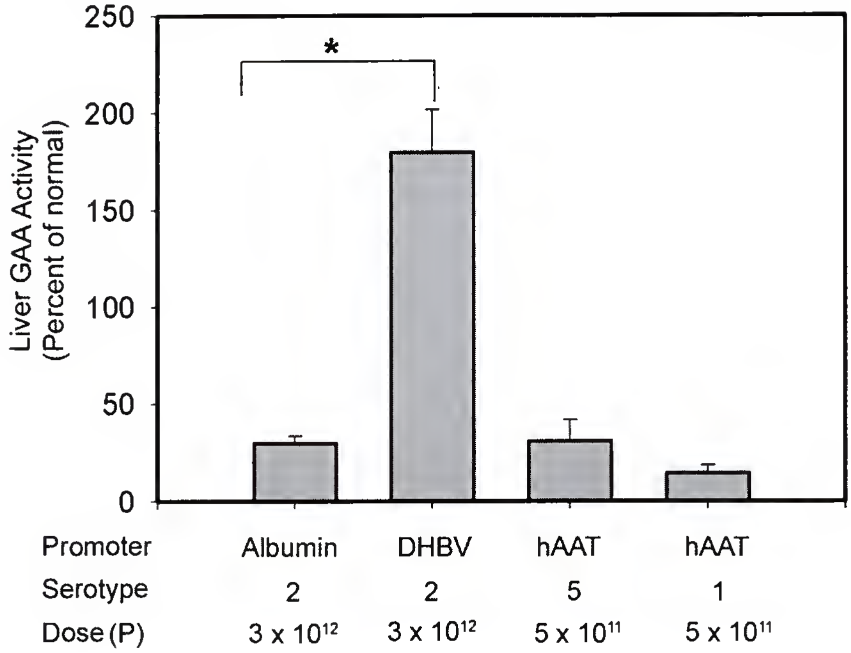

Figure 2-3. Summary of *in vivo* studies comparing liver promoters by portal vein delivery of *human GAA*-expressing rAAV vectors in adult *Gaa*$^{-/-}$ mice. Background activity in untreated *Gaa*$^{-/-}$ mice was subtracted from all values. Bars represent mean ± standard error of the mean (n=3 for albumin and DHBV vectors and n=5 for hAAT vectors) * P=<0.01.

Gaa$^{-/-}$ Mice Elicit a Humoral Immune Response to Vector-Derived Human GAA

Before planning future studies to optimize hepatic GAA expression, it was necessary to determine if lack of cross-correction was solely due to insufficient levels of hepatic GAA expression or if *Gaa*$^{-/-}$ mice were forming anti-GAA antibodies that could potentially inhibit uptake of liver-secreted GAA by other tissues. Serum samples collected weekly from rAAV1- and rAAV5-hAAT-*hGAA* treated mice were assayed for the presence of anti-GAA antibodies by ELISA. Formation of anti-GAA antibodies was observed beginning at 5 weeks post injection (Figure 2-4). Variability in the degree of immune response was observed between mice from both groups. In the rAAV1-treated group, 2 of 5 mice had elevated antibody titers peaking at 2.4 and 3.1-fold over background, respectively, while the remaining 3 had lower titers of 1.2 ± 0.06-fold over background. Antibody titers overall (as well as the degree of variability) were lower in the rAAV5-treated group, with 2 of 5 mice having elevated antibody titers of 1.6- and 2.2-fold over background, and the remaining 3 having background titers.

The significance of these values was difficult to assess, as there was no cross-correction in any of the mice, regardless of their immune response. However, we did observe an overall inverse relationship between liver GAA activity and antibody titer (Figure 2-5). In mice with liver-GAA values of ≤ 10% of normal, anti-GAA antibody titers were between 2 to 4-fold over background. In contrast, mice with higher levels of liver GAA expression (between 16% to 140% of normal) had anti-GAA antibody titers near background. The exponential decay relationship of these two variables suggests the possibility of a threshold effect where liver GAA expression values greater than 10% of normal are able to induce immune-tolerance. While the mechanism behind the idea of high dose tolerance has not been elucidated, it has been demonstrated by others studying liver-directed, rAAV-mediated gene replacement for hemophilia and Fabry disease (81,148).

Alternatively, the negative relationship observed between liver GAA activity and anti-GAA antibody titer could suggest the presence of a cell-mediated immune response (CMI). If higher antibody titers are an indication of a CMI response in these mice, then we would expect to see a loss of liver GAA activity due to destruction of transduced hepatocytes by cytotoxic T-lymphocytes in these mice. To begin evaluating this theory, liver tissues from rAAV-hAAT-*hGAA*-treated mice and saline-treated mice were sectioned, stained with hemotoxylin and eosin (H&E), and evaluated for histopathology (not shown). While no signs of infiltration or other hepatocellular changes were observed in the terminal liver tissues, it is theoretically possible that an earlier cytotoxic response would have been cleared and become undetectable at 8 wk post injection. More in depth immunologic studies will be necessary in future experiments to confirm this.

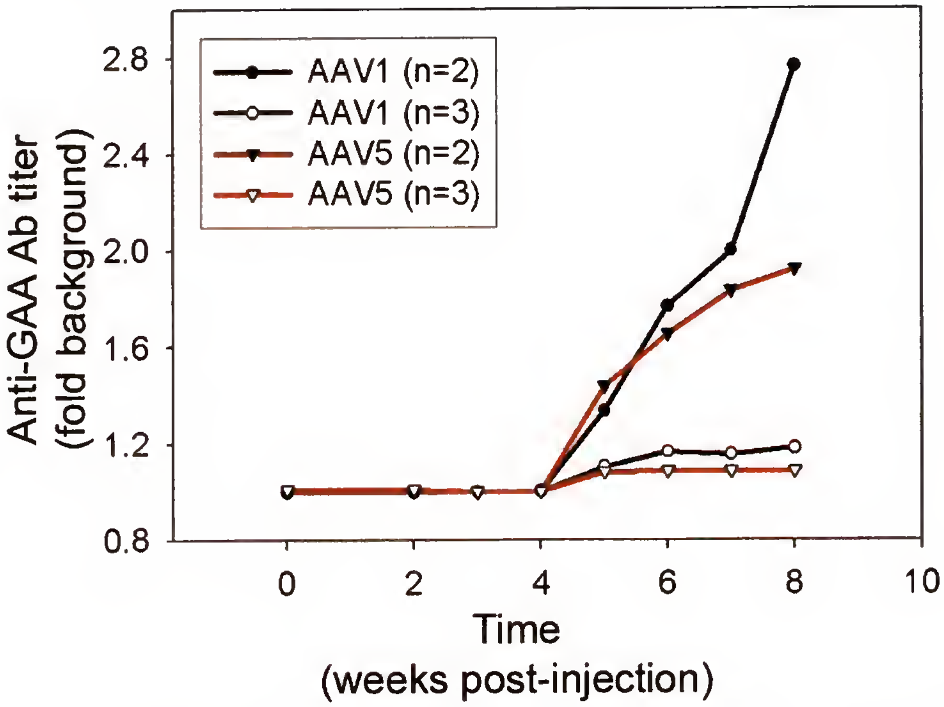

Figure 2-4. Weekly anti-GAA antibody formation in rAAV1- and rAAV5-hAAT-*hGAA* treated *Gaa*$^{-/-}$ mice.

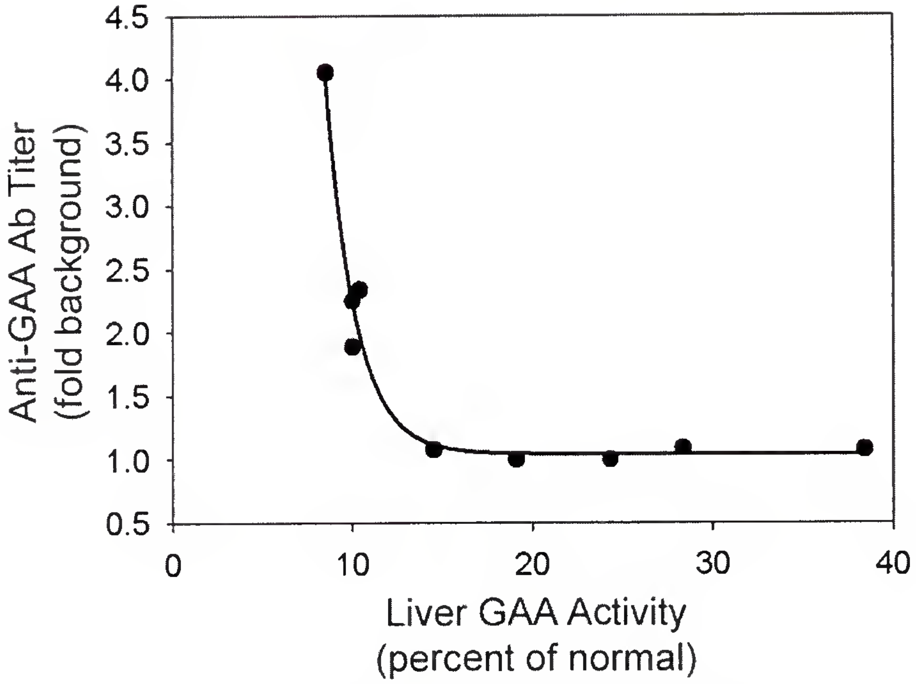

Figure 2-5. Exponential decay relationship between percent normal liver GAA activity versus terminal anti-GAA antibody titers in rAAV-hAAT-*hGAA* treated mice.

Discussion

Recombinant AAV-mediated delivery of human GAA to *Gaa*$^{-/-}$ mice was evaluated using 4 promoter/serotype combinations. Results from *in vitro* DNA transfection studies showed transgene expression from the hAAT promoter to be 2.6-fold greater than the DHBV promoter, which was approximately equal to the levels of expression observed from the albumin promoter. Conversely, *in vivo* studies showed expression from the DHBV promoter to be 6-fold greater than the albumin promoter. Surprisingly, liver transgene expression with a 6-fold lower dose using the hAAT promoter with serotypes 1 and 5 were very low. While a direct comparison of all three promoters using the same serotype and dose would be necessary to determine the relative promoter strengths, these results suggest that the hAAT promoter is weaker in the liver than both the DHBV and albumin promoters.

These initial studies to evaluate liver-directed rAAV gene therapy for GSDII were disappointing, showing up to 200% of normal liver GAA activity levels with no correction of distally affected tissues. There are two likely hypotheses for the lack of cross-correction observed in *Gaa*$^{-/-}$ mice:

- Levels of liver GAA expression were not sufficient to provide necessary amounts of secreted GAA for uptake by distal cells.
- *Gaa*$^{-/-}$ mice, recognizing the rAAV-derived human GAA as a foreign protein, formed anti-GAA antibodies, which inhibited liver-secreted human GAA preventing uptake by distal cells.

The former hypothesis can be tested only by generating higher-expressing rAAV-*hGAA* vectors, and future studies will benefit from evaluating intrahepatic delivery of rAAV5-DHBV-*hGAA* in *Gaa*$^{-/-}$ mice. The latter hypothesis is not likely to be the sole explanation of the observed results, as 6 of the 10 rAAV-hAAT-*hGAA*-treated mice had near-background to background antibody titers with no restored activity in distal tissues. It is possible that a combination of both insufficient liver GAA levels and inhibitory antibody formation is responsible for lack of cross-correction, and it will likely be necessary to overcome both of these obstacles to achieve systemic correction.

Immunologically naïve treated *Gaa*$^{-/-}$ mice showed considerable heterogeneity not only in the levels of hepatic GAA expression from identical treatments, but also in the anti-GAA antibody response. This heterogeneity in hepatic expression levels could be attributed to the interplay of unidentified modifier genes, variable success of vector administration between mice, or physiological state of the mouse at the time of treatment. While it is difficult to control for variable hepatic expression levels after identical treatments, we may be able to control for the variegated immune response. In order to determine the potential for cross-correction from liver-produced, rAAV-derived hGAA, a mechanism for inhibiting the immune response to human GAA in *Gaa*$^{-/-}$ mice will have to be developed.

CHAPTER 3
CHARACTERIZATION OF A NEONATALLY TOLERIZED GSDII MOUSE MODEL

Background

Initial studies evaluating liver-directed rAAV-mediated delivery of *hGAA* to *Gaa*$^{-/-}$ mice resulted in up to 200% of wild-type liver GAA levels with no restoration of activity in the cardiac or skeletal muscle. At this time, numerous reports were beginning to emerge investigating the immune response to rAAV-derived transgene products, (particularly for the treatment of hemophilia). While anti-GAA antibody titers were observed beginning at five weeks post delivery of rAAV-hAAT-*hGAA* to *Gaa*$^{-/-}$ mice, the peak titers were only 1.0 to 3.1-fold over background. Because of the lack of information concerning the presence of anti-GAA antibodies to hGAA (delivered by gene or enzyme replacement therapy), it was necessary to determine if the observed antibody titers were inhibitory. One approach to this is comparison of treatment outcomes in *Gaa*$^{-/-}$ mice with and without anti-GAA immune responses. To better control for the anti-GAA response, we generated a tolerant *Gaa*$^{-/-}$ mouse model. There are a variety of approaches to generating tolerance to a therapeutic foreign protein. We chose to generate a murine model of neonatal tolerization by administering a small dose of highly purified recombinant hGAA (rhGAA) to 1-day-old *Gaa*$^{-/-}$ mice. This technique is modified from the protocol described by Pittman *et al.* (96), where a low dose of various antigenic forms of hFVIII was delivered intraperitoneolly to 1 day-old mice for the purpose of studying relative antigenicty of the different isoforms.

For our studies, human GAA tolerance was confirmed by lack of antibody formation after challenge with repeated injections of a therapeutic dose of the same protein. This tolerant GSDII model will be valuable for determining the effects of anti-GAA humoral immunity and for evaluating the full potential of both gene and enzyme replacement therapies in the absence of anti-GAA antibodies.

Materials and Methods

Pretreatment of *Gaa*$^{-/-}$ Mice

All mice were house in the University of Florida SPF animal facility and all animal procedures were done in accordance with the University of Florida's Institutional Animal Care and Use Committee approval guidelines. Recombinant hGAA (25 μg), diluted in 50 μL of 0.9% saline, was injected subcutaneously in the scruff of the neck of 15-30 h old *Gaa*$^{-/-}$ mice using a 0.5 cc insulin syringe. Mice were immediately returned to the cage.

Intravenous Protein Delivery

Mice were anesthetized *via* intraperitoneal delivery of avertin (2,2,2-tribromoethanol) prepared as a 1.2% solution and used at a dose of 0.2 mL/10 g body weight. The fur surrounding the neck area was removed using a depilatory cream, followed by cleaning with 10% povodone-idodine solution. A small incision was made in the skin to provide access to the internal jugular vein, and rhGAA was injected at a dose of 10 mg/kg (diluted to a total volume of 100 μL in 0.9% saline) using a 0.5 cc insulin syringe. The incision was closed and analgesics were delivered subcutaneously.

ELISA for Detection of Anti-GAA Antibodies

Serum samples were obtained weekly *via* tail bleed of anesthetized mice. Serum, diluted 1:80, was assayed for the presence of anti-GAA antibodies by ELISA (described in chapter 2). Results were standardized to serial dilutions of rabbit anti-human GAA antibody and reported as fold over background with background equal to the anti-GAA antibody titer in untreated *Gaa*$^{-/-}$ mice.

ELISA for Detection of Distinct Isotypes

The ELISA protocol for measuring distinct antibody isotypes was performed as described in chapter 2 for the anti-GAA antibody ELISA with the following modification: After incubation of serum (diluted 1:80) on coated plates and washing, rabbit-anti mouse- IgG1, IgG2a, Ig2b or IgM (Zymed, San Francisco, CA) (diluted 1:10,000 in 10% FBS), was added to the wells for 30 min at room temperature. The remaining ELISA steps were performed as previously described.

Competition ELISA to Determine Antibody Specificity

Immulon microtiter plates (Thermo Labsystems, Franklin, MA) were coated overnight at 4°C with 200 µL 0.5 mg/ml human GAA in 0.1M $NaHCO_3$ (pH 8.2). Wells were washed three times with 300 µL PBS containing 1% Tween20 (PBS/T) and blocked with 300 µL 10% fetal bovine serum (FBS) diluted in PBS/T for 2 h at room temperature. After incubation, washing was repeated, and the competing rhGAA was added to triplicate wells in a total volume of 100 µL (diluted in 10% FBS) at the following concentrations: 0, 0.1, 0.5, 5.0, 10, and 20, µg/mL. Serum (pooled from 3 naïve *Gaa*$^{-/-}$ mice 1 wk after intravenous delivery of 10 mg/kg rhGAA) was diluted 1:80 and added to wells containing competing rhGAA. After 1 h at room temperature, wells were washed 3 times to remove antigen-bound serum. Sheep-anti-mouse IgG-HRP linked antibody (Amersham Pharamcia Biotech, Piscataway, NJ), diluted 1:10,000 in 10% FBS, was added to the wells in a total volume of 100 µL. After 30 min incubation at room temperature, washing was repeated, and 100 µL tetramethyl benzidine (Sigma-Aldrich, St. Louis, MO) was added to the wells for 1-3 min. The reaction was stopped with 100 µL 1N H_2SO_4, and absorbance was measured at 450 nm. The absorbance values obtained in the presence of competing antigen were divided by the absorbance values obtained in the absence of competing antigen to obtain the percent decrease in signal.

Lymphocyte Proliferation Assay

All techniques were performed under sterile conditions. Spleens were harvested from treated and control animals and placed in a Petri dish containing 1X Hanks Balanced Salt Solution (HBSS) (Cellgro, Herndon, VA). The spleens were then placed in 70 µm nylon mesh filters over a 50 mL conical tube. Using a 27-gauge needle and 3 cc syringe, HBSS was injected directly into the spleen to break up the tissue. The spleens were ground on the surface of the nylon mesh filter using the plunger from the 3 cc syringe. The membrane was rinsed with HBSS using a disposable transfer pipette. HBSS was added to bring the final volume to 25 mL. The cells were centrifuged at 500 *g* for 10 min. Supernatant was removed, and cells were resuspended in the remaining small volume of media. Two mL of cold NH_4Cl Solution (Stem Cell Technologies, Vancouver, BC) was added to the cells and kept on ice for 2 min (to induce lysis of the red blood cells). The reaction was stopped by adding HBSS to a final volume of 25 mL. Cells were centrifuged at 500 *g* for 10 min. Supernatants were removed, and cells were resuspended to a final volume of 5 mL in RPMI media (Cellgro) supplemented with 10% FBS, 1% penicillin/streptomycin and 2.5 % 1M HEPES. Cells were counted on a hemacytometer and splenocytes were transferred to a 96-well round-bottom dish (1 x 10^5 cells/well in a total volume of 100 µL). Conconavalin A (Con A) (Sigma) was diluted in RPMI media and added to positive control wells at 6 final concentrations ranging from

0.1 to 5 µg/mL. Recombinant human GAA was diluted in RPMI media and added to sample wells at 4 concentrations ranging from 0.5 to 10.0 µg/mL. Cells were incubated in humidified air, 5% CO_2 at 37°C. Five days after treatment, tritiated thymidine was added to wells at a final concentration of 0.2 Ci/well. Cells were incubated at 37°C for 7 h. Cells were harvested onto glass fiber multiscreen plates (Millipore, Billerica, MA) and washed 3 times with sterile water. After drying, 25 µL scintillation fluid was added to wells and radioactivity was counted using a Trilux beta counter (Wallac, Boston, MA). Responses were calculated as a stimulation index by dividing cpm of the stimulated wells by the cpm of the unstimulated wells.

In vitro GAA Inhibition Assay

HeLa cells were cultured in 1X DMEM (Cellgro) supplemented with 10% fetal bovine serum and maintained in 5% CO_2 at 37°C. Cells were seeded to 90% confluency in 12-well plates. For each treatment sample, pooled serum from 3 mice was used. Serum-free DMEM (760 µL) was added to 40 µL serum and 2 µL rhGAA (0.15 µg/µL in serum-free DMEM). The 800 µL mixture was incubated for 1 h at 4°C on an inverting platform. A control sample of rhGAA alone was also mixed for 1 h at 4°C to control for loss of activity. Medium was removed from cells, which were then washed with 1X PBS. The serum-rhGAA mixture was added to cells, and cells were incubated at 37°C, 5% CO_2 for 3.5 h. Cells were harvested in 400 µL 1X PBS per well. Cells were centrifuged and the cell pellet was resuspended in 120 µL 1X PBS. The cell lysates were subjected to 3 freeze-thaw cycles followed by centrifugation to pellet cell debris. Cell lysate (20 µL) was used in the 4-MUG-cleavage assay for determination of GAA enzymatic activity as described in chapter 2.

Results

Neonatal Pretreatment Results in Humoral Tolerance to Intravenous Protein Delivery

To induce tolerance to hGAA, *Gaa*$^{-/-}$ mice were administered 25 μg rhGAA subcutaneously between 15-30 h after birth. Eight weeks after rhGAA administration, pretreated and naïve *Gaa*$^{-/-}$ mice were administered the same protein intravenously at a dose of 10 mg/kg (which was the intermediate dose being evaluated at this time for preclinical enzyme replacement therapy trials). A second dose was delivered 4 wk after the first to boost the immune response, and serum samples were collected weekly out to 4 wk after the second injection. Anti-GAA antibody formation in naïve mice followed a typical humoral response pattern to repeated antigen exposure; antibodies were first detected 2 wk after the first injection and peaked 1 wk after the second. Antibody titers gradually fell to approximately 5-fold over background by the end of the experiment (Figure 3-1). In contrast, there was no detectable anti-GAA antibody formation for the duration of the study in pretreated *Gaa*$^{-/-}$ mice.

Antibodies are Specific to GAA

A competition ELISA was performed to confirm the specificity of antibodies detected in serum from treated mice for GAA (Figure 3-2). Six titrations of rhGAA were added to respective wells, along with serum from treated mice, to compete with well-bound rhGAA for binding of IgG in the serum. The antigen specificity of IgG is determined by the degree to which the competing GAA prevents serum IgG from binding the well-bound GAA and is measured by a loss of signal after colorometric detection of the HRP-conjugated anti-mouse IgG anitbody. After adding 0.01 μg rhGAA, an 8% decrease in signal was observed. This was followed by a 30% decrease in signal in the presence of 0.05 μg competing GAA. Percent signal reduction reached a steady state with 0.5 μg of competing GAA. This exponential curve suggests high specificity of IgG detected in the serum of rhGAA-challenged *Gaa*$^{-/-}$ mice for GAA.

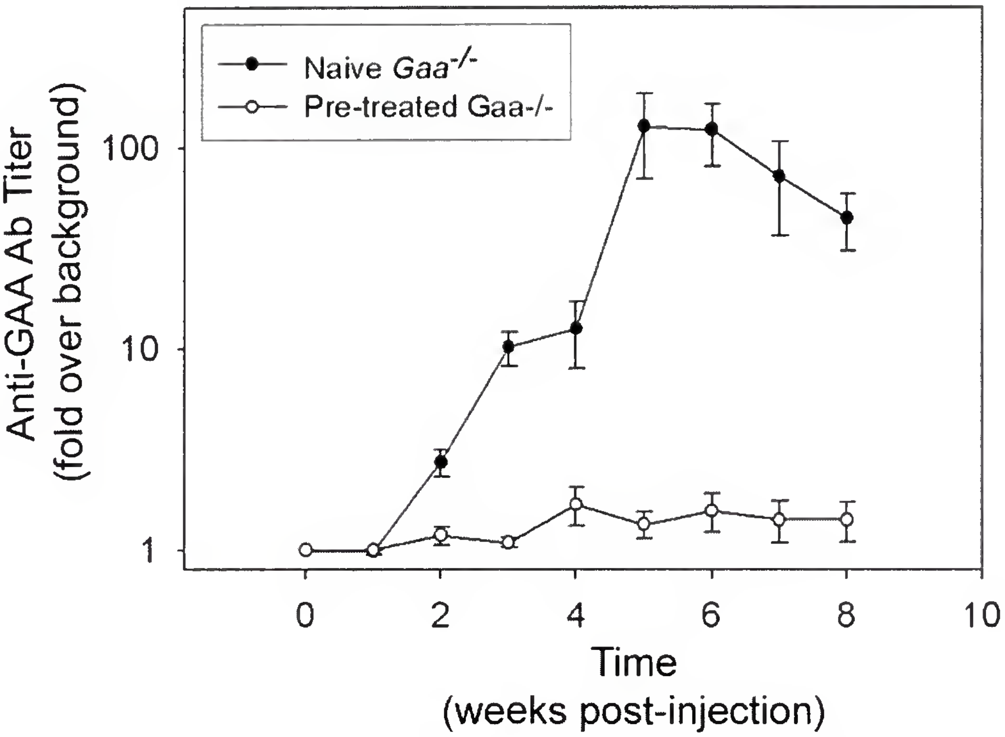

Figure 3-1. Anti-GAA antibody formation in pretreated and naïve *Gaa*$^{-/-}$ mice to rhGAA protein. Recombinant hGAA was injected *via* the jugular vein at a dose of 10 mg/kg at 0 and 4 wk (8 and 12 wk of age respectively). Anti-GAA antibodies were measured by ELISA (n=8/group). Data points represent mean anti-GAA antibody titer ± standard error of the mean.

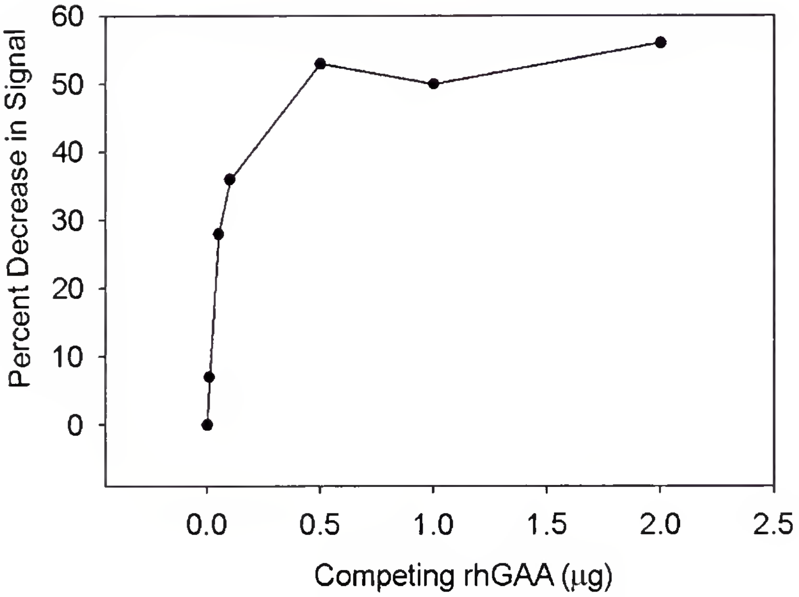

Figure 3-2. Competition ELISA of anti-GAA antibody-containing serum. Serum samples were pooled from 3 naïve *Gaa*$^{-/-}$ mice 1 wk after the second injection of 10 mg/kg rhGAA. Data points represent the percent decrease in serum to plate binding after competition with the amounts of rhGAA designated on the X-axis.

Recombinant Human GAA-Challenged Mice Show no Signs of Cell-Mediated Immunity

We previously reported in chapter 2 that naïve *Gaa*$^{-/-}$ mice show no detectable signs of cell-mediated immunity to rAAV-derived hGAA after intraheptic delivery. Because the development of a tolerant GSDII model will be useful for both gene and enzyme replacement therapies studies, it was necessary to determine if naïve *Gaa*$^{-/-}$ mice elicited a cell-mediated immune (CMI) response to direct rhGAA infusion. If a CMI response is expected, it will be necessary to confirm that the chosen approach to tolerization reduces or abolishes the CMI as well as the humoral immune response. In order to evaluate the Th1-driven CMI response to hGAA in *Gaa*$^{-/-}$ mice, we examined liver histopathology, proliferation of splenocytes from challenged mice in response to rhGAA, and formation of the Th1-indicating isotype, IgG2a.

No lymphocyte infiltration was observed on hematoxylin and eosin-stained liver sections from naïve or pretreated *Gaa*$^{-/-}$ mice after rhGAA challenge (data not shown). After stimulation of harvested splenocytes from treated mice, no proliferation was observed in rhGAA treated wells in contrast to 25-fold proliferation observed in the positive control (ConA)-treated wells (Figure 3-3).

While proliferating Th2 cells characteristically activate B cells leading to the production of IgG1, Th1 cells (which stimulate proliferation of cytoxic T-lymphocytes) can also activate B cells resulting in IgG2a production (34). Therefore, IgG2a can be considered a Th1-indicating isotype. Anti-GAA antibodies in all samples consisted predominantly of IgG1 with 3- to 6-fold lower levels of IgG2b and background levels of IgG2a (Figure 2-6). This lack of IgG2a suggests the absence of significant Th1- cell proliferation and presumably a lack of CMI. Note that IgM formation follows an expected pattern with a primary response forming at approximately 1 wk prior to class-switching to IgG followed by a secondary reaction immediately after the second dose. The results suggest a lack of CMI after two monthly doses of 10 mg/kg rhGAA and therefore tolerance to this dosing regimen of hGAA will not require inhibiting Th1-mediated responses.

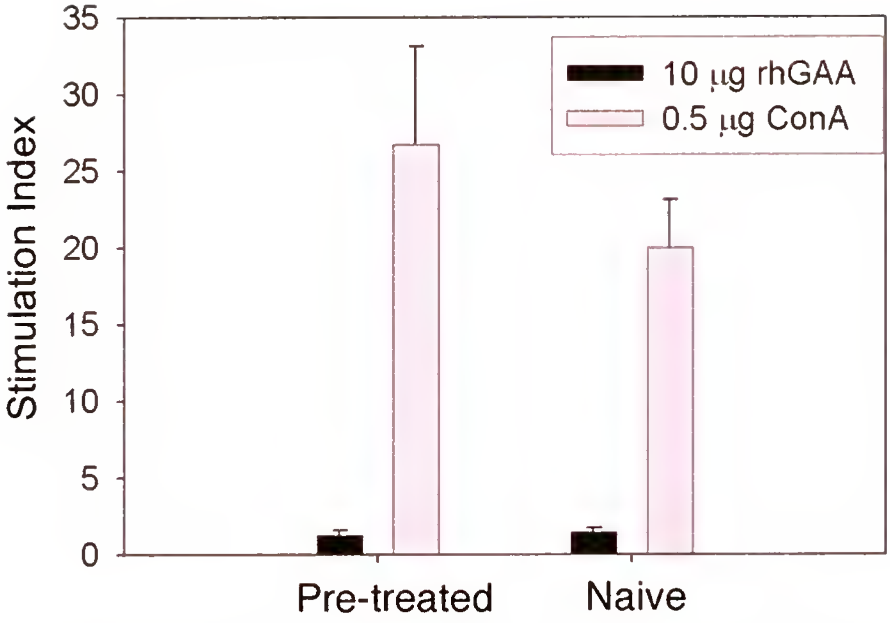

Figure 3-3. Lymphocyte proliferation assay on splenocytes from pretreated and naïve *Gaa*$^{-/-}$ mice 8 wk after challenge with 10 mg/kg rhGAA. Bars represent the mean (n=6 mice per treatment each assayed in quadruplicate) ± standard error of the mean.

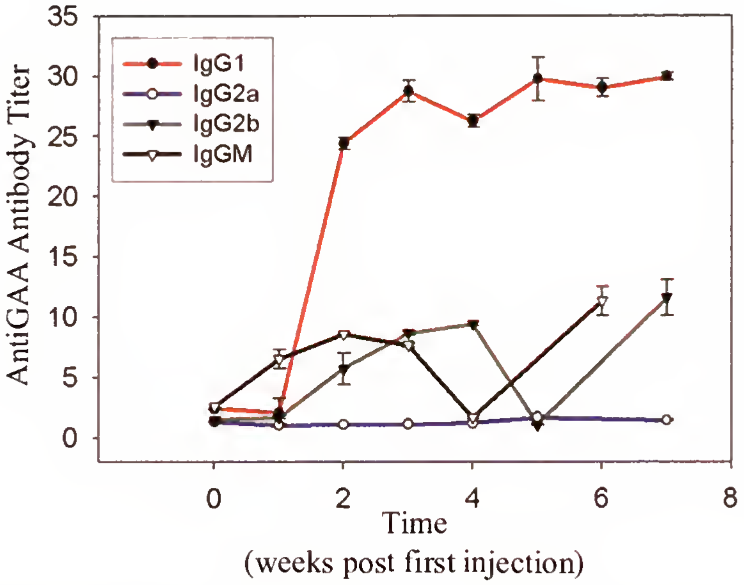

Figure 3-4. Detection of anti-GAA isotypes in naïve *Gaa*$^{-/-}$ mice after rhGAA delivery. Naïve *Gaa*$^{-/-}$ mice were administered rhGAA (10 mg/kg) *via* the jugular vein at 0 and 4 wk (8 and 12 wk of age respectively). Symbols represent the mean ± standard error of the mean (n=3).

Susceptibility to Tolerization Decreases from 1 to 7 Days after Birth

To use this neonatal tolerant GSDII model for future studies evaluating gene delivery and consequential immune response, we needed to determine the window of opportunity for successful induction of tolerance in the *Gaa*$^{-/-}$ model. The theoretical window of opportunity for neonatal tolerance varies depending on the mode of tolerance induction and nature of the toleragen. Most reported neonatal tolerance studies induce tolerance within 24 h after birth. However, we were interested in the possibility of later tolerance induction; as the immunologic development in the mouse is thought to occur throughout the first week of life (55).

Six mice were pretreated at 1, 3, or 7 days after birth and subsequently challenged with 10 mg/kg of rhGAA 8 wk later. Three weeks after challenge, serum was collected and assayed for the presence of anti-GAA antibodies (Figure 3-5). Six of 6 mice pretreated at 1 day-old had less than 2-fold over background anti-GAA antibody titers. Mice pretreated at 3 days-old showed a slightly less susceptibility to tolerance: Four of 6 mice had antibody titers of less than 2-fold over background while 2 of 6 mice had intermediate antibody titers (between 2- to 4-fold over background). Mice pretreated at 7 days-old showed even less susceptibility to tolerance: One of 6 mice had background antibody titers, 3 of 6 mice had intermediate titers and the remaining two had higher titers (4- to 5-fold over background). Despite the high antibody titers observed in 7 day pretreated mice, antibody formation was inhibited to some degree; as anti-GAA antibody titers in naïve mice receiving the same protein challenge were approximately 9-fold background at 3 weeks post-challenge (Figure 3-1).

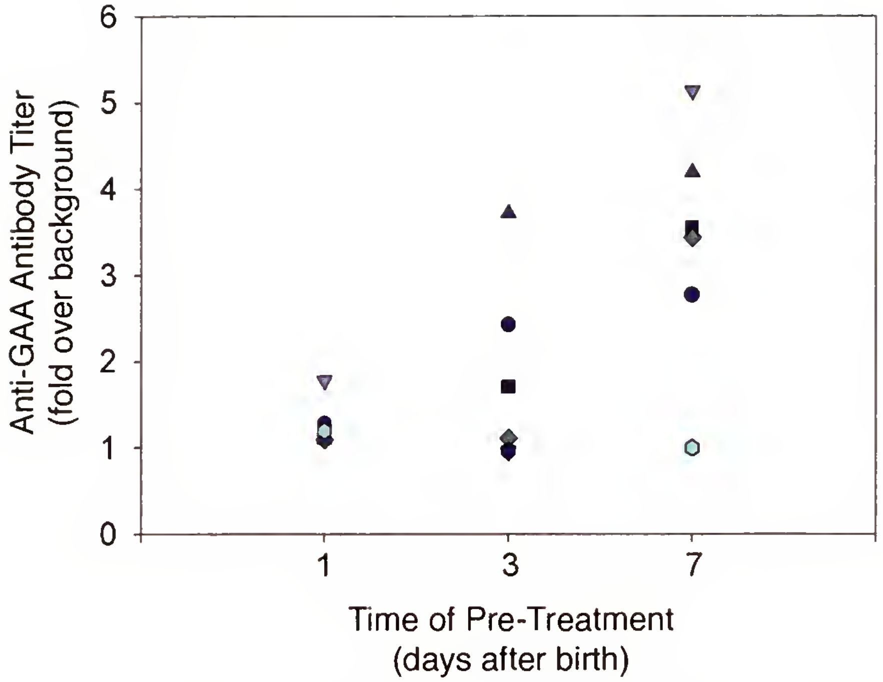

Figure 3-5. Anti-GAA antibody titer in *Gaa*$^{-/-}$ mice after pretreatment at different ages followed by rhGAA challenge. *Gaa*$^{-/-}$ mice were pretreated with 25 µg rhGAA at 1, 3, or 7 days after birth and subsequently challenged with 10 mg/kg rhGAA 8 wk later. Serum samples assayed were obtained 3 weeks post injection. Data points represent individual mice. Each group contains 6 data points.

Anti-GAA Antibodies in Treated Serum Inhibit GAA Activity *In Vitro*

Antibodies generated to a foreign protein can inhibit protein activity by a variety of mechanisms including binding of the active site, preventing uptake of the antigen-antibody complex at the receptor, and altering intracellular distribution. Alternatively, it is possible that antibodies can stabilize a foreign protein by increasing the half-life, or have no detectable effect at all (particularly at low antibody to antigen ratios). In effort to determine if anti-GAA antibodies observed in treated serum from *Gaa*$^{-/-}$ mice are inhibitory, an *in vitro* inhibition assay was performed (Figure 3-6). Recombinant hGAA was mixed at 4°C for 1 h with 1 of 5 different samples:

1. Serum from pretreated *Gaa*$^{-/-}$ mice after challenge with 10 mg/kg rhGAA
2. Serum from naive *Gaa*$^{-/-}$ mice after challenge with 10 mg/kg rhGAA
3. Serum from naive *Gaa*$^{-/-}$ mice after challenge with 5 mg/kg purified β-galactosidase

4. Serum from naive *Gaa*$^{-/-}$ mice (not challenged)
5. Serum-free DMEM (used for diluting all serum samples) alone.

After incubation, the rhGAA-serum or rhGAA-media mixture was added to HeLa cells. Cellular GAA activity was assayed 3.5 h after treatment. GAA activity in cells receiving rhGAA-serum treatment was normalized to cells receiving rhGAA-media alone. Due to the non-specific binding activity of serum, we expected a decrease in GAA activity after incubation with untreated serum when compared to cells treated with rhGAA-media alone. A 28 ± 4% decrease in GAA activity was observed after incubation with serum from untreated mice. In contrast, a 60 ± 5% decrease in GAA activity was observed after incubation with serum from naive *Gaa*$^{-/-}$ mice challenged with rhGAA (corresponding to an anti-GAA titer of approximately 15-fold background). Incubation with serum from pretreated *Gaa*$^{-/-}$ mice receiving the same protein challenge (determined to have background anti-GAA antibody titers) resulted in only a 26% ± 14% decrease in GAA activity, similar to that observed with control serum. To control for the presence of other immune-regulatory components generated from a humoral response to a foreign protein, serum from mice challenged with β-galactosidase was included as a negative control. These results demonstrate that the 15-fold background anti-GAA antibody titers observed in naive *Gaa*$^{-/-}$ mice after repeated rhGAA challenge, were sufficient to significantly inhibit GAA activity by approximately 30% *in vitro* (*P*=<0.01).

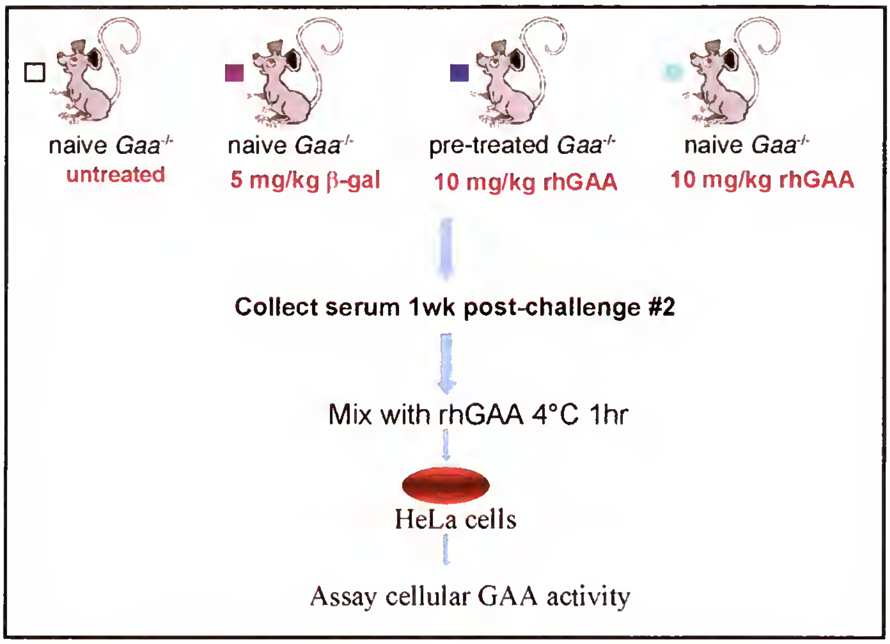

Figure 3-6. Diagram of *in vitro* GAA inhibition assay experimental design. The colored boxes correspond to the colored bars in Figure 3-7.

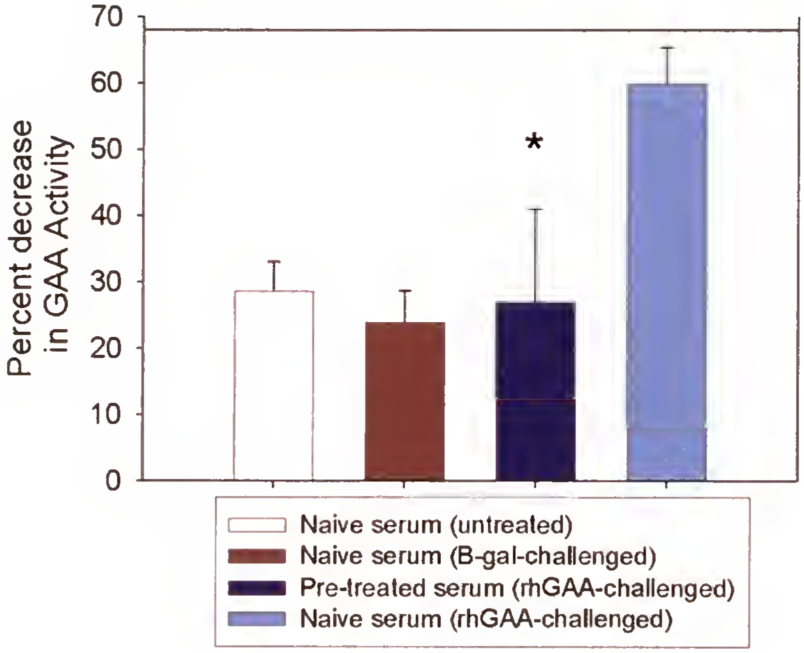

Figure 3-7. Affects of anti-GAA antibody-containing serum on GAA activity *in vitro*. Bars represent the decrease in GAA activity of HeLa cells after treatment with rhGAA mixed with serum relative to cells treated with rhGAA alone (n=3 wells). * $P=<0.05$

Discussion

For the purposes of evaluating the potential for intrahepatic rAAV-*hGAA* delivery to lead to systemic cross-correction in *Gaa*$^{-/-}$ mice without the interference of an anti-GAA humoral response, a tolerant *Gaa*$^{-/-}$ mouse model was generated by introduction of rhGAA antigen to neonatal *Gaa*$^{-/-}$ mice during a period of immunologic immaturity. Neonatal tolerance was first described in 1945 by Owen (93) and later demonstrated experimentally by Billingham *et al.* (9). Since these studies, the immunologic mechanism responsible for neonatal tolerance has remained controversial. Originally, it was believed that neonatal exposure to antigen results in clonal deletion and/or inactivation of T-cells. More recently, alternative mechanisms have been proposed including T-cell suppression, which could result in reversible tolerance, and immune deviation, leading to a skewed T helper2 (TH2) response (1,18,37). Multiple mechanisms may play a role in how neonatal tolerance is induced and could possibly depend on factors such as dose, route and immunogenicity of toleragen.

Neonatally pretreated *Gaa*$^{-/-}$ mice were shown to be 100% tolerant to hGAA after 2 injections of rhGAA at a dose that resulted in up to 100-fold over background anti-GAA antibody titers in naive *Gaa*$^{-/-}$ mice. While no signs of CMI were observed in these studies, we speculate that higher and more frequent doses would eventually lead to CMI as demonstrated by Raben *et al* (101) who observed 100% anaphylaxis after the 7th injection at a dose of 20 mg/kg.

We demonstrated that susceptibility to neonatal tolerization decreases between 1 to 7 days after birth. This is important for the use of this model in future studies evaluating rAAV-mediated treatment as inaccurate estimation of birth date by 1 or 2 days will likely skew results. Preliminary *in vitro* studies suggest that anti-GAA antibodies generated against rhGAA inhibit GAA activity. These results provide a rationale for further investigation of inhibiting anti-GAA immunity for successful gene transfer. The results from this study, however, provide no information as to the relationship between titer and degree of inhibition and what consequences the observed degree of inhibition will have on *Gaa*$^{-/-}$ mice. Determining how anti-GAA antibody formation will impact the ability to achieve cross-correction from liver-directed gene transfer will best be evaluated by comparing relative levels of GAA in distal tissues of treated naïve *Gaa*$^{-/-}$ mice versus treated tolerant *Gaa*$^{-/-}$ mice.

CHAPTER 4

AAV5-MEDIATED CROSS-CORRECTION OF GSDII: EFFECTS OF INHIBITORY ANTIBODY FORMATION AND IMMUNOMODULATION

Background

Achieving systemic correction in GSDII mice after liver-directed delivery of rAAV-*human GAA* (*hGAA*) will likely require high levels of liver-GAA expression along with inhibition of anti-GAA antibody formation. Previous experience with rAAV serotype 2 vectors encoding *hGAA* driven by the DHBV promoter resulted in superphysiologic levels of liver GAA activity with no biochemical correction of distally affected tissues. Recombinant AAV serotype 5 vectors have been shown to yield up to 10-fold greater liver transgene expression (82), however, our experience with rAAV-mediated delivery of hGAA under control of the hAAT promoter resulted in similar yet insufficient levels of liver GAA expression for cross-correction as with rAAV2. We therefore generated a rAAV vector using serotype 5 with the DHBV promoter driving expression of *human GAA*.

To address the obstacle of anti-GAA antibody formation observed in preliminary studies, we generated a tolerant *Gaa*$^{-/-}$ model by neonatal pre-treatment with low dose antigen. The anti-GAA humoral response to rhGAA, observed in naïve *Gaa*$^{-/-}$ mice, was abolished in the pretreated *Gaa*$^{-/-}$ mice. However, the affect of neonatal pretreatment on anti-GAA immunity to rAAV-derived hGAA has not been evaluated. We challenged tolerant *Gaa*$^{-/-}$ mice with rAAV5-DHBV-*hGAA* with the goal of achieving higher levels of liver GAA than previously observed; inhibition of anti-GAA antibody formation; and subsequent correction of the cardiac, respiratory and skeletal muscles. Naïve *Gaa*$^{-/-}$ mice were identically treated. Comparing outcomes in both the presence and absence of anti-GAA antibodies should answer important questions about the significance of anti-GAA humoral immunity and provide further information about the necessary approach toward clinical applications.

Materials and Methods

Cloning and Packaging of rAAV Constructs

Cloning of the pTR-DHBV-*hGAA* plasmid is described in chapter 2. The recombinant AAV5 vector (rAAV2 *rep* / rAAV 5 *cap*) was generated, purified and tittered (described in chapter 2) by the University of Florida Powell Gene Therapy Center Vector Core.

ELISA for Detection of Anti-GAA Antibodies

Serum samples were obtained weekly *via* tail bleed of anesthetized mice. Serum, diluted 1:80, was assayed for anti-GAA antibodies by ELISA (described in chapter 2). Results were standardized to serial dilutions of rabbit anti-human GAA antibody and reported as fold over background with background equal to the standardized value of serum from untreated *Gaa*$^{-/-}$ mice.

Animals

All mice were housed in the University of Florida SPF animal facility and all animal procedures were done in accordance with the University of Florida's Institutional Animal Care and Use Committee approval guidelines. The pretreated *Gaa*$^{-/-}$ mouse model was generated by subcutaneous delivery of 25 μg rhGAA at 1 day of age (described in chapter 3). Mice were treated at 10 wk of age with 5 x 10^{11} or 1 x 10^{12} vg rAAV5-DHBV-*hGAA via* portal vein delivery of rAAV as described in chapter 2. Age-matched C57B6/129 mice were used as controls.

Tissue Processing

Eight weeks post injection, animals were sacrificed and extracted tissues were immediately cut and frozen in liquid nitrogen. Skeletal muscle tissue was first crushed to a powder using a hemostat in liquid nitrogen prior to homogenization. Tissues were homogenized in sterile water with lysing matrix D using the Fast Prep Instrument (Qbiogene, Carlsbad, CA). Homogenized lysates were centrifuged to pellet the lysing matrix. Supernatants were subjected to three freeze-thaw cycles and centrifugation.

GAA Enzymatic Activity Assay

The enzymatic activity assay for GAA and the Bradford assay for total protein quantification were performed as described in chapter 2. Briefly, 20 μL of homogenized tissue lysate was added to one well of a black 96-well plate with 1.6 μL of 75mM 4-MUG (diluted in 38.4 μL of 200 mM sodium acetate, pH 3.6). After 1 h incubation at 37°C, the reaction was stopped with 200 μL of 0.5 M sodium carbonate (pH 10.7). Six standards of 4-MU ranging from 0 to 500 μm were used to generate the standard curve. Fluorescence was measured at 460 nm. Protein concentrations were determined using the Bio-Rad *DC* Protein Assay kit (Bio-Rad, Hercules, CA) according to the manufacturer's instructions. GAA activity was calculated as μM 4-MU /h/mg protein. Values are reported as percent of GAA activity in normal tissues from C57BL/6 / 129 mice (n=3) (processed and assayed at the same time) minus background.

Histological Detection of Glycogen

Tissues were fixed in 10% buffered formalin, embedded in paraffin and sectioned (4-μm thickness). For liver histopathology, paraffin-embedded liver sections stained with hematoxylin and counterstained with eosin were examined and scored for histopathology by a Veterinary Pathologist at the University of Florida Pathology Core Lab. For glycogen staining, paraffin-embedded muscle sections were stained with Periodic Acid Schiff (PAS) reagent for glycogen detection (Richard Allen, Kalamazoo, Michigan) according to the manufacturer's instructions and counterstained with toluidine blue. For immunohistochemistry, paraffin-embedded liver sections were immunostained, by the University of Florida Pathology Core Lab, using the Vectastain ABC Kit (Vector Laboratories, Burlingame, CA) as per manufacturer's instructions with the rabbit anti-human GAA antibody (1:10,000 dilution). Images were taken using a Zeiss Axioskop motorized Plus with Axiocam HR color camera. Relative transduction efficiency was determined as described by Nakai *et al.* (88). The number of positively stained cells and total number of cells were counted. Five fields of approximately 200 nuclei were counted for each section.

Determination of Vector Genome Copy Number

Quantitative PCR followed by chemiluminescent detection was performed as described by Mingozzi *et al.* (82). Briefly, using 1.25 μg genomic liver DNA as a template and biotinylated primers, co-amplification of a 2.1 kb region of the DHBV-human *GAA* DNA (5'-CCAACACATGCGCAATATCC and 5'-CCGGTCTCGTTGGTGATGAAA-3') and a 1.0 kb region of the endogenous *HPRT* gene (5'-GCTGGTGAAAAGGACCTCT-3' and 5'-CACAGGACTAGAACACCTGC-

3') was performed. In addition to the genomic DNA, standard controls included 0.01, 0.05, 0.1, 0.5 and 1.0 pg pTR-DHBV-human *GAA* plasmid DNA spiked into 1.25 µg genomic liver DNA from saline-treated *Gaa*$^{-/-}$ mice. All reactions were performed at the following conditions: hot start denaturation at 94°C for 5 min, followed by 30 cycles of denaturation at 94°C for 1 min, annealing at 57°C for 1 min, and extension at 72°C for 2 min. A final 10 min extension was done at 72°C. Products were separated by electrophoresis on a 1.0% agarose gel followed by transfer to a nylon membrane and visualized using the Southern-*Star*™ system (Applied Biosystems, Bedford, MA) as per the kit protocol. Densitometric analysis of resulting bands was performed using *Scion Image* Release Beta 4.0.2 software (Scion Corporation, Frederick, Maryland) and ratios of human *GAA/HPRT* band intensity were calculated. Gene copy numbers were estimated using the following calculations: Picrograms of *hGAA* cDNA used in the standards were converted to copies of *hGAA* per cell based on 1 pg of double-stranded DNA of 1000bp = 0.9×10^7 copies. Total copies in each standard were divided by the number of cells in the standard based on 1 cell = 15 pg DNA (71). A standard curve was generated using *hGAA/HPRT* mean pixel density ratio versus copies of human GAA per cell. Copies of human *GAA* in the samples were determined using the equation from the standard curve ($y = 0.464x + 0.20$, $R^2=0.973$).

RNA Isolation and Analysis of Human GAA Transcript

RNA was isolated using the Rneasy kit (Qiagen, Valencia, CA) according to the manufacturers instructions for RNA isolation from the respective tissue. The RNA was treated with DNAseI (Ambion, Austin, TX) for 1 h. First strand cDNA synthesis was primed from 2.5 µg of DNAseI-treated RNA using the First-strand cDNA Synthesis Kit

(Amersham Pharmacia Biotech) and 40 pmol of the reverse β-actin and human GAA primers described below. PCR amplification of a 270 bp region of the human GAA cDNA (1 μl) was done using the primer pair 5'-CCTTTCTACCTGGCGCTGGAGGAC-3' / 5'-GGTGATAGCGGTGGAGGAGTA-3'. A separate PCR reaction for amplification of a 300 bp region of the β-actin cDNA (1 μl) was performed under the same conditions using the following primer pair: 5'TCTAGGCACCAAGGTGTGAT-3' /5'- GTGGTACGACCAGAGGCATA-3'.

Immunoblot Detection of the Mannose 6-Phosphate Receptor

Protein concentrations of tissue lysates were determined by a standard Bradford assay using two dilutions of each lysate and performed in triplicate. Absorbance values were calculated using a standard curve from 8 serial dilutions of BSA. All values fell within the linear range of the standard curve. Tissue lysates (100 μg) were electrophoresed through a non-denaturing SDS-8% polyacrylamide gel and transferred to nitrocellulose membranes. The membrane was blocked for 1 h in 5% nonfat dry milk followed by three 10-min. washes. The membrane was probed with a 1:2500 dilution of a rabbit-anti-human M6P receptor antibody (gift of W. Dunn, University of Florida, Gainesville, FL) overnight at 4°C, washed and probed with a 1:10,000 dilution of horse radish peroxidase (HRP)-conjugated, donkey-anti-rabbit IgG secondary antibody (Amersham Pharamacia Biotech, Piscataway, NJ). After washing, hybridization was detected using the ECL Plus Western blotting detection system (Amersham Pharmacia Biotech).

Statistical Analysis

Unpaired t test and unpaired t test with Welch's correction (GraphPad Instat version 2.0, San Diego, CA) were used for statistical comparison between groups with statistical significance considered if $P<0.05$.

Results

Liver GAA Activity and Antibody Formation after Intrahepatic Delivery of rAAV(5)-DHBV-*hGAA* to Naïve *Gaa*$^{-/-}$ Mice

To evaluate the hepatic GAA expression levels obtainable under control of the DHBV promoter packaged in serotype 5, two doses of rAAV(5)-DHBV-*hGAA* were delivered to the portal vein of 10 wk old, female, naïve *Gaa*$^{-/-}$ mice. After low dose (5×10^{11} vg) delivery, liver GAA activity levels were 324% ± 17.5% of normal (normal) (Table 4-1). This level is 1.8-fold greater than the liver activity levels observed with the rAAV2-DHBV-*hGAA* vector at a 6-fold higher dose (3×10^{12}vg), which is consistent with observations by others (40,82) that hepatic transgene expression from rAAV5 is up to 10-fold greater than from rAAV2. Despite the presence of 3-fold normal hepatic GAA activity levels, there was no significant activity restoration in the affected distal tissues (heart, diaphragm and quadriceps).

After high dose (1×10^{12} vg) delivery of rAAV5-DHBV-*hGAA* to naïve *Gaa*$^{-/-}$ mice, 3-fold greater hepatic GAA activity levels were observed than from the low dose vector (930% ± 200% of normal; P=0.01) (Table 4-2). GAA activity was partially restored in the heart of 1 animal and the diaphragms of all 6 mice (Table 4-2). Like the low dose group, there was no significant activity observed in the quadriceps after high dose treatment. Because GAA activity levels in this group of mice receiving identical doses varied by 15-fold in the heart and 8-fold in the diaphragm, and because the immune response in naïve *Gaa*$^{-/-}$ mice is similarly heterogeneic, we hypothesized that the variability in GAA activities of distal tissues was, in part, determined by the heterogeneity of the anti-GAA immune response.

Antibodies to GAA were detected in 5 of 6 high dose-treated mice and 3 of 6 low dose-treated mice after intrahepatic delivery of rAAV(5)-DHBV-*GAA* to naïve *Gaa*$^{-/-}$ mice (Tables 1 and 2). The 3 non immune-responsive mice from the low dose group showed no significant cardiac activity (Table 1). On the other hand, the 1 non immune-responsive animal from the high dose group (#5) showed restoration to 28.7% of normal activity levels in the heart and was, in fact, the only high dose mouse to have therapeutic levels of cardiac activity (Table 2). Furthermore, while there was no diaphragm correction in any of the 6 low dose mice (Table 1), all 6 high dose mice showed some level of restored diaphragm activity (26% to 304%). Interestingly, the one non-immune-responsive mouse in the high dose group (#5) had 4-fold greater diaphragm GAA activity levels than the five that elicited an immune response (Table 2).

Table 4-1. Acid α-glucosidase activity and anti-GAA antibody titer 8 weeks after low dose vector delivery to naïve *Gaa*$^{-/-}$ mice.

Mouse	**Anti-GAA Ab titer (fold-background)**	**Percent of normal GAA activity**[a]			
		Liver	**Diaphragm**	**Heart**	**Quad.**
1	**16.5**	**304.3**	**6.8**	**1**	**0.0**
2	**1.0**	**354.3**	**NA**	**2.5**	**0.0**
3	**1.0**	**310.3**	**0.0**	**1.4**	**0.0**
4	**5.6**	**276.3**	**0.0**	**9.7**	**0.0**
5	**1.0**	**395.3**	**0.0**	**0.3**	**0.0**
6	**3.6**	**304.3**	**6.8**	**1**	**0.0**
mean	**4.8 ± 2.4**	**324 ± 17.5**	**2.7 ± 1.6**	**2.6 ± 1.4**	**0.0 ± 0.0**

[a] Background activity averaged from 3 saline-treated *Gaa*$^{-/-}$ mice was subtracted from all values.

Table 4-2. Acid α-glucosidase activity and anti-GAA antibody titer 8 weeks after high dose vector delivery to naïve $Gaa^{-/-}$ mice.

Mouse	Anti-GAA Ab titer (fold-over background)	Percent of normal GAA activity[a]			
		Liver	Diaphragm	Heart	Quad.
1	3.2	833.3	40.8	2.4	0.0
2	8.5	1403.3	26.8	0.0	0.0
3	1.9	1597.3	165.8	2.1	0.0
4	1.5	406.3	52.8	2.2	0.0
6	5.0	762.3	26.8	5.3	0.0
mean	4.0 ± 1.2	1000 ± 218	62.2 ± 26.2	2.4± 0.8	0.0 ± 0.0
5[a]	1.0	487.8	304.8	28.7	3.1

[a] Background activity averaged from 3 saline-treated $Gaa^{-/-}$ mice was subtracted from all values.

[b] Mouse 5 is separated from mice 1-4 to demonstrate difference in both antibody titer and GAA activity of diaphragm, heart and quadriceps.

Diaphragm GAA Levels are Dependent on Both Liver GAA Activity and Antibody Titer

Careful examination of liver and diaphragm GAA activities along with the respective antibody titers of individual mice reveals an important relationship. Graphical representation of diaphragm GAA activity as a function of either antibody titer or liver GAA activity alone resulted in no consistent trend. However, because the liver can be considered the source of the diaphragm GAA, the ratio of diaphragm activity was normalized to liver GAA activity and the result of graphing these values as a function of antibody titer is an exponential decay curve (Figure 4-1). This graph suggests both that the level of diaphragm cross-correction is dependent on liver GAA activity and antibody titer and, there is a small range of antibody titer where diaphragm correction is optimal. For example, diaphragm activity (normalized to liver activity) dropped by 5-fold between mouse 5 with a background antibody titer and mouse 4 with only a 1.5-fold over background titer. The effect of antibody titer on diaphragm correction is less dramatic at antibody titers of greater than 1.5-fold over background. Within this higher antibody titer range, we observed that substantially higher liver GAA levels can compensate for relatively high antibody titers. For example, high dose mouse 2 and mouse 6 achieved the same levels of diaphragm correction (26.8% of normal) with nearly 2-fold different liver GAA activity levels (14-fold and 7.6-fold over background respectively), and this is likely attributed to the nearly 2-fold lower anti-GAA antibody titer observed in mouse 6. (Table 4-2).

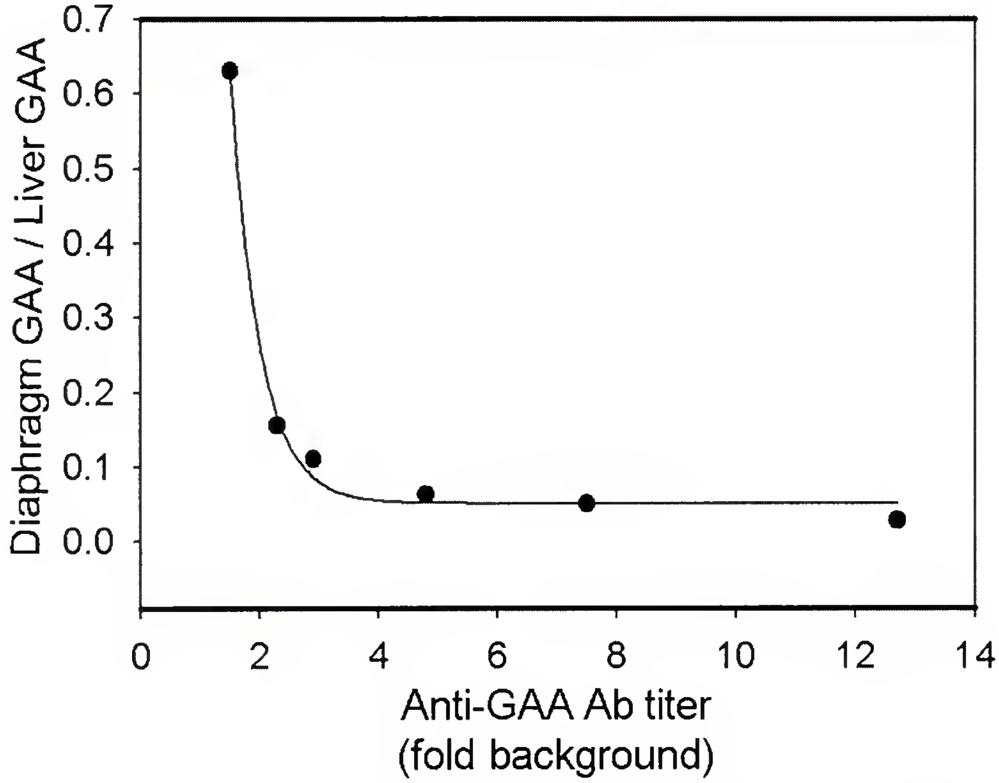

Figure 4-1. Exponential decay relationship between diaphragm activity normalized to liver activity versus anti-GAA antibody titer. Data points represent individual naïve *Gaa*$^{-/-}$ mice in the high-dose group. This relationship demonstrates the significant impact of very low antibody titers (1.5-fold background) on diaphragm activity.

Neonatally Pretreated *Gaa*$^{-/-}$ Mice do not Form Antibodies to rAAV-Derived hGAA after Low Dose Vector Delivery

Based on the previous studies suggesting that the presence of antibodies to hepatic-produced GAA inhibits correction of distal tissues, we repeated the experiment in a group of *Gaa*$^{-/-}$ mice that had previously been tolerized to human GAA protein by neonatal subcutaneous injection (described in chapter 3). Ideally, using a tolerized mouse model should provide more information regarding the relationship between dose, immune response, and correction in *Gaa*$^{-/-}$ mice. As in the initial experiment, neonatally pretreated mice received a high (1 x 10^{12} vg) or low (5 x 10^{11} vg) dose of rAAV5-DHBV-*hGAA via* the portal vein at 10 wk of age. Anti-GAA antibody formation was followed weekly for the duration of the study (Fig. 4-2). While 50% of naïve mice had background antibody titers after low dose delivery (Table 4-1), 100% of the pretreated mice had background antibody titers (Figure 4-2). Despite inhibition of the humoral response in all 4 low dose mice, we did not see any restoration of GAA activity in the heart, diaphragm, or quadriceps (Figure 4-5). This is consistent with data from the naïve group showing that the absence of an immune response in 3 of the 6 mice after low dose delivery also had no impact on correction outcome in any of the tissues examined despite having 300% to 400% of normal liver GAA levels.

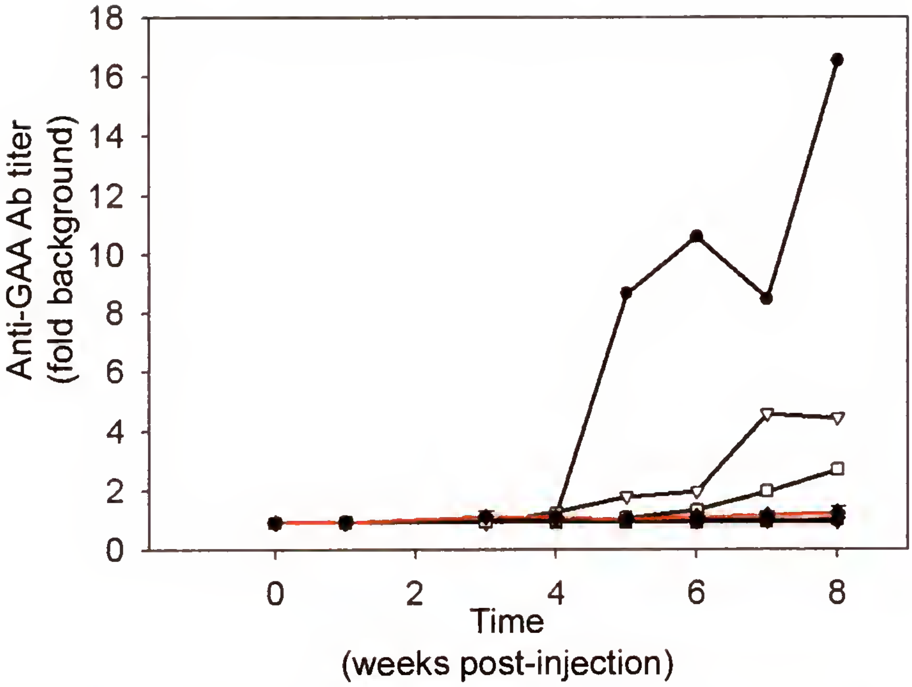

Figure 4-2. Anti-GAA antibody formation in naïve and pretreated *Gaa*$^{-/-}$ mice over time after low dose vector delivery. Black lines represent the 6 individual naïve *Gaa*$^{-/-}$ mice. The red line represents the mean and standard error of the mean of the 4 tolerized *Gaa*$^{-/-}$ mice.

Neonatal Tolerance is Broken after High Dose Delivery

The trend of anti-GAA antibody formation observed over time for all of the immune responsive mice described thus far is consistent with earlier experiments using a weaker rAAV-*hGAA* vector, where the most significant increase in antibody titer occurs between 4-5 weeks (Figure 2-2). This is not surprising based on the finding that transgene expression from an rAAV5 vector is not observed until 4 wk post injection (15,82) and formation of the primary immune response should follow within 4 to 7 days. The immune response in tolerized mice after high dose rAAV-*hGAA* delivery was different from the low dose tolerized group. Interestingly, after pretreatment of *Gaa*$^{-/-}$ mice and subsequent challenge with the high dose vector, we see a variation in the immune response among the 5 mice (Figure 4-3). Four of the 5 high dose mice elicited an immune response (Table 4-3). However, anti-GAA antibody formation in these mice was not detected until 6 to 8 wk post injection (1 to 3 weeks later than in naïve mice) suggesting the possibility of a break in tolerance (Figure 4-3).

In the pretreated group, high dose mouse 2 was the only 1 of 5 without antibody formation. This may be due to the heterogeneity of the immune response observed in the naïve mice (mouse 2 was naturally non-immune-responsive and would have not required tolerance) or this mouse was tolerized for the 8 wk duration of the study and tolerance may have been broken at a later time point. In the absence of any anti-GAA antibody formation, mouse 2 had the highest levels of biochemical correction in both the diaphragm (249%) and heart (110%). More importantly, this was the only mouse to show significant levels of GAA in the skeletal muscle with restoration to 72% of normal activity (Table 4).

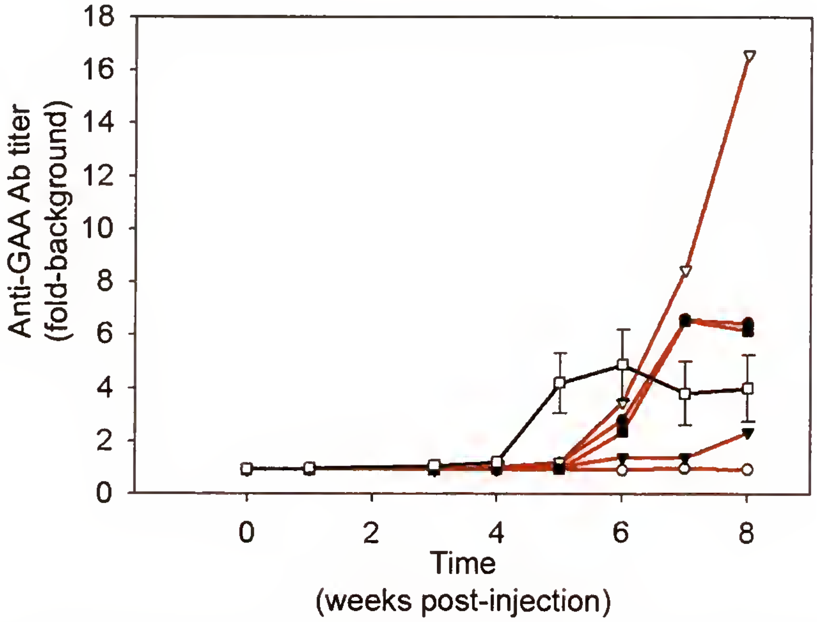

Figure 4-3. Anti-GAA antibody formation in naïve and pretreated $Gaa^{-/-}$ mice over time after high dose vector delivery. Red lines represent the 5 individual tolerized $Gaa^{-/-}$ mice. The black line represents the mean and standard error of the mean of the 6 naive $Gaa^{-/-}$ mice.

Among the high dose-treated mice from both the pretreated and naïve groups that elicited an immune response, there was overall higher level of GAA activity observed in distal tissues of pretreated mice (Figure 4-6). Higher liver GAA activities in these mice (1461% ± 160% versus 1000% ± 218% respectively; P=0.048) may have contributed to the higher average levels of distal tissue correction. However, comparison of individual pretreated and naïve mice with similar liver GAA activity levels and terminal antibody titer, yet significantly different levels of cardiac correction, suggests the role of an additional factor (such as the 1-3 week delay in antibody formation) (Tables 2 and 3).

The detailed analysis of individual mice represented on all 3 tables is represented as treatment groups in Figure 4-4. Due to the inability to successfully induce permanent tolerance in *Gaa*$^{-/-}$ mice to high dose (1 x 10^{12} vg) rAAV-derived human GAA, only 2 of 11 high dose-treated mice showed no antibody formation to rAAV-derived human GAA. However, these results show a clear relationship between absence of antibody formation and higher levels of activity in all three distal tissues examined (outliers in Fig. 4-5 represent single non-immune responsive animals).

Table 4-3. Acid α-glucosidase activity and anti-GAA Ab titer 8 weeks after high dose vector delivery to pretreated *Gaa*$^{-/-}$ mice.

Mouse	**Anti-GAA Ab titer (fold over background)**	**Percent of normal GAA activity**			
		Liver	**Diaphragm**	**Heart**	**Quad.**
1	**9.4**	1068.3	1189.8	39.9	2.1
3	**2.3**	1843.3	60.2	23	4
4	**16.6**	1396.3	244.6	49.2	4.7
5	**6.1**	1537.3	139.6	9.1	11.8
mean	8.6 ± 3.0	1461 ± 160	408 ± 263	30.3 ± 8.9	5.6 ± 2.1
2[b]	**1.0**	1646.3	2497.8	110.3	72.1

[a] Background activity averaged from 3 saline-treated *Gaa*$^{-/-}$ mice was subtracted from all values.

[b] Mouse 2 is separated from 1, 3-5 to demonstrate difference in both antibody titer and GAA activity of diaphragm, heart and quadriceps.

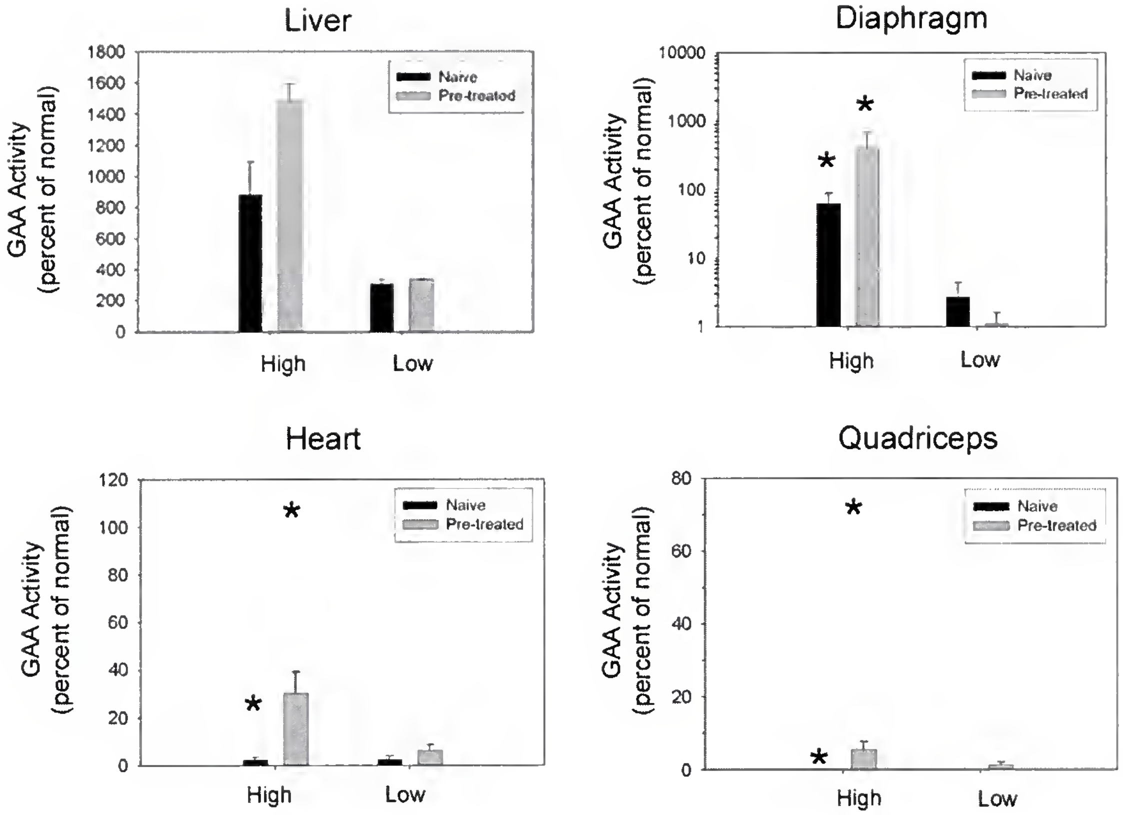

Figure 4-4. Summary of percent normal GAA activity 8 wk post delivery of rAAV5-DHBV-*hGAA* in the liver, diaphragm, heart and quadriceps of all high and low dose-treated mice from both the naïve and pretreated *Gaa*$^{-/-}$ groups. For the diaphragm, heart and quadriceps graphs, outlier symbols (*) represent the individual high dose mice from the naïve (mouse 5) and pretreated (mouse 2) groups that had background anti-GAA antibody titers. Bars represent mean (n=6 for both naïve groups, n=5 for high dose, pretreated group and n=4 for low dose, pretreated group) ± standard error of the mean. For the liver graph, all mice in each group were grouped together to determine the mean and standard error of the mean.

Lack of Cell-Mediated Immune Response After rAAV(5)-DHBV-h*GAA* Treatment

In order to further characterize the immune response to rAAV-derived hGAA, it was necessary to rule out a cell-mediated immune (CMI) response. To assess a potential CMI response, hemotoxylin and eosin (H&E)-stained liver sections were independently evaluated by the University of Florida Pathology Core for inflammatory responses.

Additionally, proliferation of rAAV-human GAA-treated splenocytes in response to rhGAA protein was measured. No signs of infiltration were observed on H&E-stained liver sections taken at sacrifice. Furthermore, there was an absence of proliferation of splenocytes from rAAV-DHBV-*hGAA*- treated mice after exposure to rhGAA compared to a 30-fold stimulation index after ConA exposure (not shown). These two assays, however, evaluate CMI in terminal tissues only and may not reveal an earlier response. Serum samples taken bi-weekly from rAAV-DHBV-*hGAA*-treated mice were assayed for the presence of IgG1, IgG2b and the Th1-indicating isotype IgG2a. We observed predominant levels of IgG1, followed by IgG2b and no detectable IgG2a (Figure 4-5) for the duration of the experiment suggesting a Th2 and not a Th1-mediated response.

As an alternative method to rule out the possibility of lower liver GAA activity levels being attributed to a CMI response, we estimated the vector genome copy number per cell using methods described by Mingozzi *et al.* (82) and looked for a correlation between copy number and terminal liver GAA activity. Liver DNA from high dose-treated mice was shown to have an average of 0.74 ± 0.05 vector genome copies per diploid genome (Fig. 4-6). Within the high dose-treated mice from both the naïve and pretreated groups, there was a strong correlation between copy number and liver GAA activity (*P*=<0.01) suggesting that relative levels of GAA activity in the transduced liver were more likely attributed to the varying degree of vector copy number per cell than to loss of activity due from a CMI response.

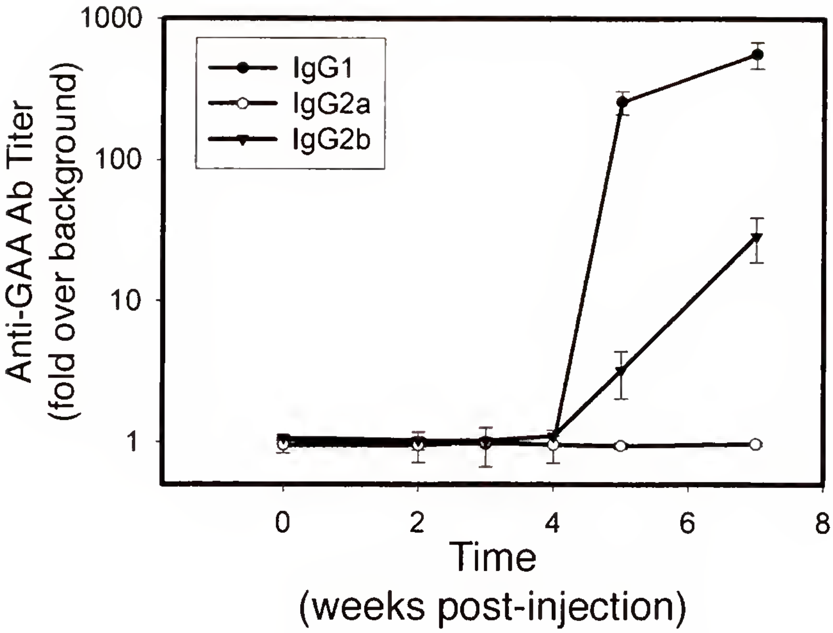

Figure 4-5. Isotype analysis of anti-GAA antibodies formed against rAAV5-derived hGAA. Symbols represent the mean ± standard error of the mean (n=3).

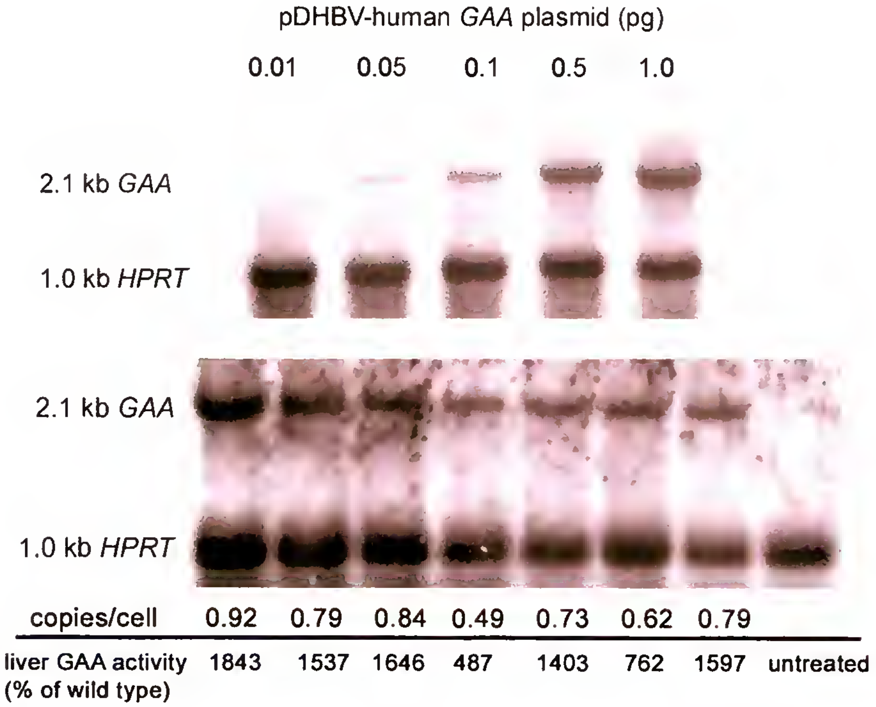
pDHBV-human GAA plasmid (pg)
0.01 0.05 0.1 0.5 1.0
2.1 kb GAA
1.0 kb HPRT
2.1 kb GAA
1.0 kb HPRT
copies/cell 0.92 0.79 0.84 0.49 0.73 0.62 0.79
liver GAA activity (% of wild type) 1843 1537 1646 487 1403 762 1597 untreated

Figure 4-6. Semi-quantitative analysis of rAAV5-*hGAA* vector genome copies per cell by Southern blot of *hGAA* and endogenous *HPRT* after chemiluminescent detection of PCR-amplified region of the vector.

Restoration of GAA Activity in Tolerized Mice Improves Glycogen Clearance

In order to evaluate whether the levels of GAA activity observed were sufficient for clearance of lysosomal glycogen, tissue sections were stained with Periodic acid-Schiff's reagent (PAS). On longitudinal muscle sections, relative amounts of glycogen can be determined by the overall intensity of the pink staining. The intensity of PAS positive staining is decreased to normal levels in the heart and quadriceps of pretreated mouse 2 (Fig. 7). This mouse had the highest levels of GAA activity in both tissues (110% in heart and 72% in quadriceps) (Table 3). After restoration to 49% of normal heart activity in pretreated mouse 4, there is no detectable difference in PAS staining (not shown). This is not surprising as the mice in this study were 3-months old (2-months past the age at which glycogen accumulation is first detected) and tissues were examined only 4 weeks after initiation of GAA expression.

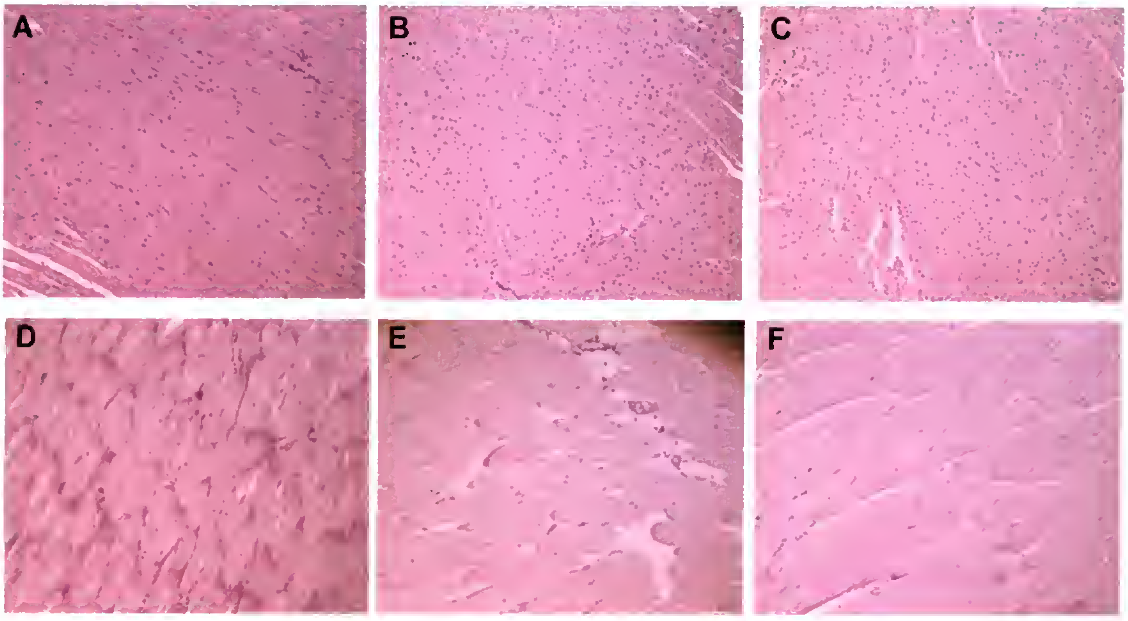

Figure 4-7. Detection of glycogen by PAS staining on longitudinal sections of cardiac and skeletal muscle. Tissues were harvested 8 wk post delivery of 1 x 10^{12} vg rAAV5-DHBV-*hGAA* and stained. Cardiac muscle is shown in A-C and quadriceps femoris muscle is shown in D-F. A and D represent an untreated, age-matched *Gaa*$^{-/-}$ mouse. B and E represent pretreated mouse 2. C and F represent an untreated, age-matched normal (C57BL6/129) mouse. Original magnification is 100X for A-C and 200X for D-F.

Human GAA Protein Observed in Corrected Tissues is Hepatic-Produced

To confirm that hGAA activity observed in distal tissues of high dose-treated mice is derived from hepatic-produced human GAA, RT-PCR of a 270 bp region of human GAA RNA was performed on corrected tissues from pretreated mouse 2 (shown), pretreated mouse 1 and naïve mouse 5. The resulting transcript was readily detected in liver RNA and was undetectable in RNA from heart, diaphragm and quadriceps (Fig. 4-8). More sensitive, quantitative RT-PCR experiments would exclude the possibility of leaky promoter activity in other tissues. However, these preliminary RT-PCR results suggest that GAA activity observed in distal tissues is liver-derived and this is consistent with the observed correlation between hepatic GAA activity and distal tissue activity after accounting for the immune response.

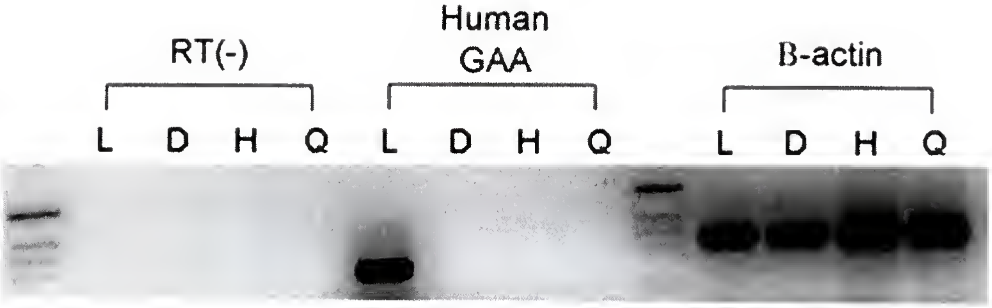

Figure 4-8. RT-PCR detection of rAAV5-delivered hGAA RNA in liver (L), Diaphragm (D), Heart (H) and Quadriceps (Q) by RT-PCR. Reverse transcription of β-actin was performed as an internal control. RT-PCR of human GAA in the absence of the reverse transcriptase enzyme was performed to control for DNA contamination in the RNA preparation.

Assessment of Hepatic Transduction Efficiency

Successful inhibition of the anti-GAA immune response may be beneficial only if sufficient levels of hepatic-GAA are produced. As only approximately 10-20% of GAA is secreted for uptake by distal tissues and high levels of activity are required for reversal of glycogen accumulation, systemic correction will rely heavily on the ability to maximize hepatic expression at both the levels of gene expression and cell transduction. In effort to begin characterizing the transduction efficiency of the vector used in these, the percentage of human GAA-expressing hepatocytes was estimated by immunohistochemical staining of liver sections from treated mice followed by cell counting as described by Nakai *et al.* (88) (Figure 4-10). In high dose-treated livers, 86% ± 2.5% (78-93%) of total hepatocytes stained positive for human GAA. This number closely reflects the vector copy number per cell data for high dose-treated mice (Fig. 6B) showing 0.74 ± 0.05 copies per cell. In low dose-treated livers, we observed 29% ± 1.3% (26-32%) of positive cells. This 3-fold difference in GAA-expressing cells between the high and low dose groups correlates with the 3-fold difference in liver GAA activity observed (Table 1 and 2).

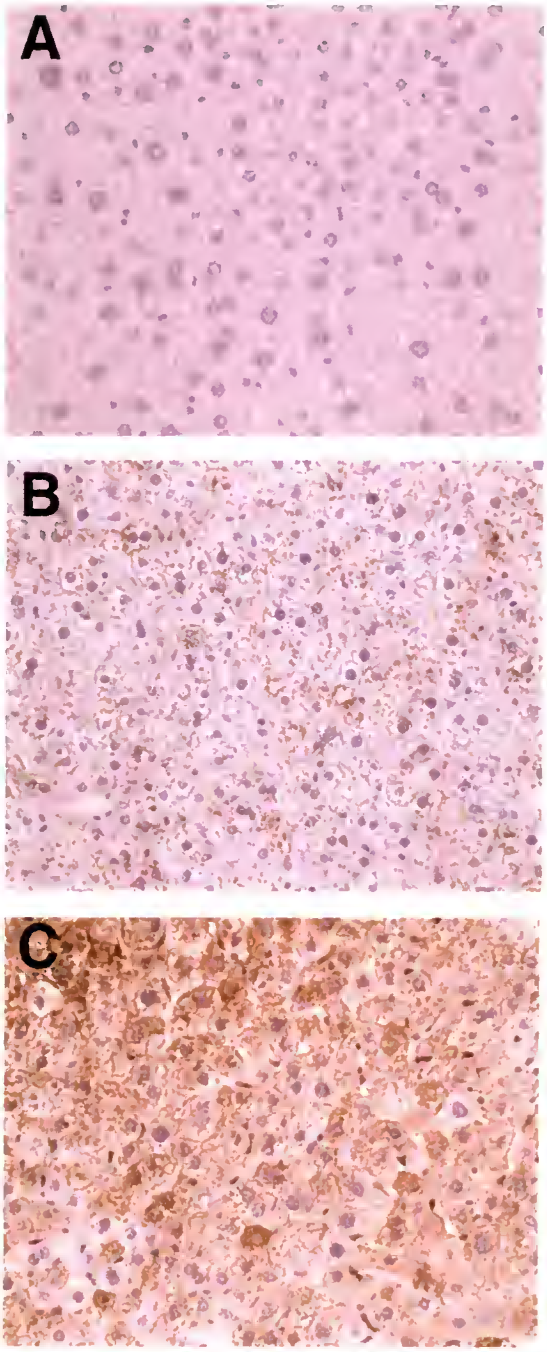

Figure 4-9. Immunhistochemical detection of human GAA-expressing hepatocytes of (A) saline-treated *Gaa*$^{-/-}$ mouse, (B) low dose-treated *Gaa*$^{-/-}$ mouse (naïve 1), and (C) high dose-treated *Gaa*$^{-/-}$ mouse (naïve 2). Original magnification is 400X.

Poor Correction of Quadriceps Correlates with Lower Levels of Mannose 6-Phosphate Receptor

The differences in the ability to correct diaphragm versus cardiac versus ambulatory muscles has been observed in enzyme replacement therapy studies in the *Gaa*$^{-/-}$ mouse model (101) and is recapitulated in these rAAV-mediated gene replacement studies. One likely explanation is the difference in the M6P receptor population. After examining M6P amounts (relative to total protein) in the diaphragm, heart, and quadriceps by immunoblot, we find lower levels in the quadriceps than in the heart and diaphragm (Fig. 4-10). Based on the cross-correction results of this study, we would expect to see higher relative M6P receptor levels in the diaphragm than in the heart. Other factors may influence diaphragm correction, such as the high surface area and vascularity to mass ratios, allowing for maximal exposure to and uptake of circulating GAA. While more sensitive assays need to be performed to look at M6P receptor expression levels, the Immunoblot analysis data does suggest that the reason for varying susceptibility to correction in the three tissues examined may be, at least partially, due to the receptor availability.

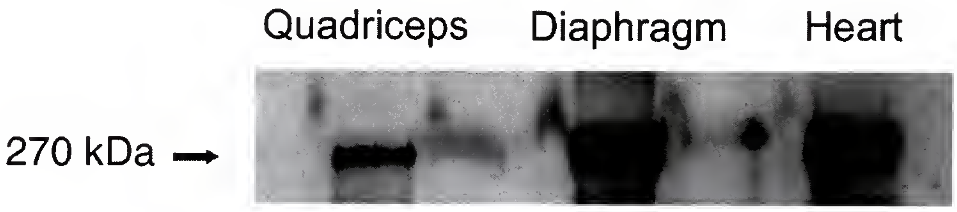

Figure 4-10. Immunodetection of the 220-kDA mannose 6-phosphate receptor in the quadriceps, diaphragm and heart tissue lysate (100 µg) from 4 wk-old *Gaa*$^{-/-}$ mice.

Discussion

Impact of Immune Responses to Intrahepatic Delivery of rAAV-hGAA

Earlier studies evaluating cross-correction after rAAV-*hGAA* delivery to *Gaa*$^{-/-}$ mice led to local correction without correction of distally affected tissues. These results were likely attributed to both insufficient hepatic GAA expression and anti-GAA antibody formation. Using the high expressing, rAAV5-DHBV-*hGAA* vector we were able to observe, for the first time, restoration of proposed therapeutic levels of GAA in the heart, diaphragm and quadriceps of *Gaa*$^{-/-}$ mice after intrahepatic delivery of a rAAV vector.

At a high dose (1 x 10^{12} vg), the rAAV5-DHBV-*hGAA* vector produced between 4-fold to 16-fold normal hepatic GAA levels in naïve *Gaa*$^{-/-}$ mice, whereas the low dose produced 2.7-fold to 3.5-fold normal levels. These results correlated with the percentage of GAA-expressing hepatocytes. Upon closer examination, similar liver GAA activities observed in the higher expressing low dose mice and the lower expressing high dose mice could not be accounted for by the 2-fold difference in dose. However, as these values represent terminal activity values only (8 weeks post injection), more significant variation may have occurred between 4 to 7 weeks post injection, particularly if the kinetics of expression are dose-dependent.

In the high dose-treated naïve *Gaa*$^{-/-}$ group, the one mouse that failed to elicit an immune response had the highest level of GAA activity in distal tissues, despite having the lowest hepatic GAA activity. The naïve *Gaa*$^{-/-}$ mice that did elicit an immune response to rAAV-derived human GAA had varying levels of diaphragm correction, and these levels correlated with both the anti-GAA antibody titer and hepatic GAA activity.

The variability in hepatic GAA activity levels between mice receiving high dose vector is likely due to the observed range in vector genome copy number. The variegated immune response within both the high and low dose groups is likely attributed to unidentified modifier genes in the mixed background of the *Gaa*$^{-/-}$strain. A better understanding of how both hepatic GAA expression levels and immune response cooperate to impact cross-correction can be gained from controlling for the variability in at least one of these two parameters.

We attempted to control for the immune response by tolerizing *Gaa*$^{-/-}$ mice to human GAA protein using a model of neonatal tolerance. The failure to successfully induce tolerance in *Gaa*$^{-/-}$ mice was surprising as preliminary studies testing this method of tolerance by challenge with rhGAA protein resulted in complete tolerance in 8 out of 8 mice. One potential explanation for a break in tolerance in 4 of the 5 pretreated mice is greater overall immunogenicity of rAAV-derived human GAA versus direct enzyme delivery. This theory is unlikely as anti-GAA antibody titers were approximately 6-fold over background after high dose delivery versus the 100-fold over background titer observed after direct enzyme delivery.

A second possible explanation would involve the difference in time lapse between pre-treatment and protein challenge (8 weeks) versus pre-treatment and vector challenge (10 weeks). If neonatal tolerance was occurring by T-cell suppression or inactivation, and not deletion, it is possible that the absence of a stimulus for a sustained period of time can re-activate suppressed or inactivated T-cells. A protocol involving multiple injections of toleragen throughout the first two weeks may have been required to sustain tolerance as demonstrated by others (31,32). Conversely, it is possible that neonatal antigen exposure primed the TH2 response, as observed by others (37) prior to vector delivery. If this were the case, we would have expected to see significantly higher antibodies titers at the same time or earlier as in naïve *Gaa*$^{-/-}$ mice. A 2.5-fold higher antibody titer was observed in 1 of the 4 pretreated mice that elicited an immune response, however, this difference is within the range of variability observed within treatment groups and is therefore not to likely a relevant indicator of T-cell priming.

A third potential explanation would involve structural differences between the directly infused rhGAA and the vector-produced, hepatic-secreted hGAA protein. While the amino acid sequence of the hGAA used in both the transfection of CHO-cells to produce rhGAA and in the rAAV vector are identical, post-translational modifications of GAA in CHO cells versus murine liver cells may vary. Additionally, pharmacological modifications were made in the development of rhGAA to increase the degree of phosphorylation for more efficient receptor-mediated uptake of circulating GAA.

Biochemical and Histological Assessment of Cross-Correction

Along with developing a further understanding of the immune response to hepatic-secreted human GAA, we also wanted to assess the feasibility of rAAV-mediated cross-correction from the liver for the treatment of GSDII. We were able to demonstrate GAA activity levels that were > 20% of normal in the diaphragms of 100% of high dose-treated mice. We were also able to achieve these proposed therapeutic levels of GAA activity in the hearts of 45% of high dose-treated mice and the quadriceps of one mouse.

The relationship between percent restoration of activity and ability to clear lysosomal glycogen after short-term studies in the mouse model is not yet fully understood. While 100% normal heart activity resulted in obvious reduction in positive PAS staining for glycogen, 50% normal heart activity levels led to no detectable improvement. Due to difficulties in processing of diaphragm sections, histochemical staining of the treated diaphragms is not available. However, Mah *et al.* (72) demonstrated near complete reversal of glycogen accumulation in the diaphragm with 120% normal GAA activity levels obtained 6-weeks after direct delivery of rAAV-*GAA* to the diaphragms of the same *Gaa*$^{-/-}$ mouse model. A better understanding of the relationship between age of treatment, levels of activity restoration and ability to reduce accumulated lysosomal glycogen in different tissues will be necessary for both outcome assessment during clinical trials and further defining corrective levels for *Gaa*$^{-/-}$ mice.

The more stringent requirements for correction of the quadriceps and potentially other skeletal muscles may be attributed to decreased levels of M6P receptor in hind-limb skeletal muscles versus the cardiac and diaphragm muscle. Raben *et al.* (101) suggested that, in skeletal muscle, type I fibers (slow-twitch) have greater levels of M6P receptor than type II (fast-twitch). The diaphragm predominately consist of type I fibers, and cardiomyocytes behave more like type I than type II skeletal muscle fibers. However, the quadriceps are a mixture of type I and type II fibers. Examining the ability to correct different types of skeletal muscles to confirm this theory will be beneficial for future cross-correction studies.

Summary

In summary, we showed that the immune response to rAAV-derived *hGAA* in naïve *Gaa*$^{-/-}$ mice is inhibitory. We found that in naïve *Gaa*$^{-/-}$ mice, a high dose (1×10^{12} vg) of vector is required for diaphragm correction. Additionally, we observed that diaphragm correction is primarily dependent on antibody titer; presence of relatively low antibody titers can substantially decrease GAA activity levels in the diaphragm. However GAA activity can still be restored in the diaphragm in the presence of antibodies provided sufficient levels of liver GAA activity levels are present. Correction of the heart and quadriceps was only observed after high dose delivery in the absence of antibodies. While myopathies of the cardiac and diaphragm muscles are the most threatening to Pompe patients, correction of the functional, anti-gravity muscles (including quadriceps) would greatly improve the quality of life in patients once cardiac and diaphragm muscle function is improved.

Achieving the higher levels of liver GAA expression that will be necessary for systemic muscle correction may be possible with a higher dose. However, using rAAV serotype 2, Nakai *et al.* (88) showed saturation of precent hepatocyte transduction and a loss of a linear dose-response in number of vector genomes per hepatocyte at a dose of 1.8×10^{12} vg. Alternative serotypes will be investigated to improve overall level of hepatic GAA activity. Additionally, an alternative tolerant GSDII model will be necessary to fully evaluate the potential for correction of GSDII in the absence of an immune response.

CHAPTER 5
DEVELOPMENT AND CHARCTERIZATION OF A GSDII MOUSE MODEL THAT CONDITIONALLY EXPRESSES HUMAN GAA

Background

In order to effectively evaluate the therapeutic potential for liver-directed, rAAV-mediated cross-correction of GSDII, a truly tolerant GSDII mouse model will be necessary. Previous attempts to generate a tolerant model involved a method of subcutaneous, low-dose delivery of recombinant human GAA protein (rhGAA) to 1 day-old mice. This method of tolerance resulted in complete inhibition of anti-GAA antibody formation in adult mice after challenge by intravenous delivery of rhGAA. However, after challenge with a high-expressing rAAV-*hGAA* vector, tolerance failed to be induced or was only temporarily induced. There are many possible explanations for the variation in ability to induce tolerance to the two different treatments, all of which involve the inability to successfully tolerize by clonal T-cell deletion.

We generated an alternative model of hGAA tolerance using the same exon 6 knockout $Gaa^{-/-}$ mouse model. This model (skin-*hGAA* / $Gaa^{-/-}$) has the identical $Gaa^{-/-}$ genotype as previously described and expresses tetracycline-regulatable human *GAA* under control of the keratin5 promoter. The ability to induce low-level, transient expression during embryonic development confers complete tolerance in adult mice to hGAA protein. Furthermore, this low level of *hGAA* expressed in limited tissues does not alter the muscle biochemical or histological phenotype characteristic of $Gaa^{-/-}$ mice that recapitulates the GSDII pathophysiology. Generating the skin-*hGAA* / $Gaa^{-/-}$ line was done by crossing *Gaa*$^{-/-}$ mice transgenic for the human *GAA* cDNA under control of the tetracycline response element (TRE) to mice expressing the tetracycline-controlled transcriptional activator, *tTA* (which binds TRE in the absence of tetracycline), under control of the keratin5 promoter. These studies describe the genetic, biochemical and immunologic characterization of the skin-*hGAA* / *Gaa*$^{-/-}$ mice that will be used as an alternative tolerant GSDII model for assessment of future cross-correction mediated gene replacement and potentially enzyme replacement therapies.

Materials and Methods

Generation of the Transgenic Skin-*hGAA* / *Gaa*$^{-/-}$ Strain

All mice were housed in the University of Florida SPF animal facility and all animal procedures were done in accordance with the University of Florida's Institutional Animal Care and Use Committee approval guidelines. *Gaa*$^{-/-}$ mice transgenic for the human GAA cDNA under control of the tetracycline response element (Tre-*hGAA* / Gaa$^{-/-}$) were provided by and generated in collaboration with N. Raben (NIH, Bethesda, MD) (102). The keratin5-tTA (K5*tTA*) transgenic line maintained on the FVB background was generated and provided by A. Glick (NCI, Bethesda, MD) (26). The K5*tTA* strain was first crossed to *Gaa*$^{-/-}$ mice for two generations to yield K5*tTA*$^{+}$ / *Gaa*$^{-/-}$ mice. Mice that were PCR-positive for *K5tTA*$^{+}$ and *Gaa*$^{-/-}$ were crossed to the Tre-*hGAA*$^{+}$/ *Gaa*$^{-/-}$ strain to generate K5*tTA*$^{+}$/ TRE-*hGAA*$^{+}$ / *Gaa*$^{-/-}$ mice (referred to as skin-*hGAA* / *Gaa*$^{-/-}$). A schematic of the crosses is shown in Figure 5-1.

Doxycycline Administration

To expose mice to the tetracycline derivative, doxycycline, mice were fed mouse chow formulated with 200 mg/kg doxycycline (# S3888, Bio-Serv, Frenchtown, NJ). Based on the assumption that a mouse eats 5g of food per day, these formulations result in approximately 1 mg of doxycycline per day. A schematic of the tetracycline-regulated gene expression system is shown in Figure 5-1.

Genotyping of Transgenic Lines by PCR

Tail clips were taken from mice at 3 to 4 weeks of age and DNA was isolated using the Qiagen DNeasy kit (Qiagen, Valencia, CA) according to the manufacturer's instructions. A 1 kb region of the *tTA* gene, 1 kb region of the *hGAA* gene and the exon 5-7 region of the *Gaa* gene were PCR-amplified from 100 ng genomic tail DNA. Due to the exon 6 *neo* insertion, the heterozygous *Gaa* genotype results in two bands after amplification of a region containing exons 5 to 7 (the wild type band at 0.7 kb and the mutant GAA band at 2.0 kb). The homozygous mutant genotype results in one band at 2.0 kb. The following primer pairs were used: tTA5'/tTA3 (5'-TGATTAACAGCGCATTAGA-3' / 5'-CCCACCGTACTCGTCAA-3'); minCMV/hGAA1744 (5'-CGTTTAGTGAACCGTCAG-3' / 5'-AAGGAACTGGTCCGCAA-3') and Gaa exon5/Gaa exon 7 (5'-CCTTTCTACCTGGCACTGGAGG-3' / 5'-GGACAATGGCGGTCGAGGAG-3'). All reactions were performed separately. PCR conditions were as follows: hot start denaturation at 94°C for 3 min, followed by 30 cycles of denaturation at 94°C for 1 min, annealing for 1 min (at 60°C for the *tTA* and *Gaa* PCR and 51°C for the *hGAA* PCR), extension at 72°C for 2 min and a final 10 min extension at 72°C. PCR products were separated by electrophoresis on a 1% agarose gel.

GAA Staining of Tail Snips and Skin

GAA expression can be detected in tissues by staining with the chromogenic substrate for GAA, 5-bromo-4-choloro-3-indolyl-α-D-glucopyranoside (X-Gluc, Calbiochem, San Diego, CA). X-Gluc was prepared as a 1 mg/mL solution in PBS with 0.25 mM potassium ferriccyanide, 0.25 mM potassium ferrocyanide, and 1 mM magnesium chloride, pH 3.6. Tail snips were rinsed in PBS and placed in a 1.5 mL tube with 0.3 mL X-Gluc. Tubes were covered in aluminum foil and visualized 24 h later. For X-Gluc staining of skin, a depilatory cream was applied to the area of the skin to be removed for 3-5 min prior to sacrifice. The cream and excess hair were removed with gauze. After sacrifice, a small section of the skin was cut and placed into a dish containing PBS for 10 min to rinse off remaining cream and hair. The skin was transferred to a dish containing 1 mg/mL X-Gluc. The dish was covered in aluminum foil and visualized 24 h later.

Tissue Processing

At the time of sacrifice, tissues were extracted and immediately cut and frozen in liquid nitrogen. Skeletal muscle tissue was first crushed to a powder using a hemostat in liquid nitrogen prior to homogenization. Tissues were homogenized in sterile water with lysing matrix D using the Fast Prep Instrument (Qbiogene, Carlsbad, CA). Homogenized lysates were centrifuged to pellet the lysing matrix. Supernatants were subjected to three freeze-thaw cycles and centrifugation.

GAA Enzymatic Activity Assay

The GAA activity assay and the Bradford assay for quantification of total protein were performed as described in chapter 2. Briefly, 20 μL of homogenized tissue lysate was added to one well of a 96-well plate with 1.6 μL 75mM 4-MUG diluted in 38.4 μL of 200 mM sodium acetate (pH 3.6). After 1 h incubation at 37°C, the reaction was stopped with 200 μL of 0.5 M sodium carbonate (pH 10.7). Six standards of 4-MU ranging from 0 to 500 μm were used to generate the standard curve. Fluorescence was measured at 460 nm. Protein concentrations were determined using the Bio-Rad *DC* Protein Assay kit (Bio-Rad, Hercules, CA) according to the manufacturer's instructions. Values are reported as units/mg (μM 4-MU/hr/mg protein).

Intravenous Protein Delivery

Intravenous delivery of recombinant human GAA was performed as described in chapter 3. Briefly, mice were anesthetized *via* intraperitoneal delivery of avertin. After removing hair, a small incision was made in the skin and rhGAA was injected at a dose of 10 mg/kg (diluted to a total volume of 100 μL in 0.9% saline) using a 0.5 cc insulin syringe. The incision was closed and analgesics were delivered subcutaneously.

ELISA for Detection of Anti-GAA Antibodies

Serum samples were obtained weekly *via* tail bleed of anesthetized mice. Serum, diluted 1:80, was assayed for anti-GAA antibodies by ELISA as described in chapter 2. Results were standardized to serial dilutions of rabbit anti-human GAA antibody and reported as fold over background with background equal to Ab titer in untreated *Gaa*$^{-/-}$ mice.

Results

Generation of Skin-*hGAA* / *Gaa*$^{-/-}$ Mice

Three generations of crosses were performed before obtaining skin-*hGAA* / *Gaa*$^{-/-}$ mice. We expected these mice to express the human *GAA* gene in specific keratin-containing tissues in the absence of doxycycline (Dox) (Figure 5-1A). To first generate

K5-*tTA*$^{+}$ / *Gaa*$^{+/-}$ mice, K5*tTA*$^{+}$ mice were crossed with *Gaa*$^{-/-}$ mice (Figure 5-1B). Subsequent F1 crosses resulted in approximately 20-30% of mice that were PCR positive for both K5-*tTA* and the homozygous knockout *Gaa* genotypes. These mice were crossed to the TRE-*hGAA*$^{+}$ / *Gaa*$^{-/-}$ strain to yield approximately 20-30% of mice PCR positive for all 3 required genotypes: K5-*tTA*$^{+}$, TRE-*hGAA*$^{+}$ and *Gaa*$^{-/-}$. Tail snips of the first generation of mice that were shown to be skin-*hGAA*/*Gaa*$^{-/-}$ by PCR were stained with the chromogenic substrate for GAA, X-Gluc, to determine if the expected phenotype would be observed without having to sacrifice the animals (Figure 5-2). Because mice were first crossed to the *Gaa*$^{-/-}$ background, all mice that were PCR positive for both K5*tTA* and TRE-*hGAA* should synthesize *hGAA* in the skin and hair follicles with no background murine Gaa. All *Gaa*$^{-/-}$ mice that were shown to be positive for both K5-*tTA* and TRE-*hGAA* by PCR were also positive for GAA expression on the surface of the tail, as was determined by the blue-green color of the X-Gluc solution. Mice that were only single positives by PCR resulted in no change in the yellow X-Gluc color (Figure 5-2).

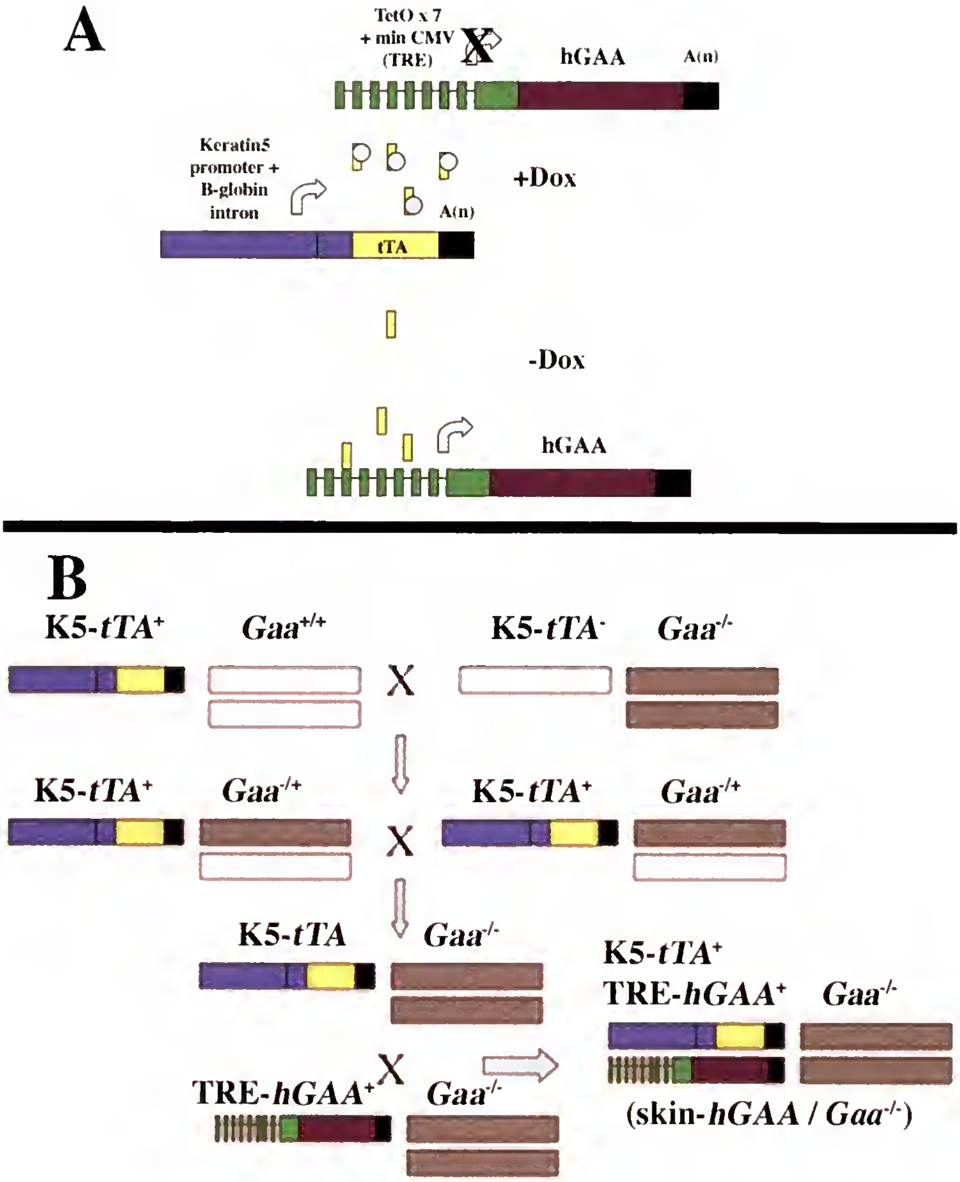

Figure 5-1. Schematics of the tetracycline-mediated gene regulation system (tet-off) and breeding strategy. (A) In the absence of Dox, the tetracycline transactivator is able to bind the tetracycline response element (TRE), which consist of 7 repeats of the tet-operator sequence upstream of a minimal TATA sequence of the CMV promoter. Activation of the TRE results in *hGAA* transcription only in tissues where *tTA* is expressed. When Dox is added to the system, it binds the tTA protein preventing activation of the TRE and resulting in inhibition of *hGAA* transcription. (B) Breeding strategy for generation of skin-*hGAA*/*Gaa*$^{-/-}$ mice. Grey boxes represent mutant *Gaa* allele and white boxes indicate wild-type *Gaa* allele. Colored boxes correspond to those in (A). Blue and yellow boxes represent the K5-*tTA* genotype and green and purple boxes represent the TRE-*hGAA* genotype. Because the genotyping methods do not detect zygosity, only one box is shown for these two genotypes.

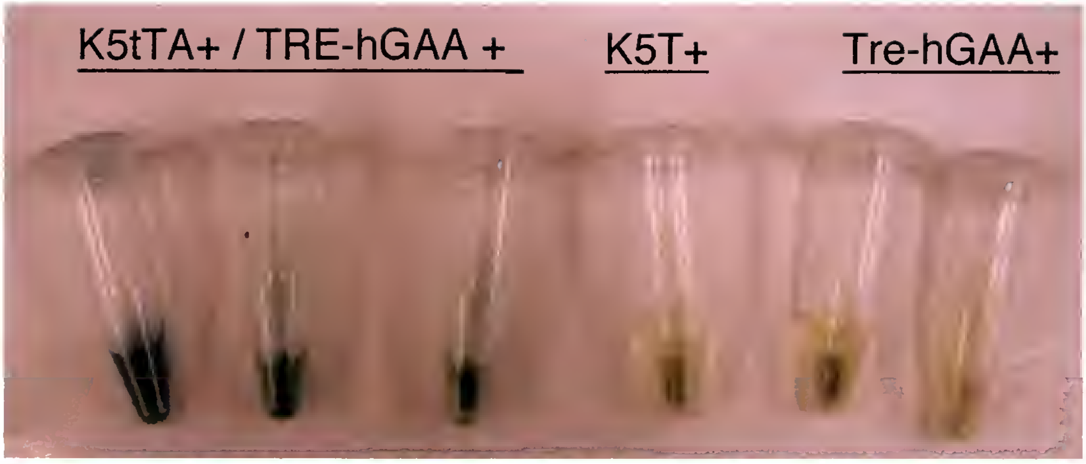

Figure 5-2. X-Gluc detection of GAA on tails of mice after PCR determination of genotype. Blue-Green color indicates positive GAA staining. Samples shown are from a representative litter.

Human GAA Transcript Detected in Skin, Spleen and Stomach

Once the skin-*hGAA / Gaa*$^{-/-}$ line was established, we assayed 9 tissues from 4 wk-old skin-*hGAA / Gaa*$^{-/-}$ mice with no previous exposure to Dox for the presence of human GAA transcript by RT-PCR (Figure 5-3A). We were primarily concerned with transcript activity in the liver and muscle tissues, as this would prevent accurate analysis of rAAV-mediated treatment. The keratin5 promoter is expressed in stratified squamous epithelial cells in tissues such as the skin, eye, cervix, stomach and esophagus. Non-squamous bilary epithelium is present in the liver but contains predominately Keratin19 and not Keratin5. No keratin expression is observed in muscle (90). Along with the 4 tissues of interest (liver, diaphragm, heart and quadriceps), the skin, spleen, and stomach were also assayed as these tissues were shown to have promoter activity from the keratin5 promoter in a similar transgenic model expressing skin-specific β-galactosidase in the absence of Dox (26). Human GAA transcript was detected predominately in the skin followed by the spleen and minimally detected levels in the stomach as well. As expected, there was no human GAA transcript detected in the liver, diaphragm, heart or quadriceps of skin-*hGAA* / *Gaa*$^{-/-}$ mice.

GAA Activity Detected in All Examined Tissues

While GAA expression was detected only in keratin5-expressing tissues, we expected to see GAA activity in all examined tissues as the skin is the largest organ in the body and highly efficient at protein secretion. Ten tissues from 4 week-old skin-*hGAA* / *Gaa*$^{-/-}$ mice with no previous exposure to Dox were assayed for GAA activity. GAA activity was highest in the skin, spleen and stomach (1015, 387 and 563 units/mg over background respectively) (Figure 5-3B). Tissues with no detectable GAA transcript also showed high levels of activity compared to *Gaa*$^{-/-}$ mice (Figure 5-3C). Interestingly, in the transcript (-) tissues, the highest levels of expression were observed in the quadriceps followed by lower levels in the diaphragm and significantly lower levels in the heart. This is inconsistent with the receptor availability hypothesis suggesting that the lower M6PR levels in the quadriceps (compared to the diaphragm and heart) observed by us (Figure 4-10) and others (101) is the primary reason for lower levels of cross-correction in the quadriceps. It is possible that the amount of hGAA secreted by the *hGAA*-expressing cells in the skin-*hGAA*/*Gaa*$^{-/-}$ mice may be in sufficient excess to overwhelm the available M6P receptors. Therefore, an alternative mechanism regulating uptake and processing of GAA in various cell types may be involved.

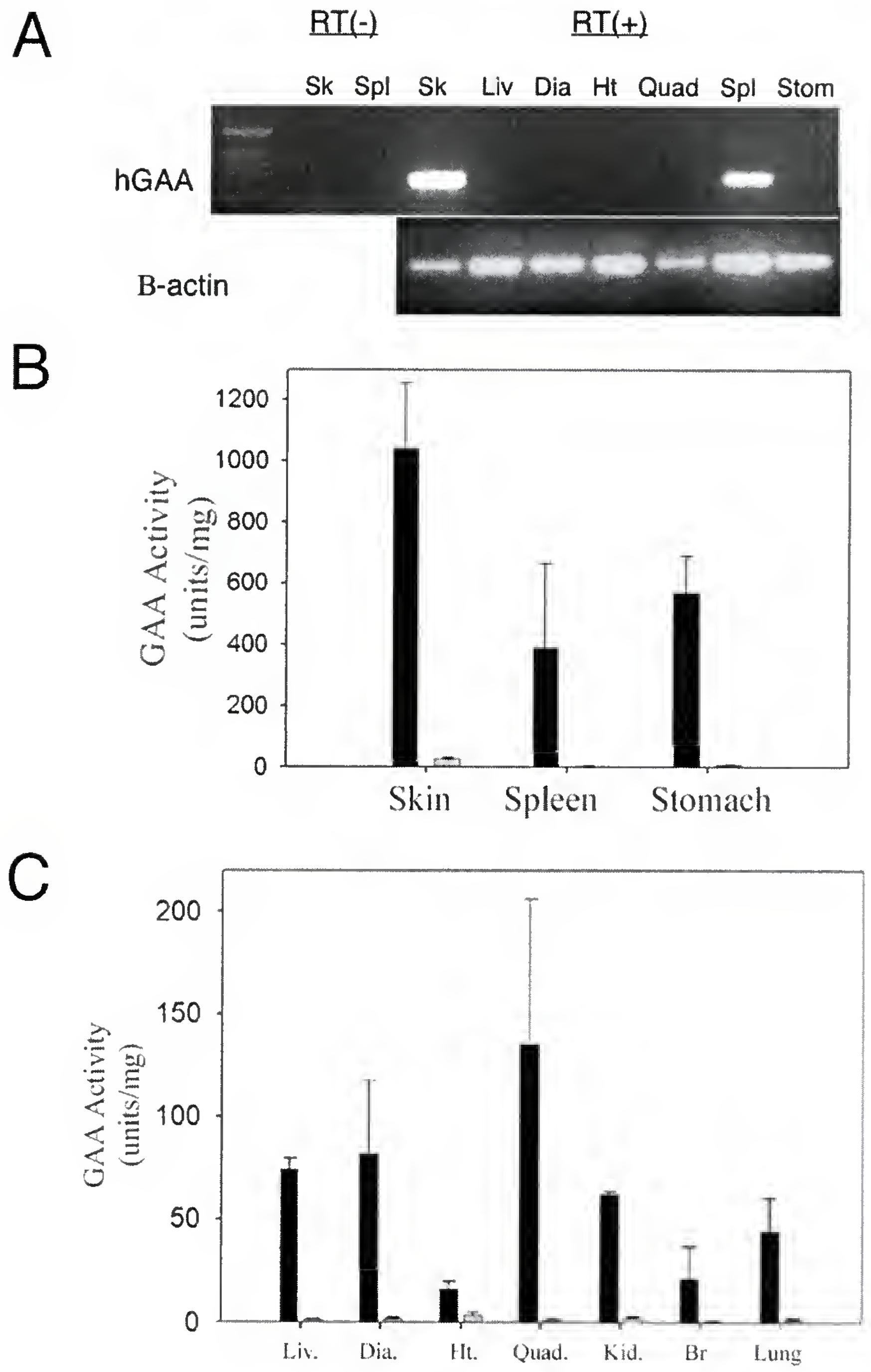

Figure 5-3. Genetic and biochemical characterization of skin-*hGAA* / *Gaa*$^{-/-}$ mice and their single transgenic littermates. (A) RT-PCR was used to detect human GAA transcript. RT(-) controls were used to control for DNA contamination. (B) GAA activity analysis of the 3 hGAA transcript (+) tissues. (C) GAA activity analysis of the 3 transcript (-) tissues along with the kidney, brain and lung. Black bars represent skin-*hGAA* / *Gaa*$^{-/-}$ mice (n=6) and grey bars represent single-transgenic littermates (n=4).

Doxycycline-Mediated Repression of GAA Expression Leads to *Gaa*$^{-/-}$ Phenotype

In order to use the skin-*hGAA* / *Gaa*$^{-/-}$ model for evaluating gene and enzyme replacement therapies, the model must recapitulate the biochemical and functional phenotype of *Gaa*$^{-/-}$ mice. Therefore, GAA gene expression must be shut off by administration of Dox sufficiently to reduce GAA activity in both expressing and non-expressing tissues to background levels early enough to prevent rescue of the functional phenotype, while maintaining tolerance to human GAA. At 3 wk of age (the earliest date for weaning and genotyping) normal diet food was replaced with Dox-formulated food. Two weeks later, mice were sacrificed and the critical tissues were analyzed for GAA activity (Figure 5-4A). GAA activity was reduced to background in only the heart and quadriceps and was significantly higher than background in the skin, liver and diaphragm. After waiting 6 wk post-Dox feeding, activity in all tissues, including the skin, was reduced to the levels observed in *Gaa*$^{-/-}$ mice, suggesting that future treatment studies using these mice will require at least 6 wk of Dox feeding when initiated at 3 wk of age.

The relative activity levels in the skin at 0, 2 and 6 wk on Dox are consistent with RT-PCR identification of human GAA transcript in the skin at the same time points (Figure 5-4B). It is understood that the tetracycline operon-based gene regulation systems such as the one used in these mice has low levels of leakiness and therefore, more sensitive and quantitative methods for RNA detection would likely reveal human GAA transcript in the skin even at 6 wk on Dox. However, this level of regulation in the skin is not necessary for our studies.

Because human GAA expression was not shut-off until 3 wk of age, it is possible that exposure to GAA for this length of time would be sufficient to clear accumulated lysosomal glycogen. PAS staining of cardiac, diaphragm and quadriceps tissue sections revealed no detectable change in the degree of accumulated glycogen compared to *Gaa*$^{-/-}$ mice (not shown).

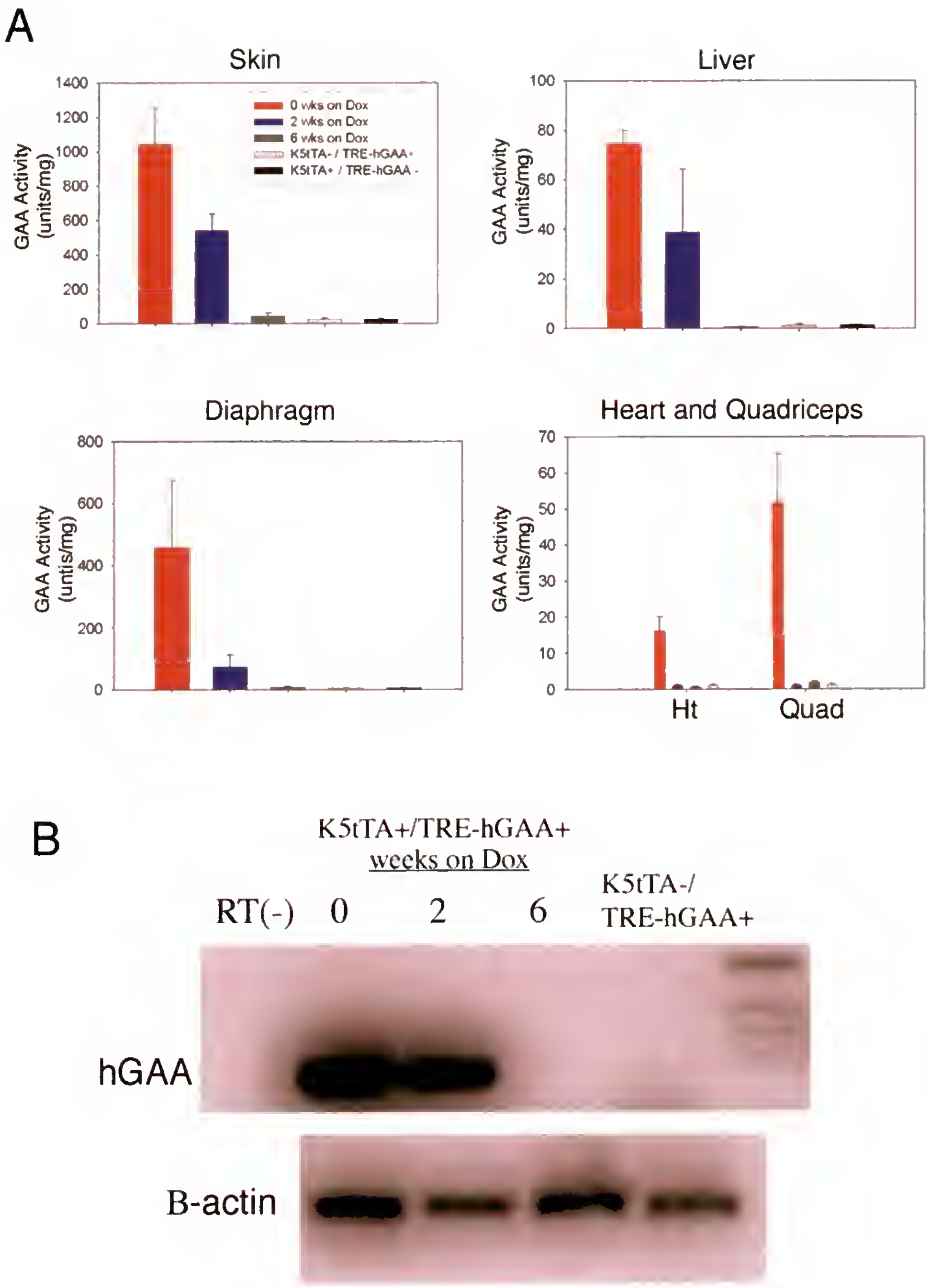

Figure 5-4. Biochemical and genetic affects of Dox-mediated repression. (A) GAA activity levels in the skin and distal tissues. Bars represent mean ± standard error of the mean (n=4). (B) RNA levels in the skin of mice from 0, 2 and 6 wk on Dox. After RT, cDNA was pooled from 3 mice for PCR. The RT(-) sample (lane 1) represents RT-PCR of the 0 wk Dox sample (lane 2).

Anti-GAA Humoral Response is Completely Inhibited in Skin-hGAA / *Gaa*$^{-/-}$ Mice

To confirm that early exposure to human GAA induced tolerance to exogenously introduced human GAA, skin-*hGAA* / *Gaa*$^{-/-}$ mice were intravenously administered 10 mg/kg rhGAA 8 wk after Dox feeding was initiated. Anti-GAA antibody formation was followed for 7 wk and compared to antibody formation both in naïve *Gaa*$^{-/-}$ mice and the pretreated *Gaa*$^{-/-}$ mice described in chapter 4 (Figure 5-5). Antibody titers in naïve *Gaa*$^{-/-}$ mice peaked at 100-fold over background. In contrast, there was no increase in anti-GAA antibody titer in skin-hGAA/*Gaa*$^{-/-}$ mice. Anti-GAA antibody titers in the pretreated *Gaa*$^{-/-}$ mice were low enough to be considered background (1.0-1.18 fold over background) during initial characterization studies (chapter 3). However, after comparison of these values with those from the skin-hGAA/*Gaa*$^{-/-}$ mice, it is apparent that complete inhibition of anti-GAA immunity was not induced in the pretreated model.

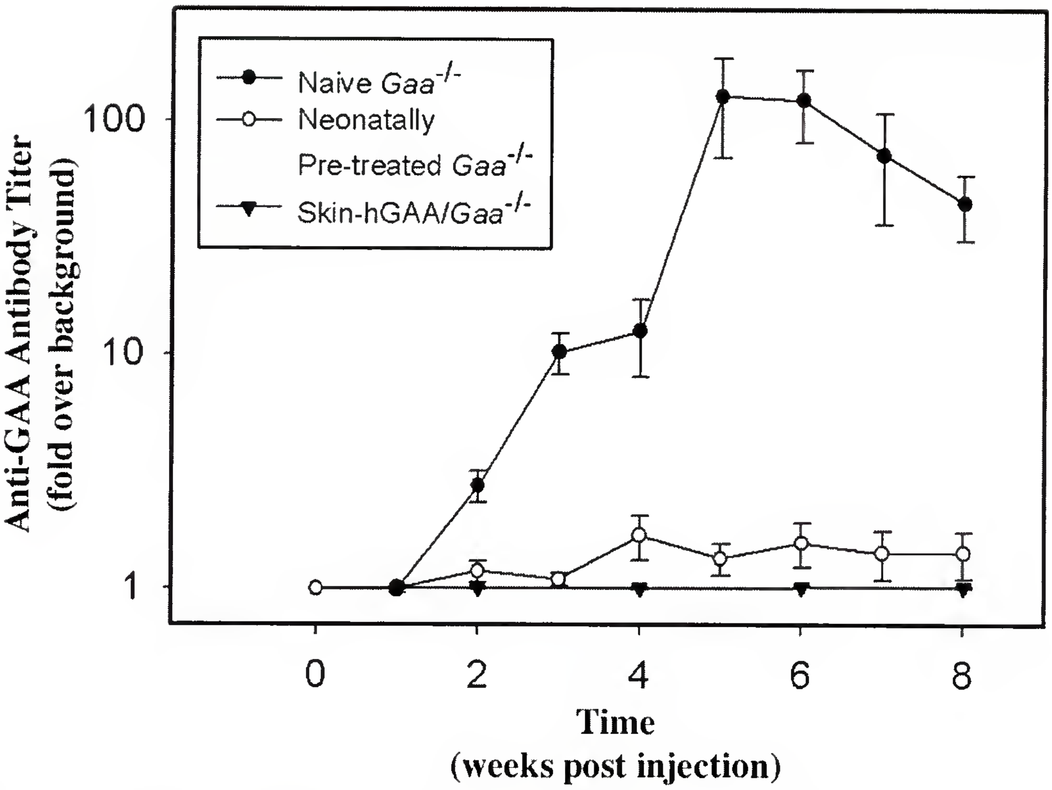

Figure 5-5. Anti-GAA antibody formation in skin-*hGAA*/*Gaa*$^{-/-}$, naïve *Gaa*$^{-/-}$ and neonatally pretreated *Gaa*$^{-/-}$ mice after intravenous delivery of rhGAA at 0 and 4 wk (n=6). Note, data from pretreated and naïve groups are from experiments shown in figure 3-1.

Unexpected Observations of the Skin-*hGAA* / *Gaa*$^{-/-}$ Phenotype

At the time of weaning mice from the first skin-*hGAA* / *Gaa*$^{-/-}$ cross, we observed an obvious difference in appearance between mice that were PCR positive for both K5-*tTA* and TRE-*hGAA* versus mice only positive for one of the two. These mice were smaller (68 ± 10% of the weight of their single transgenic littermates) and had patchy hair loss (Figure 5-6). After administering Dox for 3 wk to half of the skin-*hGAA* / *Gaa*$^{-/-}$ mice, hair growth and weight gain were restored. In the absence of Dox, the remaining mice maintained the lower body weight and hair growth did not reach the level observed in mice exposed to Dox.

Over the next 14 months of breeding, the degree of poor weight gain and hair loss varied with no particular trend over time. The poor weight phenotype was so severe in some mice that they could not maneuver through the bedding. This was likely exacerbated by the inability to compete for food from the mother, leading to weakness and occasionally death (if not euthanized first). Others had no detectable weight or hair loss phenotype and yet others had a mild phenotype that was restored to varying degrees 2 to 3 wk after initiating Dox feeding. Additionally, we noted in two of the initial breeding pairs that both skin-*hGAA* / *Gaa*$^{-/-}$ parents had a normal appearance 1 wk before weaning. However, at the time of weaning, the mother (who was 3 wk pregnant with the second litter) had patchy hair loss, which was restored by 2 wk after birth.

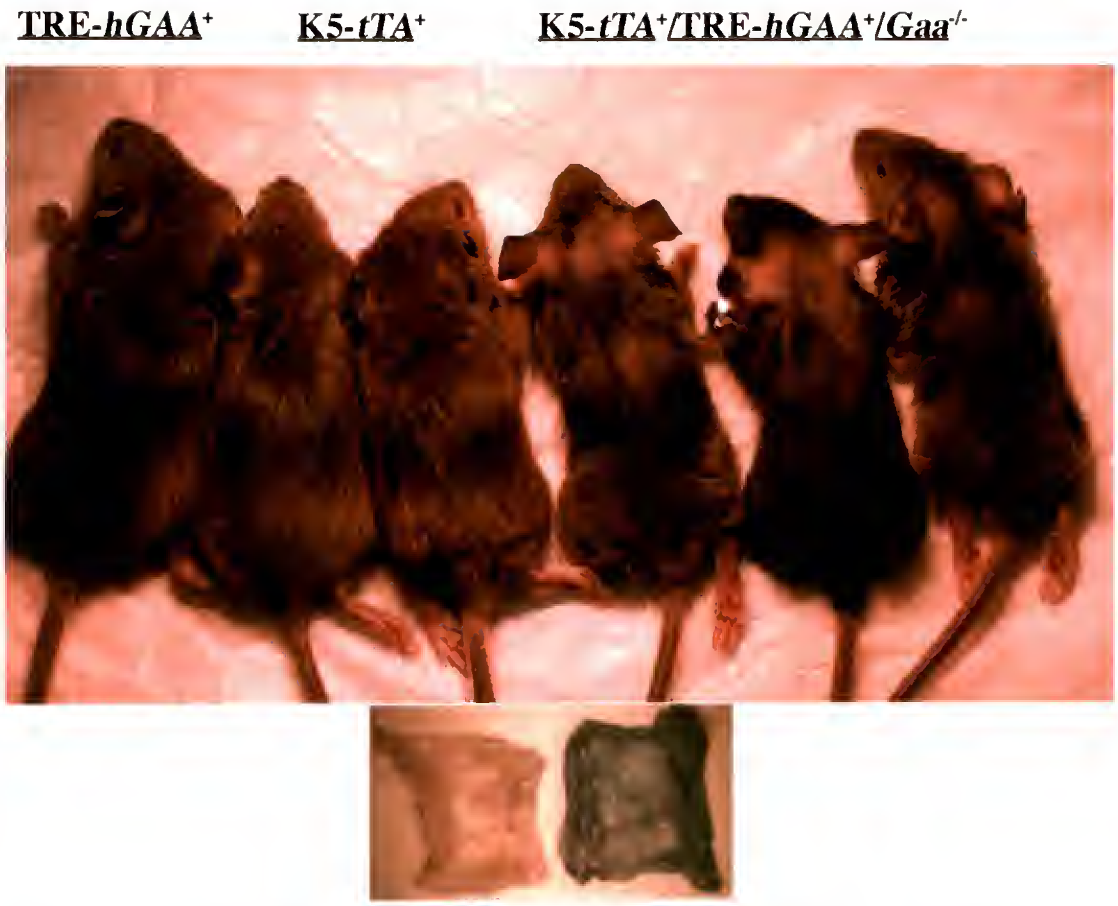

Figure 5-6. Photograph of skin-$hGAA/Gaa^{-/-}$ mice with single transgenic littermates demonstrating patchy hair loss and smaller size. X-Gluc staining of skin from a representative skin-$hGAA/Gaa^{-/-}$ mouse and the TRE-$hGAA/Gaa^{-/-}$ mouse shown in the picture demonstrates obvious biochemical phenotype.

Conclusions

A variety of approaches can be taken to manipulate the immune system in transgenic mice for the purposes inducing tolerance to a foreign therapeutic protein. The approach taken in the studies described in this chapter was to induce complete and irreversible tolerance to human GAA, a technique that while not clinically applicable, will provide a best-case scenario to truly evaluate the potential for cross-correction mediated gene therapy for GSDII. In our model, high enough levels of hGAA expression were induced to mimic a self-protein during the clonal selection process of immunologic development, while not interfering with the biochemical and histological phenotype of the GSDII mouse model. This was achieved by generating a tissue-restricted, conditionally expressing GSDII model.

Not surprisingly, GAA protein detection was ubiquitous. However, this could be completely shut-off after 6 wk on Dox. As hGAA expression throughout gestation alone should be sufficient to confer complete and irreversible tolerance, future studies will likely involve initiation of Dox feeding 1 to 3 wk earlier than the 3 wk time point used in these characterization studies. This should result in lower background tissue activity levels and possibly a shorter period of Dox exposure required to knock down GAA activity to background levels.

Previous experiments evaluating the ability of neonatally pretreated *Gaa*$^{-/-}$ mice to form an immune response to directly infused rhGAA and rAAV-derived hGAA showed tolerance to directly infused rhGAA only. It is theoretically possible that the tolerance observed to rhGAA in the skin-*hGAA/Gaa*$^{-/-}$ mice will not be recapitulated after rAAV-delivery of hGAA as well. However, we expect that the endogenous, long-term, *in-utero* exposure to the human GAA gene product (as opposed to the endocytosed, exogenous CHO-cell derived hGAA used in previous tolerization studies) will allow for irreversible tolerance. A similar model was generated by Raben *et al.* (101) (described in chapter 1) where liver-restricted hGAA was synthesized under control of the tetracycline response element and these mice were shown to be 100% tolerant to a dosing regimen of rhGAA that otherwise resulted in death due to anaphylaxis in 100% of naïve *Gaa*$^{-/-}$ mice. However, these mice were not ideal for liver-directed gene therapy studies due to the background levels of GAA transcript, even after long-term Dox exposure.

The patchy hair phenotype observed in skin-*hGAA*/*Gaa* $^{-/-}$ mice was surprising but is consistent with Chen *et al.* (17) showing patchy to complete hair loss in a double transgenic model that expressed both *tTA* under control of an alternative skin-active promoter (modified NSE promoter) and luciferase under control of the TRE. Hair loss in the skin-*luciferase* mice was also reversed after 1 wk of Dox exposure. The authors speculate that the hair loss is due to high levels of tTA bound to the TRE in the skin and not luciferase; as single transgenic (TRE-*luc* or Skin-*tTA*) mice had no hair loss phenotype. The mechanism responsible for this is unknown, however could be related to disturbance of the normal transcriptional activity in the skin that is specifically caused by tTA-mediated activation; as no hair loss was observed in similar inducible transgenic models expressing ΔFosB or other transcription factors in place of tTA. Additionally, Chen *et al.* reported that their ideas are supported by the fact that gonadal steroid hormones, which have been linked to hair loss in humans, bind to similar transcription factors that regulate expression of other genes (123). In that case, the change in hair loss observed in our studies from 2-3 wk after conception may also be due to fluctuations in these hormones. While Chen *et al.* did not report observations of low weight in their Skin-*tTA* / TRE-*Luc* mice, it is possible that a similar mechanism of altered transcriptional activation is responsible for weight gain.

While these findings are interesting and may lay important foundations for the study of hair loss and weight gain, they do not impact the utility of this model for gene delivery studies. Our current interests are evaluating the full potential of rAAV-mediated cross-correction of GSDII in a diseased mouse model in the absence of anti-GAA immunity. The model generated in these studies fulfills those requirements. However, in the event that these mice are used for future FDA-regulated, preclinical trials for gene or enzyme replacement therapy for GSDII, a further understanding of the hair loss and weight gain phenotype will be required.

CHAPTER 6
BIOCHEMICAL, HISTOLOGICAL, FUNCTIONAL, AND IMMUNOLOGIC ASSESSMENT OF RECOMBINANT AAV(8)-MEDIATED CROSS-CORRECTION IN TWO MURINE MODELS OF GSDII

Background

The identification of new AAV serotypes for the purpose of creating vectors capable of higher levels of transgene expression and tissue specific tropism is a rapidly growing area of research. Numerous reports have demonstrated enhanced transduction with AAV2 genomes packaged in capsids from alternative serotypes (pseudotypes) (15,39,40,82). As of 2001, rAAV5 vectors were shown to yield the highest levels of transgene expression in the liver and this was, in part, attributed to an increase in the percentage of transduced hepatocytes over rAAV2 vectors (82).

Our experience with rAAV5 vectors after intrahepatic delivery of 1 x 10^{12} vg resulted in 5 to 16-fold normal levels of liver GAA. However, the therapeutic efficacy with these levels of activity was difficult to assess due to inhibitory anti-GAA antibody formation in both the naïve *Gaa*$^{-/-}$ and pretreated *Gaa*$^{-/-}$ mouse models. Only 2 mice were tolerant to hGAA and had liver activity values of 5-and 16-fold normal, respectively. Histological improvement, however, was observed only in the latter animal.

The AAV8 serotype was isolate from heart DNA of rhesus monkeys in 2002 by Gao *et al.* (40), and was shown to yied 15-fold greater expression levels in the murine liver compared to the rAAV5 vector. To better evaluate the full potential of rAAV-mediated cross-correction of GSDII, we generated both an alternative model of hGAA tolerance (described in chapter 5) and a higher-expressing rAAV-*hGAA* vector (rAAV8-DHBV-*hGAA*). This vector was made using the same rAAV-DHBV-*hGAA* genome as that used with rAAV5 studies but packaged in rAAV8 capsids

These studies evaluate intrahepatic delivery of rAAV8-DHBV-*hGAA* to both the skin-*hGAA/Gaa*$^{-/-}$ and the neonatally pretreated *Gaa*$^{-/-}$ models of tolerance (described in chapters 3 and 4). As discussed previously, the neonatally pretreated *Gaa*$^{-/-}$ animals gave rise to varying degrees of transgene expression in the liver, anti-GAA antibody titer, and time of immune onset in response to rAAV-derived hGAA. Studying the spectrum of effects of antibody formation on the success of therapeutic outcome requires the analysis of immune-responsive animals with differential responses to therapy, we therefore treated 10 neonatally pretreated *Gaa*$^{-/-}$ mice. However, when both liver GAA values and antibody titers are highly variable within the same group, it is difficult to make statistically significant conclusions about the success of therapy. To eliminate one of these variables, skin-*hGAA/Gaa*$^{-/-}$ mice were also treated; as these mice are more likely to be irreversibly tolerant to rAAV-derived hGAA than the neonatally pretreated animals. Therapeutic efficacy was determined by GAA activities measured in 6 muscle types, histological assessment of glycogen levels, and measurement of soleus muscle contractile function.

Materials and Methods

Cloning and Packaging of rAAV8 construct

Cloning of the pTR-DHBV-*hGAA* plasmid is described in chapter 2. Recombinant AAV8 vectors were generated by triple transfection of 293 cells with the following plasmids: The DHBV-*hGAA* expression cassette flanked by the AAV2 ITRs (described in chapter 2), the pXX6 plasmid containing the adenoviral helper genes, and the *rep-cap* expression construct (p5E18-VD2/8, gift of J.M. Wilson, The University of

Pennsylvania, Philadelphia, PA), which contains the AAV8 *cap* gene and AAV2 *rep* genes. Vectors were purified on an idodixanol gradient and Q-Sepharose column and tittered by dot blot method as previously described (150). Titers were reported as vector genomes (vg)/mL.

Animals and Vector Delivery

All mice were housed in the University of Florida SPF animal facility and all animal procedures were done in accordance with the University of Florida's Institutional Animal Care and Use Committee approval guidelines. The pretreated *Gaa*$^{-/-}$ mouse model was generated by subcutaneous delivery of 25μg rhGAA at 1 day of age (described in chapter 3). The skin-hGAA/*Gaa*$^{-/-}$ mouse model is a conditional, tissue-restricted human GAA-expressing *Gaa*$^{-/-}$ mouse model and is described in chapter 5. Mice were treated at 8 to 10 wk of age with 1 x 10^{12} vg rAAV8-DHBV-*hGAA*. Methods for portal vein delivery of rAAV are described in chapter 2. Age-matched C57B6/129 mice were used as controls.

Tissue Processing

Sixteen weeks post injection, mice were euthanized by intraperitoneal injection of Pentobarbital sodium solution (150mg/kg) and extracted tissues were immediately cut and frozen in liquid nitrogen. Hind-limb skeletal muscle tissues were first crushed to a powder using a hemostat in liquid nitrogen prior to homogenization. Tissues were homogenized in sterile water with lysing matrix D using the Fast Prep Instrument (Qbiogene, Carlsbad, CA). Homogenized lysates were centrifuged to pellet the lysing matrix. Supernatants were subjected to three freeze-thaw cycles and centrifugation.

GAA Enzymatic Activity Assay

The enzymatic activity assay for GAA and the Bradford assay for total protein quantification were performed as described in chapter 2. Briefly, 20 µL of homogenized tissue lysate was added to one well of a black 96-well plate with 1.6 µL 75mM 4-MUG diluted in 38.4 µL 200 mM sodium acetate (pH 3.6). After 1 h incubation at 37°C, the reaction was stopped with 200 µL 0.5 M Na_2CO_3 (pH 10.7). Six standards of 4-MU ranging from 0 to 500 µm were used to generate the standard curve. Fluorescence was measured at 460 nm. Protein concentrations were determined using the Bio-Rad *DC* Protein Assay kit (Bio-Rad, Hercules, CA) according to the manufacturer's instructions. Values are reported as percent of normal GAA activity (minus background). Background was based on activity values measured in untreated *Gaa*$^{-/-}$ tissues, which were processed and assayed at the same time as treated tissues.

ELISA Detection of Anti-GAA Antibodies and Isotypes

Serum samples were obtained weekly *via* tail bleed of anesthetized mice. Serum samples (diluted 1:80) were assayed for anti-GAA antibodies by ELISA as described in chapter 2. Twelve dilutions of rabbit-anti-human GAA polyclonal serum were used to generate the standard curve. All values are reported as fold over background anti-GAA antibody titer with background equal to antibody titer in untreated *Gaa*$^{-/-}$ mice. The ELISA methods for detection of specific anti-GAA isotypes is described in chapter 3 and is similar to the standard anti-GAA antibody ELISA with the following exception: After incubation of serum with well-bound rhGAA, HRP-conjugated, rabbit anti-mouse IgG1, IgG2a, IgG2b, or IgGE (1:10,000 dilution) were added to the wells for 30 min at room temperature to detect specific anti-GAA isotypes. Standardized values are obtained by dividing absorbance units for treated serum by absorbance units for untreated *Gaa*$^{-/-}$ serum. All samples were assayed at the same time.

Histology

For evaluation of liver and spleen histopathology, tissues were fixed in 10% buffered formalin, embedded in paraffin and sectioned. Sections were stained with hematoxylin and counterstained with eosin (H&E). H&E-stained liver and spleen sections were examined for histopathology by a veterinary pathologist at the University of Florida Pathology Core Lab. For histological assessment of glycogen, tissues were fixed overnight in 2% gluteraldehyde in PBS, TAAB-embedded, sectioned (1µm thickness), and stained with Periodic Acid Schiff (PAS) reagent (Richard Allen, Kalamazoo, Michigan) according to the manufacturers instructions. PAS positive staining of glycogen on muscle cross-sections reveals distinct pink foci.

Western Blot Detection of GAA in Immunoprecipitated Serum

Serum samples collected from tail-bleeds of anesthetized mice were stored at -20°C. After thawing serum, 4 µg purified goat anti-human GAA antibody was added to 100 µL serum and 150 µL NP-40 buffer (50mM Tris-HCL pH 8.0, 150mM NaCl and 1% NP-40) and incubated overnight at 4°C on a rotating platform. Protein G-Agarose (Roche Diagnositcs, Manheim, Germany) was washed 3 times with NP-40 buffer and resuspended in an equal volume of buffer to generate 50% Protein G. Fifty µL of 50% Protein G was added to the serum/anti-GAA Ab mixture and incubated for 4 h at 4°C on an inverting platform. After centrifugation, the supernatant was removed and the pellet was washed with NP-40 buffer twice. The final pellet containing the Protein G/goat anti-human GAA IgG/serum human GAA complexes were resuspended in an equal volume of 2X SDS loading buffer. Samples were heated to 100°C for 5 min and centrifuged. The total volume of supernatant was separated on an 8% SDS-polyacrylamide gel and transferred to a nitrocellulose membrane. After transfer, the membrane was blocked with 5% nonfat dry milk and washed with PBS/T. The membrane was probed with a 1:1000 dilution of rabbit anti-human GAA polyclonal serum for 1 hr at room temperature. Washing was repeated and the blot was probed with a 1:10,000 dilution of horseradish peroxidase-conjugated, donkey-anti-rabbit IgG (Amersham Pharamcia Biotech). After washing, hybdridization was detected using the ECL Plus Western blotting detection system (Amersham Pharmacia Biotech).

In Vitro Force Frequency Measurement

In vitro contractile measurements were performed by T. Fraites as described previously (38). Briefly, the mouse was anesthetized with sodium pentobarbital. Soleus muscles were surgically excised and placed in a dissecting chamber with Krebs-Henseleit solution equilibrated with a 95% O_2 / 5% CO_2 gas mixture. The soleus muscle was suspended vertically between two lightweight plexiglass clamps connected to force transducers (Model FT03, Grass Instruments, West Warwick, RI) in a water jacketed tissue bath containing Krebs-Henseleit solution equilibrated with a 95% O_2 / 5% CO_2 gas (bath 37°C, pH 7.4, osmality 290mOsm). Transducer output was amplified and differentiated by operational amplifiers and underwent A/D conversion for analysis using a computer-based data acquisition system (Polyview, Grass Instruments). *In vitro* contractile measurements began with determination of the muscle's optimal length for isometric titanic tension development. The muscle was field-stimulated using a stimulator (Model S48, Grass Instruments) along its entire length with platinum electrodes. Muscle length was progressively increased until maximal isometric twitch tension was obtained. Once the highest twitch force was achieved, all contractile properties were measured isometrically at optimal length. At the end of the study, the muscle strip length and weight are determined in order to calculate the normalized force generated.

Results

Intrahepatic Delivery of rAAV8-DHBV-*hGAA* Vectors Leads to Higher Levels of Liver GAA Expression than Previously Observed

Earlier studies demonstrated the necessity of achieving liver GAA activity levels in the range of 16-fold normal for successful cross-correction in the absence of an immune response. To determine the potential for rAAV8 vectors to yield sufficient levels of GAA under control of the liver-enhanced DHBV promoter, two models of *Gaa*$^{-/-}$ mice (skin-*hGAA/Gaa*$^{-/-}$ and neonatally pretreated *Gaa*$^{-/-}$) were administered 1 x 10^{12} vg rAAV8-DHBV-hGAA *via* the portal vein, and liver GAA activity levels were determined 16 wk post injection. Tissues were analyzed after 16 wk for this study (compared to 8 wk for the rAAV5 study) to allow for more time to reverse glycogen accumulation and restore muscle function. Terminal liver GAA activity levels after rAAV8 treatment ranged from 11.7-fold to 56.5-fold normal (mean 27.3 ± 3.9) (Table 6-1). Eleven of the 16 mice had expression levels greater than 16-fold normal, which was shown to be sufficient to improve glycogen accumulation as determined by PAS staining after rAAV5-*hGAA* delivery. In addition, mean terminal liver GAA values were 3-fold greater than observed using the rAAV5 vector, however, these values were measured at different wk post injection.

Skin-hGAA/*Gaa*$^{-/-}$ Mice are Tolerant to rAAV8-Derived hGAA

The skin-hGAA/*Gaa*$^{-/-}$ mouse model was shown to be completely tolerant to directly delivered rhGAA (chapter 5). However, the pretreated *Gaa*$^{-/-}$ model was also tolerant to rhGAA, but had varying degrees of immunologic response to rAAV5-derived hGAA. The most likely reason for failed tolerance to rAAV-derived hGAA in mice pretreated with rhGAA is the difference in the endogenously expressed versus exogenous antigen. Because the toleragen for the skin-hGAA/*Gaa*$^{-/-}$ mice is endogenously-expressed antigen, we expected to avoid this problem. Skin-hGAA/*Gaa*$^{-/-}$ mice (for the rAAV8 study) were given Dox-formulated chow within 1 day after birth instead of 3 wk after birth as was done for protein-challenge studies. This change was made in effort to decrease the likelihood of a phenotypic effect by human GAA production that may not have been detected in previous characterization studies. In doing this, it was therefore possible that shutting off hGAA expression while immunologic development was still occurring could result in incomplete tolerance.

After intrahepatic delivery of 1 x 10^{12} vg rAAV8-DHBV-*hGAA* to 6 skin-hGAA/*Gaa*$^{-/-}$ mice, no anti-GAA antibody formation was observed in any of the mice over the 16 wk course of the study (Table 6-1 and Figure 6-1). This suggests that tolerance in *Gaa*$^{-/-}$ mice can be irreversibly induced by the induction of *hGAA* expression from conception to birth.

Recombinant AAV8-DHBV-*hGAA* Delivery to Pretreated *Gaa*$^{-/-}$ Mice Results in Early Formation of High Titer Antibodies

It has been suggested by others (81) that tolerance to rAAV-derived transgene products can be induced simply the use of high expressing vectors delivered to the liver. Because the rAAV8 vector led to higher liver GAA levels than previously observed, it is possible that high dose tolerance could be induced. Alternatively, it is also possible that higher levels of GAA expression from the rAAV8 vector could lead to the production of higher titer antibodies and potentially a more serious cell-mediated immune response.

After delivery of 1 x 10^{12}vg rAAV8-DHBV-*hGAA* to 8 to 10 wk-old neonatally pretreated *Gaa*$^{-/-}$ mice, 6 of the 10 mice formed anti-GAA antibodies (Table 6-1 and Figure 6-1). Two unexpected observations were made among these 6 mice. First, anti-GAA antibody formation was initially detected at 2 wk post injection in 3 of the 6 immune-responsive mice (Figure 6-1). This suggests that transgene expression from the rAAV8 vector began earlier than from the rAAV2 and rAAV5 vectors (which both resulted in antibody formation between 5 to 8 wk post injection). Two of the remaining 3 mice had detectable antibody formation at 5 wk post injection and 1 at 10 wk post injection. The early expression seen from rAAV8 vectors compared to rAAV2 vectors is consistent with findings by others (115,125). If early gene expression is occurring, it is possible that the 3 to 8 wk delay in antibody formation observed in the other 3 mice is due to a break in tolerance induced by neonatal pretreatment as described in chapter 4.

The second unexpected observation was extremely high anti-GAA antibody titers that reached nearly 1000-fold over background in 3 of the 6 immune-responsive mice (Figure 6-1). This value is 62-fold greater than the highest antibody titer observed after rAAV5 delivery to the same mouse model (Table 4-3) and more surprisingly, 10-fold greater than peak antibody titers observed after a second injection of rhGAA in naïve *Gaa*$^{-/-}$ mice (Figure 3-1). Interestingly, the 3 mice with antibody titers in this high range had significantly lower GAA levels in the liver than the remaining pretreated *Gaa*$^{-/-}$ mice ($P<0.0001$) (Table 6-1). This suggests that a mechanism of high-dose induced tolerance (or partial tolerance in this case) in the liver observed by Mingozzi *et al.* (81) may similarly be occurring.

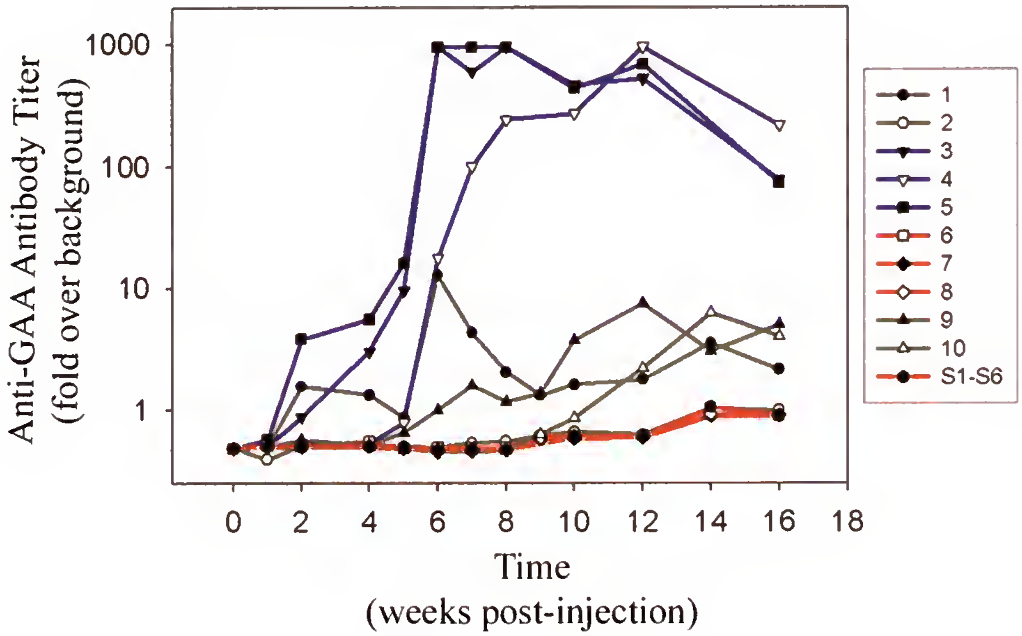

Figure 6-1. Anti-GAA antibody formation in pretreated *Gaa*$^{-/-}$ mice (1-10) and skin-*hGAA*/*Gaa*$^{-/-}$ mice (S1-S6) after intrahepatic delivery of 1 x 10^{12} vg of rAAV8-DHBV-*hGAA* at week 0.

Lack of Evidence For a Cell-Mediated Immune Response to rAAV8-Derived hGAA

Very high antibody titers in rAAV8-treated mice were observed with 4 to 11-fold normal terminal liver GAA levels whereas similar terminal liver GAA levels after rAAV5 delivery resulted in significantly lower antibody titers (Figure 4-3). This could suggest that earlier liver GAA levels in rAAV8-treated mice were higher than terminal levels (enough to induce this degree of humoral immunity), and that the lower terminal GAA levels were due to a loss of transduced hepatotcytes by a cell-mediated immune response.

To determine if such a response was occurring, liver and spleen tissue taken at the time of sacrifice were H&E-stained and evaluated for histopathology. No hepatocellular changes were observed in any of the rAAV8-treated mice (Figure 6-2). Additionally, relative levels of IgG1, IgG2a, IgG2b and IgE were also measured over time, as significantly high levels of IgG2a could be indicative of a Th1-mediated response. IgG1 was the predominant isotype followed by 1- to 5-fold lower levels of IgG2b. Only 2 animals had 1.5-fold over background IgG2a levels (Figure 6-3), but showed no evidence of a Th1 response by histology. We speculate that if there is any Th1-mediated response, it is insignificant. IgE was also measured, as it can be an indication of a skewed Th2 response, as well as a possible anaphylactic-like response. Three animals had detectable but relatively low levels of anti-GAA IgE compared to IgG1 (between 1.5- to 1.7-fold over background). The possibility of an anaphylactic-like response was ruled out due to the absence of clinical signs and this was confirmed by the absence of high levels of IgE. Together, these results suggest a lack of a cell-mediated immune response. However, more in depth immunologic studies will need to be done to confirm this.

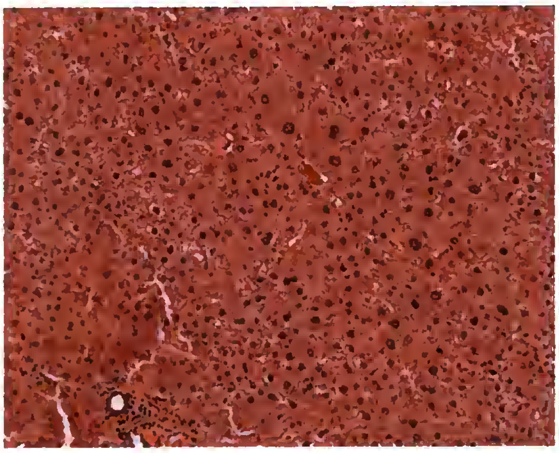

Figure 6-2. Hematoxylin and eosin-stained section of liver 16 wk after rAAV8-DHBV-*hGAA*-treatement. Section shown is from pretreated mouse 4. In a blind study, the image was chosen as a representative field to demonstrate absence of lymphocyte infiltration.

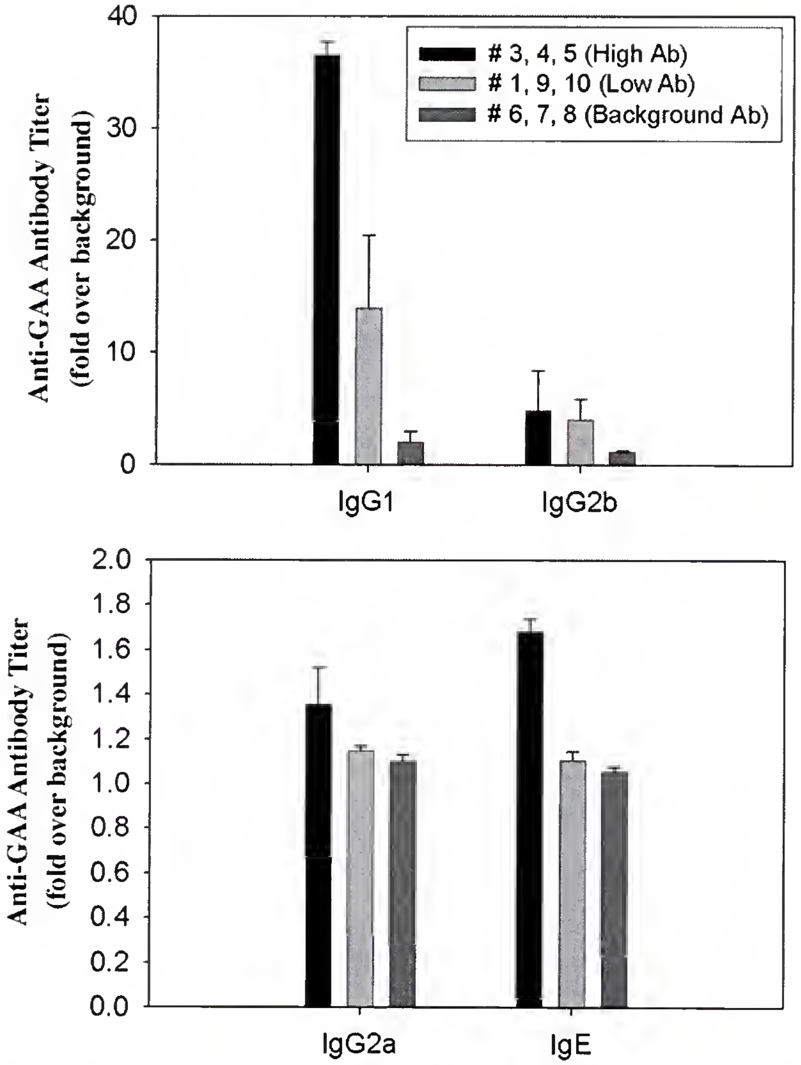

Figure 6-3. Relative levels of IgG1, IgG2b, IgG2a and IgE in pretreated $Gaa^{-/-}$ mice 12 wk post injection of rAAV8-DHBV-*hGAA*.

Partial Restoration of Heart GAA Activity Observed After rAAV8-DHBV-*hGAA* Delivery

With 10 of 16 mice (6 skin-*hGAA*/$Gaa^{-/-}$ and 4 pretreated $Gaa^{-/-}$) having no anti-GAA antibody formation and liver activity values in the range of 11- to 56-fold normal in these mice, we expected to see some degree of cross-correction in the heart. Of the 10 tolerant mice, 5 mice (6, 7, 8, S1, S2) showed significant improvement in heart GAA activity (compared to untreated and immune-responsive mice), ranging from 25% to 36% of normal (Table 6-1 and Figure 6-4). The remaining 5 tolerant mice had background to low levels of GAA activity in the heart and this is likely attributed to the significantly lower liver GAA levels (1576 ± 237% versus 4121 ± 526%, *P*=0.005) with the exception of one outlier (mouse 2).

Unexpectedly, mouse 10 had 31.3% of normal heart GAA activity in the presence of an immune response (4.5-fold over background antibody titer). However, anti-GAA antibodies in this mouse were not detected until 12 wk post injection (7 to 10 wk later than other mice) (Figure 6-1). This delayed antibody formation, maybe due to a break in tolerance, and may also be less inhibitory than earlier antibody formation. This is consistent with observations from the rAAV5 study (Table 4-3).

Superphysiologic Levels of Diaphragm GAA Result in Reversal of Glycogen Accumulation After rAAV8-DHBV-*hGAA* Delivery

Previous studies with rAAV5-*hGAA* showed a high percentage of mice with significant levels of GAA activity with higher overall GAA activity values in the diaphragm as compared to other tissues. This trend was recapitulated with rAAV8 treatment. Nine of the 10 tolerant mice had high levels of GAA activity in the diaphragm (43% to 2444% of normal) (Table 6-1 and Figure 6-4). Additionally, 3 of the 6 immune-responsive mice also had restoration of diaphragm GAA (41% to 119% of normal). Not surprisingly, the remaining 3 immune-responsive mice, with significantly higher anti-GAA antibody titers (62-fold over background) and lower liver GAA levels (3, 4, 5), had less than 20% of normal diaphragm activity levels.

The wide range of GAA levels in the diaphragm allowed us to determine therapeutic efficacy of relative enzyme activity values, as determined by the degree of glycogen accumulation *via* PAS staining. A reduction in glycogen was observed beginning with 40% of normal diaphragm GAA levels (mouse 1). More significant improvement was observed with 100% of normal diaphragm GAA (mouse 9) and complete clearance was observed in mice S1 and S2 with 18-fold and 24-fold normal diaphragm GAA levels, respectively (Figure 6-5).

Low Levels of GAA Activity Observed in Hind-Limb Skeletal Muscles Despite High Levels of Liver GAA in Tolerant Mice

The varying levels of cation-independent mannose 6-phosphate receptor (CI-M6PR) (observed by us (Figure 4-7) and others (101)) in the heart and diaphragm versus the hind-limb skeletal muscles are likely to play a role in susceptibility to correction. Additionally, it has been suggested that type I fibers ("slow-twitch") have greater levels of CI-M6PR on the cell surface than type II fibers ("fast-twitch") (101). Therefore, we analyzed 4 different skeletal muscles of the hind-limb, all of which have varying ratios of type I to type II fibers,

The ability to restore GAA activity in rAAV8-treated hind-limb skeletal muscles varied between tissue type and between individual mice, and was primarily dependent on the immune response. The soleus muscle (which has the highest ratio of type I to type II fibers compared to other examined muscle groups) had the highest levels of GAA activity. Five mice had GAA activity levels ranging from 12% to 128% of normal. However, unlike the heart and diaphragm, this 10-fold range is not explained by terminal liver GAA levels. For example, two skin-*hGAA*/*Gaa*$^{-/-}$ mice with 49- and 56-fold normal liver GAA levels had soleus GAA levels of 128% and 12% of normal respectively (Table 6-1).

The quadriceps and gastrocnemius had similar levels of restoration that were overall lower than those observed in the soleus. Four mice had increased GAA activities in the quadriceps ranging from 10 to 22% of normal and 5 mice had increased GAA activities in the gastrocnemius ranging from 13 to 15% of normal. In the soleus, quadriceps and gastrocnemius, the difference in activities between tolerant and immune-responsive mice was not statistically significant (Figure 6-4). No significantly increased levels of GAA activity were observed in the tibialis anterior (TA) of any mice.

Table 6-1. Acid α-glucosidase activity and anti-GAA antibody values after intrahepatic delivery of rAAV8-DHBV-*hGAA* to two *Gaa*$^{-/-}$ mouse models.

					GAA Activity (Percent of Normal)^{a}					
Mo.	Peak Ab titer^{c}	1st Ab detect. (week)^{b}	Term. Ab titer^{c}	Liv.	Ht.	Dia.	Sol.	TA	Qd.	Gast
1	14.1	2	2.1	4682	3.5	41.8	0.0	2.1	3.2	1.3
2	1.0	-	1.0	3891	7.4	63.7	5.2	1.2	5.0	7.1
3	942	2	77	406	1.4	10.3	0.3	0.0	3.2	0.0
4	942	5	216	1136	3.5	19.2	3.2	1.4	2.2	0.3
5	942	2	72	1132	2.2	5.4	1.2	2.2	3.2	3.3
6	1.0	-	1.0	3746	33.1	46.4	14.3	3.1	7.5	10.8
7	1.0	-	1.0	2633	34.3	55.9	16.0	1.4	10.7	5.2
8	1.0	-	1.0	3657	35.0	203.5	26.0	6.5	21.8	12.8
9	7.4	5	5.0	2475	0.15	106.1	0.0	0.7	3.1	3.0
10	4.0	12	4.0	3007	31.4	119.9	18.1	4.5	5.8	15.7
Skin-hGAA										
S1	1.0	-	1.0	4924	37.5	1803	127.9	4.4	9.9	14.1
S2	1.0	-	1.0	5646	25.0	2444	12.1	3.9	11.4	14.7
S3	1.0	-	1.0	1177	7.5	20.8	6.2	2.2	4.0	4.9
S4	1.0	-	1.0	2119	4.1	16.1	8.2	0.0	3.1	0.2
S5	1.0	-	1.0	1829	6.1	43.1	5.0	10.2	2.1	2.0
S6	1.0	-	1.0	1180	9.0	29.3	0.4	0.0	5.8	0.0

a= Background activity values (averaged from 3 untreated pretreated *Gaa*$^{-/-}$ mice or 4 skin-hGAA/*Gaa*$^{-/-}$ mice) were subtracted from all values.
b=The first week that anti-GAA antibodies were detected by ELISA.
c= Anti-GAA antibody (Ab) titers are represented as fold over background with background equal to mean antibody titer observed in untreated *Gaa*$^{-/-}$ mice.
Yellow boxes highlight higher values (>20% in heart and diaphragm columns and >10% in hind-limb skeletal muscle columns). Blue boxes highlight tolerant animals.

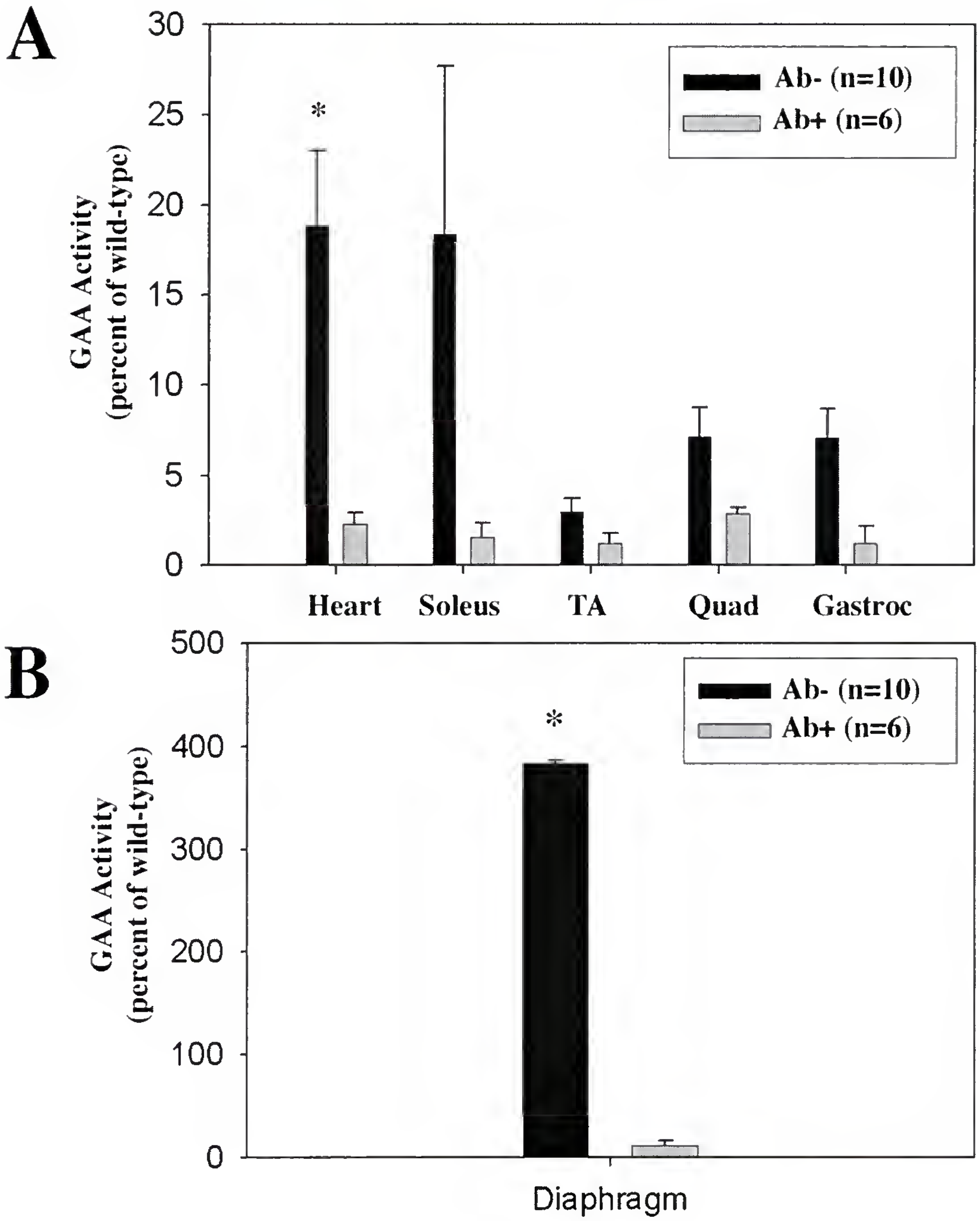

Figure 6-4. Acid α-glucosidase activity values in the 6 distal tissues of tolerant (Ab-) versus immune-responsive (Ab+) mice. * represents statistical significance (*P*=0.05 for heart and *P*=<0.01 for diaphragm).

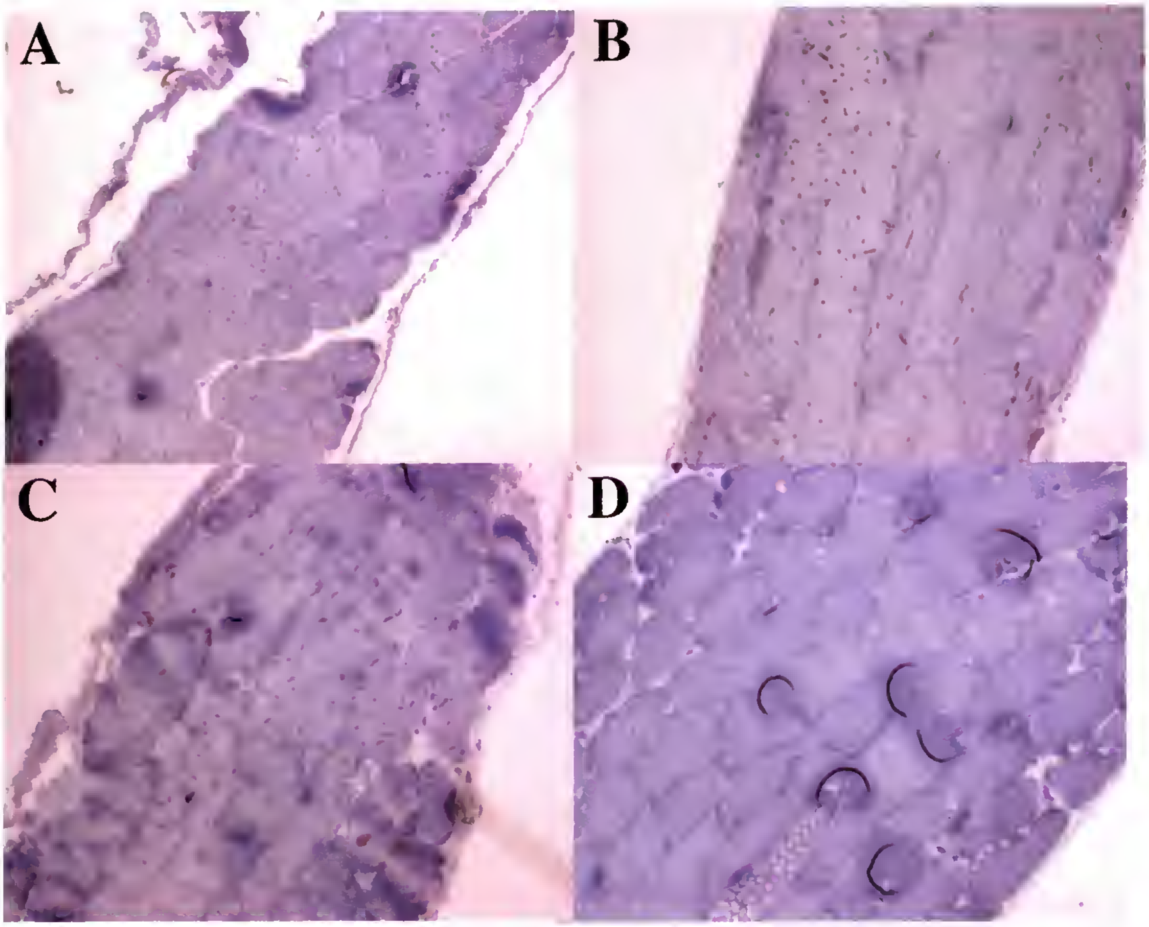

Figure 6-5. Detection of glycogen by PAS staining of diaphragm sections. (A) Untreated, age-matched $Gaa^{-/-}$ mouse, (B) mouse 1 with 40% of normal diaphragm GAA activity levels, (C) mouse 10 with 100% of normal diaphragm GAA activity levels, and (D) mouse S1 with 18-fold normal diaphragm GAA activity levels. Original magnification is 400X.

110-kDa Circulating GAA Detected in rAAV8-Treated Mice

Detecting GAA in the serum has been difficult due to the relatively low levels of circulating GAA and high levels of neutral glucosidases that have similar specificity for the enzyme activity assay substrate. However, confirming that cross-correction is occurring relies on the ability to show a positive correlation between serum GAA and distal tissue activity.

Optimizing immunoprecipitation protocols allowed us to detect GAA in the serum of the liver-*hGAA*-expressing transgenic mice (described in chapter 1). However, serum

GAA was not detected by this method in any of the rAAV5-treated mice. With the relatively high levels of liver GAA activity observed after rAAV8-treatment, we hoped to see detectable levels of the unprocessed, 110-kDa, circulating GAA in some of the tolerant mice.

Serum GAA was detected in 6 of the 16 mice (6, 7, 8, 10, S1, S2) (Figure 6-6). Five of these 6 had no immune response and the highest levels of liver GAA activity (26 to 56-fold normal). Surprisingly, 1 of these 6 mice (mouse 10) had similarly high levels of liver GAA (30-fold normal), but also had anti-GAA antibody formation that peaked at 4.5-fold over untreated. As mentioned previously, antibody formation in this mouse was not detected until 12 wk post injection. The presence of detectable levels of serum GAA in mouse 10 is consistent with the unexpected level of cardiac GAA activity (Table 6-1). Additionally, mouse 2 that had 39-fold normal liver GAA and no immune response also had no detectable serum GAA which is consistent with the surprising lack of cardiac GAA activity as well.

A

Mouse	+	1	2	3	4	5	6	7	8	9	10
Liver GAA	40	47	39	4	11	11	37	26	36	24	30
Peak Ab titer		14	1.0	942	942	942	1.0	1.0	1.0	7.4	4.0
Cardiac GAA		-	-	-	-	-	+	+	+	-	+

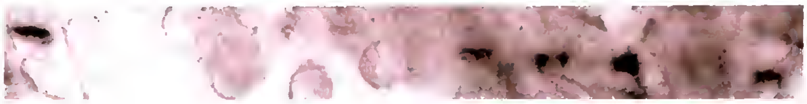

B

Mouse	+	S1	S2	S3	S4	S5	S6
Liver GAA	40	49	56	12	21	18	12
Cardiac GAA		+	+	-	-	-	-

Figure 6-6. Western blot analysis of hGAA in the serum of rAAV8-DHBV-*hGAA*-treated mice 16 wk post injection. The positive control sample (+) is serum from a liver-hGAA expressing transgenic mouse. Liver GAA values represent percent of normal GAA activity. Peak Ab titer values represent antibody titer (fold over background). Cardiac GAA refers to mice with (+) or without (-) greater than 20% of normal GAA activity in the heart.

Partial Restoration of Soleus Muscle Function in rAAV8-DHBV-*hGAA*- Treated mice

To determine if rAAV8-mediated delivery of hGAA lead to functional improvement, contractile function of the soleus muscle was measured. Fraites *et al* (38) was able to demonstrate a significant difference in soleus muscle function between normal mice and *Gaa*$^{-/-}$ mice using this technique (38). Overall, there was a detectable, but not statistically significant difference between rAAV8-*hGAA*-treated mice and untreated *Gaa*$^{-/-}$ mice (Figure 6-7). Additionally, there was no correlation between soleus GAA enzyme activity and contractile force.

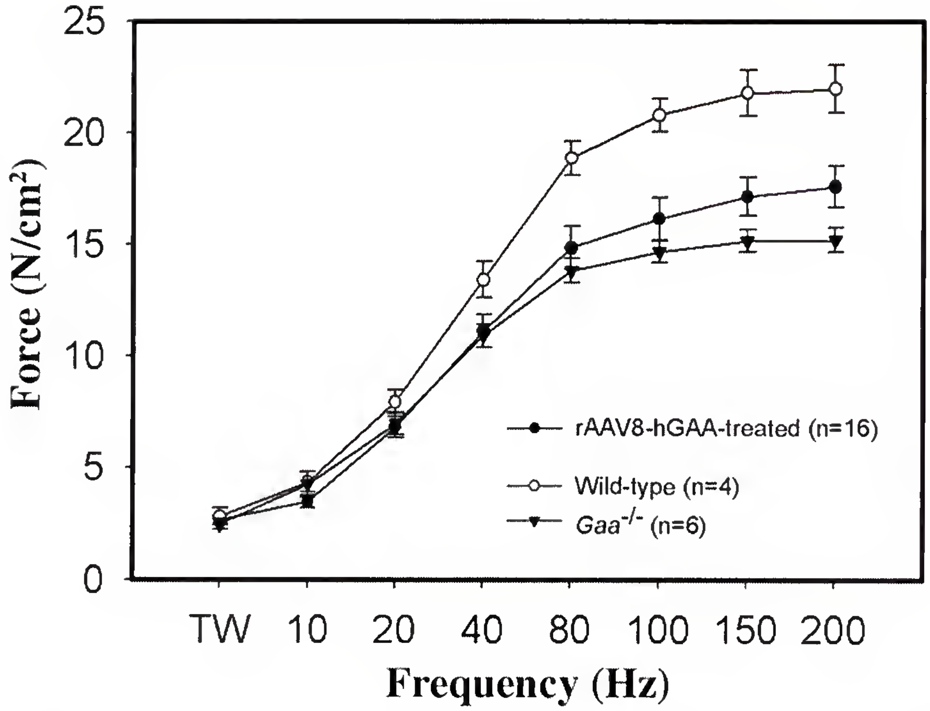

Figure 6-7. Force-frequency relationship of intact soleus muscle 16 wk after intraheptic delivery of 1 x 10^{12} vg rAAV8-DHBV-*hGAA*. Four age-matched, C57BL6/129 mice were used for normal controls. Untreated controls consisted of 4 age-matched *Gaa*$^{-/-}$ mice and 2 age-matched skin-hGAA/*Gaa*$^{-/-}$ mice (with the same Doxycycline feeding schedule as treated mice).

Human GAA RNA from the rAAV8-DHBV-*hGAA* Vector is Expressed in Multiple Tissues

The DHBV promoter appears to have strong liver-specificity based on reported *in vitro* studies (68) and RT-PCR of *human GAA* from rAAV5-*hGAA*-treated tissues (Figure 4-5). To determine if *hGAA* expression from the rAAV8-DHBV-*hGAA* vector was similarly restricted to the liver, RT-PCR was performed on 9 tissues. Results revealed high levels of *hGAA* transcript not only in the liver, but also in the heart. Low but detectable levels were observed in the diaphragm, gastrocnemius and quadriceps as well (Figure 6-8).

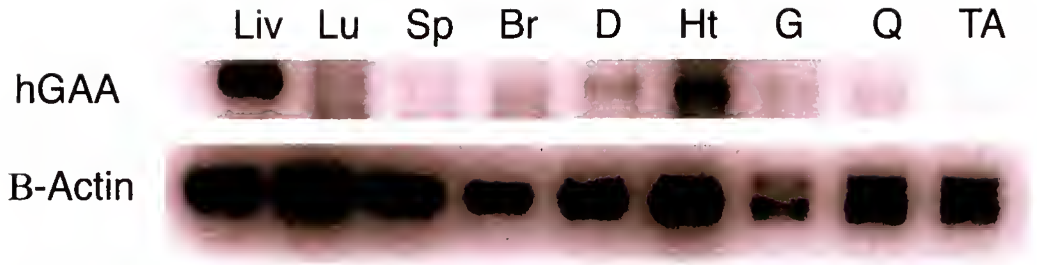

Figure 6-8. RT-PCR of rAAV8-delivered *hGAA* in the liver (Liv), lung (Lu), spleen (Sp), brain (Br), diaphragm (D), heart (Ht), gastrocnemius (G), quadriceps (Q), and tibialis anterior (TA) of mouse 6, 16 wk after rAAV8-DHBV-*hGAA* delivery.

Discussion

Relative Success of rAAV8-*hGAA* in the Liver

The goals of this study were to generate higher levels of liver GAA expression than previously observed, using the rAAV8 vector, and to evaluate the therapeutic efficacy of this vector (in both the absence and presence of an immune response) by using two immune-modulated GSDII mouse models.

The rAAV8 vector resulted in 3-fold greater liver GAA expression levels (at 16 wk post injection) than the rAAV5 vector (at 8 wk post injection). This is a significantly smaller difference than reported by Gao *et al*, (40) who showed 15-fold greater β-gal expression in the liver from a rAAV8 vector. As Gao *et al.* (40) evaluated expression levels at 4 wk post injection (8 wk earlier than our study), it possible that transgene expression peaked prior to the 16 wk time point and subsequently dropped. This theory is supported by studies from Sarkar *et al.* (115), who observed a 3.6-fold greater expression level (with rAAV8 versus rAAV5) at 13 weeks post injection which then dropped to result in only a 2-fold difference by 38 wk.

Alternatively, it is possible that hepatocytes have a saturation point for processing translated GAA, and that further maximizing transgene expression levels are futile. A quantitative assessment of vector copy number and *hGAA* RNA levels along with weekly assessment of liver and distal tissue activities will be necessary to determine if this is true.

Lastly, an assay to determine the infectious particle titer of the rAAV5 and rAAV8 vectors has not been optimized and therefore titers are reported as total particles/mL. Significant differences in the ratio of infectious to total particles could explain the discrepancy between various groups.

Immune Responses to rAAV8-Derived Human GAA

It was not surprising that the skin-*hGAA/Gaa*$^{-/-}$ model did not elicit an anti-GAA immune response to rAAV-derived hGAA while the pretreated *Gaa*$^{-/-}$ mice did. After rAAV5 delivery, there was a slight increase in the percentage of tolerant mice in the pretreated group versus the naïve group (55% versus 33%) suggesting that neonatal pretreatment has limited success of inducing tolerance. After rAAV8 delivery, 40% of pretreated *Gaa*$^{-/-}$ mice were tolerant to rAAV8-derived hGAA and the variation in both titer and week of onset in pretreated mice allowed us to further dissect the impact of anti-GAA immune response on cross-correction.

The ability to detect antibodies at 2 wk post injection suggests that transgene expression is occurring at 1 wk (3 wk earlier than with the rAAV5 or rAAV2 vector) and is consistent with studies by others (115,125) and also similar to observations seen with rAAV1 studies (39). The molecular mechanism responsible for increased transduction with alternative serotypes (which differ only in the capsid) is not fully elucidated. The rate-limiting factor for the onset of transgene expression from rAAV vectors remains controversial. Proposed theories include second-strand synthesis, uncoating of vector genomes in the nucleus, and accumulation of single-stranded genomes (30,87,125). In

2000, Nakai *et al.*(87) suggested that a threshold of accumulation of plus and minus-strand complementary rAAV genomes in the cell can result in annealing of these strands to form biologically active double-stranded molecular forms. Furthermore, recent studies by Thomas *et al* (125) showed that the rate of uncoating of vector genomes determines the ability of these complementary plus and minus single-stranded genomes to anneal together, and that rAAV2 genomes packaged in rAAV8 capsids are more efficient at uncoating than those packaged in rAAV2 capsids. Our conclusions for early transgene expression are based on antibody formation kinetics only, and a better understanding of relative expression kinetics will require analyzing liver GAA levels at earlier time points.

After observing the nearly 1000-fold over background anti-GAA antibody titers in rAAV8-treated mice, we were concerned that this degree of immunogenicity would result in a cell-mediated immune response. The potential for a CMI response to rAAV-derived transgenes is underestimated due to the notion that rAAV is non-immunogenic because of its inability to efficiently infect dendritic cells. However, these conclusions are based on rAAV2 only and parallel studies have not been reported with rAAV8. The possibility of a CMI response to rAAV8-derived hGAA would significantly hinder the progress of clinical applications. However, the lack of such a response observed in these studies suggests that tolerance will only be necessary to prevent inhibitory antibody formation, and this information is important for developing the appropriate immune-modulation protocols.

Cross-Correction of Affected Tissues

The greater susceptibility to correction of the heart and diaphragm muscles compared to other skeletal muscle is important, as the cardio-respiratory pathology is the most life threatening aspect of GSDII. Tolerant mice with GAA levels between 26- and 56-fold normal liver GAA had greater levels of heart, diaphragm and serum GAA than those with liver GAA levels between 11 and 21-fold normal liver GAA. However, there was loss of dose-responsiveness in the heart among the higher-expressing mice. It is possible that cardiomyocytes are resistant to uptake and processing of GAA beyond a given threshold. The higher levels of heart GAA observed in tolerant, rAAV5-treated mice measured at 8 wk post injection suggest that the kinetics of GAA uptake in the heart may be a reflection of the expression levels in the liver (which was shown by Sarkar *et al.*(115) to drop after 13 wk post injection) The high levels of diaphragm GAA, in response to high liver GAA in tolerant mice, resulted in complete reversal of glycogen accumulation. Intermediate levels of diaphragm GAA were also observed in immune-responsive mice and led to partial clearance of glycogen.

The poor uptake of GAA by skeletal muscle compared to heart and diaphragm muscles was similarly observed by Raben *et al* (101) after enzyme replacement therapy. One proposed strategy to better target skeletal muscle is intramuscular delivery of rAAV-*GAA* to achieve both local muscle correction and cross-correction of distal cardiac and skeletal muscles. However, this approach did not result in uptake of significant levels of GAA in the heart or diaphragm at the doses tested by Fraites *et al.* (38). In order to achieve global correction of the heart, diaphragm and skeletal muscles, a protocol involving both intrahepatic delivery and intramuscular delivery to the most severely affected skeletal muscles may be necessary.

The lack of correlation between soleus GAA activity and functional improvement was similarly observed by Fraites *et al.* (38). It is possible that very low levels of GAA

(<10% normal) in the soleus are sufficient to see mild improvement in soleus function, and that above this minimal threshold, there is loss of dose-responsiveness. It is also possible that soleus GAA levels were high enough (prior to 16 wk post injection) to improve function and although these levels variably dropped in different mice by 16 wk, functional improvement was maintained. A time course study evaluating GAA activities, histology and soleus muscle function will be beneficial in future studies to answer these questions.

Correlation Between Human GAA Gene Expression and Cross-Correction

We would expect the relatively high levels of transcript observed in the hearts of rAAV8-treated mice to contribute to higher levels of heart GAA than observed with the rAAV5 vector (that showed no detectable heart *hGAA* expression). The reason for lack of *hGAA* expression in the heart after rAAV5 delivery is not likely due the serotype tropism, as others have shown successful rAAV5 transduction in the heart (115). It is more likely that expression levels from the rAAV5 vector (compared to the rAAV8) were too low to detect transcript. In our studies, transcript was not detected in the heart 8 wk post injection of rAAV5 (4 wk post gene expression), but was detected 16 wk post injection of rAAV8 (15 wk post gene expression). If transduction kinetics are less efficient in the heart than in the liver, it is possible that *hGAA* transcript would have been observed at a later time point from the rAAV5 vector as well. If this theory is true, it is also possible that the synthesis of cardiac *hGAA* in rAAV8-treated mice was not early enough to see higher levels of cardiac GAA activity in these mice.

Summary

In summary, we have shown that the rAAV8-DHBV-*hGAA* vector is capable of producing up to 56-fold normal liver GAA expression levels. Furthermore, we have shown that with this level of liver expression, GAA levels can be restored in the heart and diaphragm, and that these levels are sufficient to completely reverse glycogen accumulation in the diaphragm. Further optimizing high expressing rAAV-*hGAA* vectors may increase liver GAA levels but may not result in significantly greater levels of cardiac GAA. We have confirmed our preliminary findings (using rAAV5) that complete humoral tolerance will be necessary for therapeutic effect. Partial tolerance or delayed tolerance may be able to prevent complete inhibition of cross-correction; however, this is not likely to be true for long-term studies.

CHAPTER 7
CONCLUSIONS AND FUTURE DIRECTIONS

The success of gene replacement therapy for inherited diseases will depend on multiple factors including the ability to generate high-expressing, non-immunogenic vectors. The discovery of AAV2 as a relatively non-immunogenic viral vector was a significant contribution to the field of gene therapy. However, lower expression levels observed from rAAV2 vectors (compared to adenoviral-based vectors) can be a limiting factor for achieving global correction of many candidate diseases. This obstacle led to the isolation and characterization of alternative AAV serotypes, which have resulted in higher transgene expression levels in a variety of tissues. In addition to rAAV vector development studies, the search continues for candidate promoters and other gene regulatory elements capable of yielding high levels of transgene expression with varying tissue specificities.

Despite advances in vector development, the therapeutic efficacy of these high-expressing vectors will rely heavily on the immunologic background of the subject. For lysosomal storage diseases (including Gaucher's disease, MPSVII, and GSDII) and diseases such as hemophilia (in which correction relies on the survival of vector-derived protein secreted from a transduced tissue bed), a thorough understanding of the immune response to vector-derived transgene products will be necessary. Because the therapeutic agents in these cases are soluble, secreted, circulating proteins, neutralizing immune responses can completely prevent or reverse correction. In the worst case, these responses can also prevent future or repeated therapy — genetic or otherwise.

The initial goal of these studies was to achieve therapeutic levels of GAA activity in affected tissues of GSDII mice by uptake of rAAV-derived, hepatic-secreted GAA. Our first studies were not successful. In effort to understand the failure of this approach, we discovered that treated mice were mounting an anti-GAA humoral immune response to vector-derived hGAA. This response contributed to the lack of observable correction in distal tissues. This finding led us to develop methods to manipulate the immune system in GSDII mice.

As a result, two alternative GSDII mouse models were developed, characterized, and evaluated for their immune responses to both enzyme and gene replacement therapies. Results obtained from studying rAAV-mediated gene replacement in these two models provided us with an appreciation for the significant impact of anti-GAA immunity in GSDII mice, which we expect to be recapitulated in the most severely affected patient population. In particular, we found that immune responses to GAA can be substantially reduced in vector-treated mice with appropriate induction of immune tolerance. Our results clearly establish a rationale for investigating this technique in larger animal models and potentially human gene therapy trial subjects.

Future work will also involve the development of clinically applicable immunomodulation protocols. Immunosuppressive agents that reduce lymphoid cell activation and proliferation will be evaluated for the ability to block anti-GAA antibody formation to rAAV-derived hGAA in naïve *Gaa*$^{-/-}$ mice. Once a clinically applicable approach to immunosuppression is achieved, we will further evaluate liver-directed versus muscle-directed therapy or a combination of the two in appropriately immunosuppressed animals. A safe and effective therapeutic protocol (involving immunosuppression followed by rAAV-meditaed delivery of *hGAA* in GSDII mice) will hopefully provide a clear foundation on which to initiate clinical trials of rAAV-mediated gene therapy for Pompe patients.

Ongoing efforts in our laboratory continue to try to understand the underlying factors that lead to the success or failure of rAAV-mediated gene transfer. While we are hopeful and confident that human clinical trials for GSDII and other genetic diseases will be safe, effective, and long lasting, our continuing work will attempt to predict and identify potential pitfalls. In particular, conditional GSDII mouse models (including the one developed during this project) will allow our laboratory to try to understand the timescale of GSDII pathogenesis and its reversibility. Current studies are also focused on the effects of GSDII on the expression profile of genes throughout the genome using gene arrays. Likewise, the expression profiles of affected cells after rAAV infection — with and without therapeutic transgenes — will hopefully provide even more predictive value for longitudinal animal and patient studies.

APPENDIX
LIST OF ABBREVIATIONS

AAV	Adeno-associated virus
Ab	Antibody
Alb	Albumin
B-gal	Beta-galactosidase
BSA	Bovine serum albumin
CHO	Chinese hamster ovary
CMI	Cell-mediated immune
CTL	Cytotoxic T-lymphocyte
DHBV	Duck hepatitis B virus
Dox	Doxycycline
FBS	Fetal bovine serum
GAA	Acid alpha-glucosidase protein
GAA	Acid alpha-glucosidase gene
$Gaa^{-/-}$	Acid alpha-glucosidase knockout mouse model
GSDII	Glycogen storage disease type II
H&E	Hematoxylin and Eosin
hAAT	human alpha 1-antitrypsin
hFIX	human factor IX protein

hGAA	human GAA protein
hGAA	human GAA gene
HRP	Horse radish peroxidase
ITR	Inverted terminal repeat
K5	Keratin 5 promoter
M6PR	Mannose 6-phosphate receptor
min	minute
PAS	Periodic Acid Schiff
PBS	Phosphate Buffered Solution
rAAV	Recombinant adeno-associated virus
rhGAA	Recombinant human GAA protein
TRE	Tetracycline response element
TTR	Transthyretin
vg	vector genomes
wk	week/s

LIST OF REFERENCES

1. **Adkins, B. and R. Q. Du**. 1998. Newborn mice develop balanced Th1/Th2 primary effector responses in vivo but are biased to Th2 secondary responses. J.Immunol. **160**:4217-4224.

2. **Amalfitano, A., A. J. McVie-Wylie, H. Hu, T. L. Dawson, N. Raben, P. Plotz, and Y. T. Chen**. 1999. Systemic correction of the muscle disorder glycogen storage disease type II after hepatic targeting of a modified adenovirus vector encoding human acid-alpha-glucosidase. Proc.Natl.Acad.Sci.U.S.A **96**:8861-8866.

3. **Arruda, V. R., P. A. Fields, R. Milner, L. Wainwright, M. P. De Miguel, P. J. Donovan, R. W. Herzog, T. C. Nichols, J. A. Biegel, M. Razavi, M. Dake, D. Huff, A. W. Flake, L. Couto, M. A. Kay, and K. A. High**. 2001. Lack of germline transmission of vector sequences following systemic administration of recombinant AAV-2 vector in males. Mol.Ther. **4**:586-592.

4. **Bartlett, J. S., R. Wilcher, and R. J. Samulski**. 2000. Infectious entry pathway of adeno-associated virus and adeno-associated virus vectors. J.Virol. **74**:2777-2785.

5. **Baudhuin, P., H. G. Hers, and H. Loeb**. 1964. An electron microscopic and biochemical study of type II glycogenosis. Lab Invest **13**:1139-1152.

6. **Berns, K. I. and R. M. Linden**. 1995. The cryptic life style of adeno-associated virus. Bioessays **17**:237-245.

7. **Bijvoet, A. G., M. A. Kroos, F. R. Pieper, d. Van, V, H. A. De Boer, A. T. Van der Ploeg, M. P. Verbeet, and A. J. Reuser**. 1998. Recombinant human acid alpha-glucosidase: high level production in mouse milk, biochemical characteristics, correction of enzyme deficiency in GSDII KO mice. Hum.Mol.Genet. **7**:1815-1824.

8. **Bijvoet, A. G., H. Van Hirtum, M. A. Kroos, E. H. Van de Kamp, O. Schoneveld, P. Visser, J. P. Brakenhoff, M. Weggeman, E. J. van Corven, A. T. Van der Ploeg, and A. J. Reuser**. 1999. Human acid alpha-glucosidase from rabbit milk has therapeutic effect in mice with glycogen storage disease type II. Hum.Mol.Genet. **8**:2145-2153.

9. **Billingham, R. E., L. Brent, and P. B. Medawar**. 1953. Activity acquired tolerance of foreign cells. Nature **172**:603-606.

10. **Blacklow NR**. 1988. Adeno-associated Viruses of Humans, p. 165-174. *In* Pattison J (ed.), Parvoviruses and Human Diseaes. CRC Press, Boca Raton.

11. **Bradford, M. M.** 1976. A rapid and sensitive method for the quantitation of microgram quantities of protein utilizing the principle of protein-dye binding. Anal.Biochem. **72**:248-254.

12. **Brockstedt, D. G., G. M. Podsakoff, L. Fong, G. Kurtzman, W. Mueller-Ruchholtz, and E. G. Engleman**. 1999. Induction of immunity to antigens expressed by recombinant adeno-associated virus depends on the route of administration. Clin.Immunol. **92**:67-75.

13. **Brooks, D. A.** 1999. Immune response to enzyme replacement therapy in lysosomal storage disorder patients and animal models. Mol.Genet.Metab **68**:268-275.

14. **Burton, M., H. Nakai, P. Colosi, J. Cunningham, R. Mitchell, and L. Couto**. 1999. Coexpression of factor VIII heavy and light chain adeno-associated viral vectors produces biologically active protein. Proc.Natl.Acad.Sci.U.S.A **96**:12725-12730.

15. **Chao, H., Y. Liu, J. Rabinowitz, C. Li, R. J. Samulski, and C. E. Walsh**. 2000. Several log increase in therapeutic transgene delivery by distinct adeno-associated viral serotype vectors. Mol.Ther. **2**:619-623.

16. **Chao, H., L. Mao, A. T. Bruce, and C. E. Walsh**. 2000. Sustained expression of human factor VIII in mice using a parvovirus-based vector. Blood **95**:1594-1599.

17. **Chen, J., M. B. Kelz, G. Zeng, C. Steffen, P. E. Shockett, G. Terwilliger, D. G. Schatz, and E. J. Nestler**. 2002. Inducible, reversible hair loss in transgenic mice. Transgenic Res. **11**:241-247.

18. **Chen, N., Q. Gao, and E. H. Field**. 1995. Expansion of memory Th2 cells over Th1 cells in neonatal primed mice. Transplantation **60**:1187-1193.

19. **Chen, Y. T. and A. Amalfitano**. 2000. Towards a molecular therapy for glycogen storage disease type II (Pompe disease). Mol.Med.Today **6**:245-251.

20. **Cordier, L., G. P. Gao, A. A. Hack, E. M. McNally, J. M. Wilson, N. Chirmule, and H. L. Sweeney**. 2001. Muscle-specific promoters may be necessary for adeno-associated virus-mediated gene transfer in the treatment of muscular dystrophies. Hum.Gene Ther. **12**:205-215.

21. **Corr, M., D. J. Lee, D. A. Carson, and H. Tighe**. 1996. Gene vaccination with naked plasmid DNA: mechanism of CTL priming. J.Exp.Med. **184**:1555-1560.

22. **Daly, T. M., K. K. Ohlemiller, M. S. Roberts, C. A. Vogler, and M. S. Sands**. 2001. Prevention of systemic clinical disease in MPS VII mice following AAV-mediated neonatal gene transfer. Gene Ther. **8**:1291-1298.

23. **de Barsy, T., P. Jacquemin, F. Van Hoof, and H. G. Hers**. 1973. Enzyme replacement in Pompe disease: an attempt with purified human acid alpha-glucosidase. Birth Defects Orig.Artic.Ser. **9**:184-190.

24. **De Duve, C., B. C. Pressman, R. Gianetto, R. Wattiaux, and F. Appelmans**. 1955. Tissue fractionation studies. 6. Intracellular distribution patterns of enzymes in rat-liver tissue. Biochem.J. **60**:604-617.

25. **Descamps, V., M. T. Duffour, M. C. Mathieu, N. Fernandez, L. Cordier, M. A. Abina, E. Kremer, M. Perricaudet, and H. Haddada**. 1996. Strategies for cancer gene therapy using adenoviral vectors. J.Mol.Med. **74**:183-189.

26. **Diamond, I., T. Owolabi, M. Marco, C. Lam, and A. Glick**. 2000. Conditional gene expression in the epidermis of transgenic mice using the tetracycline-regulated transactivators tTA and rTA linked to the keratin 5 promoter. J.Invest Dermatol. **115**:788-794.

27. **Ding, E., H. Hu, B. L. Hodges, F. Migone, D. Serra, F. Xu, Y. T. Chen, and A. Amalfitano**. 2002. Efficacy of gene therapy for a prototypical lysosomal storage disease (GSD-II) is critically dependent on vector dose, transgene promoter, and the tissues targeted for vector transduction. Mol.Ther. **5**:436-446.

28. **Doe, B., M. Selby, S. Barnett, J. Baenziger, and C. M. Walker**. 1996. Induction of cytotoxic T lymphocytes by intramuscular immunization with plasmid DNA is facilitated by bone marrow-derived cells. Proc.Natl.Acad.Sci.U.S.A **93**:8578-8583.

29. **Engel, A. G. and A. J. Dale**. 1968. Autophagic glycogenosis of late onset with mitochondrial abnormalities: light and electron microscopic observations. Mayo Clin.Proc. **43**:233-279.

30. **Ferrari, F. K., T. Samulski, T. Shenk, and R. J. Samulski**. 1996. Second-strand synthesis is a rate-limiting step for efficient transduction by recombinant adeno-associated virus vectors. J.Virol. **70**:3227-3234.

31. **Field, A. C., M. F. Bloch, and B. Bellon**. 2003. Neonatal tolerance to a Th2-mediated autoimmune disease generates CD8+ Tc1 regulatory cells. J.Autoimmun. **21**:201-212.

32. **Field, A. C., L. Caccavelli, M. F. Bloch, and B. Bellon**. 2003. Regulatory CD8+ T cells control neonatal tolerance to a Th2-mediated autoimmunity. J.Immunol. **170**:2508-2515.

33. **Fields, P. A., V. R. Arruda, E. Armstrong, K. Chu, F. Mingozzi, J. N. Hagstrom, R. W. Herzog, and K. A. High**. 2001. Risk and prevention of anti-factor IX formation in AAV-mediated gene transfer in the context of a large deletion of F9. Mol.Ther. **4**:201-210.

34. **Fields, P. A., D. W. Kowalczyk, V. R. Arruda, E. Armstrong, M. L. McCleland, J. N. Hagstrom, K. J. Pasi, H. C. Ertl, R. W. Herzog, and K. A. High**. 2000. Role of vector in activation of T cell subsets in immune responses against the secreted transgene product factor IX. Mol.Ther. **1**:225-235.

35. **Fisher, K. J., G. P. Gao, M. D. Weitzman, R. DeMatteo, J. F. Burda, and J. M. Wilson**. 1996. Transduction with recombinant adeno-associated virus for gene therapy is limited by leading-strand synthesis. J Virol **70**:520-532.

36. **Flotte, T. R. and T. W. Ferkol**. 1997. Genetic therapy. Past, present, and future. Pediatr.Clin.North Am. **44**:153-178.

37. **Forsthuber, T., H. C. Yip, and P. V. Lehmann**. 1996. Induction of TH1 and TH2 immunity in neonatal mice. Science **271**:1728-1730.

38. **Fraites, T.** Muscle-directed Gene and Enzyme Replacement Therapies for Glycogen Storage Disease Type II, Pompe Disease 2003. Ph.D. thesis. University of Florida, Gainesville, Florida.

39. **Fraites, T. J., Jr., M. R. Schleissing, R. A. Shanely, G. A. Walter, D. A. Cloutier, I. Zolotukhin, D. F. Pauly, N. Raben, P. H. Plotz, S. K. Powers, P. D. Kessler, and B. J. Byrne**. 2002. Correction of the enzymatic and functional deficits in a model of Pompe disease using adeno-associated virus vectors. Mol.Ther. **5**:571-578.

40. **Gao, G. P., M. R. Alvira, L. Wang, R. Calcedo, J. Johnston, and J. M. Wilson**. 2002. Novel adeno-associated viruses from rhesus monkeys as vectors for human gene therapy. Proc.Natl.Acad.Sci.U.S.A **99**:11854-11859.

41. **Gao, G. P., Y. Yang, and J. M. Wilson**. 1996. Biology of adenovirus vectors with E1 and E4 deletions for liver-directed gene therapy. J.Virol. **70**:8934-8943.

42. **Ge, Y., S. Powell, M. Van Roey, and J. G. McArthur**. 2001. Factors influencing the development of an anti-factor IX (FIX) immune response following administration of adeno-associated virus-FIX. Blood **97**:3733-3737.

43. **Geddes, R. and G. C. Stratton**. 1977. The influence of lysosomes on glycogen metabolism. Biochem.J. **163**:193-200.

44. **Haines, J. L., L. J. Ozelius, H. McFarlane, A. Menon, S. Tzall, F. Martiniuk, R. Hirschhorn, and J. F. Gusella**. 1990. A genetic linkage map of chromosome 17. Genomics **8**:1-6.

45. **Hermans, M. M., M. A. Kroos, J. A. Smeitink, A. T. Van der Ploeg, W. J. Kleijer, and A. J. Reuser**. 1998. Glycogen Storage Disease type II: genetic and biochemical analysis of novel mutations in infantile patients from Turkish ancestry. Hum.Mutat. **11**:209-215.

46. **Hermans, M. M., M. A. Kroos, J. van Beeumen, B. A. Oostra, and A. J. Reuser**. 1991. Human lysosomal alpha-glucosidase. Characterization of the catalytic site. J.Biol.Chem. **266**:13507-13512.

47. **Hers, H. G.** 1963. Alpha-glucosidase deficiency in generalized glycogen storage disease (Pompe's disease). Biochem.J. **86**:11.

48. **Herzog, R. W., P. A. Fields, V. R. Arruda, J. O. Brubaker, E. Armstrong, D. McClintock, D. A. Bellinger, L. B. Couto, T. C. Nichols, and K. A. High**. 2002. Influence of vector dose on factor IX-specific T and B cell responses in muscle-directed gene therapy. Hum.Gene Ther. **13**:1281-1291.

49. **High K.A.** 2003. AAV-mediated gene transfer for hemophilia. Trans AM Clin Climatol Assoc **114**:337-351.

50. **High, K. A.** 2002. Adeno-associated virus-mediated gene transfer for hemophilia B. Int.J.Hematol. **76**:310-318.

51. **Hildinger, M. and A. Auricchio**. 2004. Advances in AAV-mediated gene transfer for the treatment of inherited disorders. Eur.J.Hum.Genet.

52. **Hirschhorn, R. and A. J. J. Reuser**. 2000. Glycogen storage disease II: acid-alpha glucosidase (acid maltase) deficiency, p. 3389-3420. *In* C. R. Scriver, A. L. Beaudet, W. S. Sly, and D. Valle (ed.), Metabolic Basis of Inherited Disease. McGraw Hill, New York.

53. **Hoefsloot, L. H., M. Hoogeveen-Westerveld, M. A. Kroos, J. van Beeumen, A. J. Reuser, and B. A. Oostra**. 1988. Primary structure and processing of lysosomal alpha-glucosidase; homology with the intestinal sucrase-isomaltase complex. EMBO J. **7**:1697-1704.

54. **Huie, M. L., A. S. Chen, S. Tsujino, S. Shanske, S. DiMauro, A. G. Engel, and R. Hirschhorn**. 1994. Aberrant splicing in adult onset glycogen storage disease type II (GSDII): molecular identification of an IVS1 (-13T-->G) mutation in a majority of patients and a novel IVS10 (+1GT-->CT) mutation. Hum.Mol.Genet. **3**:2231-2236.

55. **Janeway, C., P. Travers, M. Walport, and M. Shlomchik**. 2001. Immunobiology. Garland Publishing, New York, NY.

56. **Jarriault, S., C. Brou, F. Logeat, E. H. Schroeter, R. Kopan, and A. Israel**. 1995. Signalling downstream of activated mammalian Notch. Nature **377**:355-358.

57. **Jooss, K. and N. Chirmule**. 2003. Immunity to adenovirus and adeno-associated viral vectors: implications for gene therapy. Gene Ther. **10**:955-963.

58. **Jooss, K., Y. Yang, K. J. Fisher, and J. M. Wilson**. 1998. Transduction of dendritic cells by DNA viral vectors directs the immune response to transgene products in muscle fibers. J.Virol. **72**:4212-4223.

59. **Jung, S. C., I. P. Han, A. Limaye, R. Xu, M. P. Gelderman, P. Zerfas, K. Tirumalai, G. J. Murray, M. J. During, R. O. Brady, and P. Qasba**. 2001. Adeno-associated viral vector-mediated gene transfer results in long-term enzymatic and functional correction in multiple organs of Fabry mice. Proc.Natl.Acad.Sci.U.S.A **98**:2676-2681.

60. **Kay, M. A., C. S. Manno, M. V. Ragni, P. J. Larson, L. B. Couto, A. McClelland, B. Glader, A. J. Chew, S. J. Tai, R. W. Herzog, V. Arruda, F. Johnson, C. Scallan, E. Skarsgard, A. W. Flake, and K. A. High**. 2000. Evidence for gene transfer and expression of factor IX in haemophilia B patients treated with an AAV vector. Nat.Genet. **24**:257-261.

61. **Kessler, P. D., G. M. Podsakoff, X. Chen, S. A. McQuiston, P. C. Colosi, L. A. Matelis, G. J. Kurtzman, and B. J. Byrne**. 1996. Gene delivery to skeletal muscle results in sustained expression and systemic delivery of a therapeutic protein. Proc.Natl.Acad.Sci.U.S.A **93**:14082-14087.

62. **Kikuchi, T., H. W. Yang, M. Pennybacker, N. Ichihara, M. Mizutani, J. L. Van Hove, and Y. T. Chen**. 1998. Clinical and metabolic correction of pompe disease by enzyme therapy in acid maltase-deficient quail. J.Clin.Invest **101**:827-833.

63. **Kotin, R. M., M. Siniscalco, R. J. Samulski, X. D. Zhu, L. Hunter, C. A. Laughlin, S. McLaughlin, N. Muzyczka, M. Rocchi, and K. I. Berns**. 1990. Site-specific integration by adeno-associated virus. Proc Natl Acad Sci U S A **87**:2211-2215.

64. **Kramer, M. G., M. Barajas, N. Razquin, P. Berraondo, M. Rodrigo, C. Wu, C. Qian, P. Fortes, and J. Prieto**. 2003. In vitro and in vivo comparative study of chimeric liver-specific promoters. Mol.Ther. **7**:375-385.

65. **Kunita R, Nakabayashi O, Wu JY, Hagiwara Y, Mizutani M, Pennybacker M, Chen YT, and Kikuchi T**. 1997. Molecular cloning of acid alpha-glucosidase cDNA of Japanese quail (Coturnix coturnix japonica) and the lack of its mRNA in acid maltase deficient quails. Biochim Biophys Acta **1362**:269-278.

66. **Kuo, W. L., R. Hirschhorn, M. L. Huie, and K. Hirschhorn**. 1996. Localization and ordering of acid alpha-glucosidase (GAA) and thymidine kinase (TK1) by fluorescence in situ hybridization. Hum.Genet. **97**:404-406.

67. **Lejeune, N., D. Thines-Sempoux, and H. G. Hers**. 1963. Tissue fractionation studies. 16. Intracellular distribution and properties of alpha-glucosidases in rat liver. Biochem.J. **86**:16-21.

68. **Liu, C., L. D. Condreay, J. B. Burch, and W. Mason**. 1991. Characterization of the core promoter and enhancer of duck hepatitis B virus. Virology **184**:242-252.

69. **Liu, D. W., Y. P. Tsao, C. H. Hsieh, J. T. Hsieh, J. T. Kung, C. L. Chiang, S. J. Huang, and S. L. Chen**. 2000. Induction of CD8 T cells by vaccination with recombinant adenovirus expressing human papillomavirus type 16 E5 gene reduces tumor growth. J.Virol. **74**:9083-9089.

70. **Liu, J. K., C. M. DiPersio, and K. S. Zaret**. 1991. Extracellular signals that regulate liver transcription factors during hepatic differentiation in vitro. Mol.Cell Biol. **11**:773-784.

71. **Lodish, H., D. Baltimore, A. Berk, S. Zipursky, P. Matsudaira, and J. Darnell**. 2004. Molecular Cell Biology. Scientific American Books, New York, NY.

72. **Mah, C., T. J. Fraites, Jr., K. O. Cresawn, I. Zolotukhin, M. A. Lewis, and B. J. Byrne**. 2004. A New Method for Recombinant Adeno-associated Virus Vector Delivery to Murine Diaphragm. Mol.Ther. **9**:458-463.

73. **Mah, C., R. Sarkar, I. Zolotukhin, M. Schleissing, X. Xiao, H. H. Kazazian, and B. J. Byrne**. 2003. Dual vectors expressing murine factor VIII result in sustained correction of hemophilia A mice. Hum.Gene Ther. **14**:143-152.

74. **Manning, W. C., X. Paliard, S. Zhou, B. M. Pat, A. Y. Lee, K. Hong, C. M. Walker, J. A. Escobedo, and V. Dwarki**. 1997. Genetic immunization with adeno-associated virus vectors expressing herpes simplex virus type 2 glycoproteins B and D. J.Virol. **71**:7960-7962.

75. **Manno, C. S., A. J. Chew, S. Hutchison, P. J. Larson, R. W. Herzog, V. R. Arruda, S. J. Tai, M. V. Ragni, A. Thompson, M. Ozelo, L. B. Couto, D. G. Leonard, F. A. Johnson, A. McClelland, C. Scallan, E. Skarsgard, A. W. Flake, M. A. Kay, K. A. High, and B. Glader**. 2003. AAV-mediated factor IX gene transfer to skeletal muscle in patients with severe hemophilia B. Blood **101**:2963-2972.

76. **Manno, C. S., A. J. Chew, S. Hutchison, P. J. Larson, R. W. Herzog, V. R. Arruda, S. J. Tai, M. V. Ragni, A. Thompson, M. Ozelo, L. B. Couto, D. G. Leonard, F. A. Johnson, A. McClelland, C. Scallan, E. Skarsgard, A. W. Flake, M. A. Kay, K. A. High, and B. Glader**. 2003. AAV-mediated factor IX gene transfer to skeletal muscle in patients with severe hemophilia B. Blood **101**:2963-2972.

77. **Martiniuk, F., M. Bodkin, S. Tzall, and R. Hirschhorn**. 1991. Isolation and partial characterization of the structural gene for human acid alpha glucosidase. DNA Cell Biol. **10**:283-292.

78. **Martiniuk, F., A. Chen, A. Mack, V. Donnabella, A. Slonim, L. Bulone, E. Arvanitopoulos, N. Raben, P. Plotz, and W. N. Rom**. 2002. Helios gene gun particle delivery for therapy of acid maltase deficiency. DNA Cell Biol. **21**:717-725.

79. **Martiniuk, F., M. Mehler, A. Pellicer, S. Tzall, G. La Badie, C. Hobart, A. Ellenbogen, and R. Hirschhorn**. 1986. Isolation of a cDNA for human acid alpha-glucosidase and detection of genetic heterogeneity for mRNA in three alpha-glucosidase-deficient patients. Proc.Natl.Acad.Sci.U.S.A **83**:9641-9644.

80. **Miao, C. H., H. Nakai, A. R. Thompson, T. A. Storm, W. Chiu, R. O. Snyder, and M. A. Kay**. 2000. Nonrandom transduction of recombinant adeno-associated virus vectors in mouse hepatocytes in vivo: cell cycling does not influence hepatocyte transduction. J.Virol. **74**:3793-3803.

81. **Mingozzi, F., Y. L. Liu, E. Dobrzynski, A. Kaufhold, J. H. Liu, Y. Wang, V. R. Arruda, K. A. High, and R. W. Herzog**. 2003. Induction of immune tolerance to coagulation factor IX antigen by in vivo hepatic gene transfer. J.Clin.Invest **111**:1347-1356.

82. **Mingozzi, F., J. Schuttrumpf, V. R. Arruda, Y. Liu, Y. L. Liu, K. A. High, W. Xiao, and R. W. Herzog**. 2002. Improved hepatic gene transfer by using an adeno-associated virus serotype 5 vector. J.Virol. **76**:10497-10502.

83. **Nabel, G. J., Z. Y. Yang, E. G. Nabel, K. Bishop, M. Marquet, P. L. Felgner, D. Gordon, and A. E. Chang**. 1995. Direct gene transfer for treatment of human cancer. Ann.N.Y.Acad.Sci. **772**:227-231.

84. **Nakai, H., R. W. Herzog, J. N. Hagstrom, J. Walter, S. H. Kung, E. Y. Yang, S. J. Tai, Y. Iwaki, G. J. Kurtzman, K. J. Fisher, P. Colosi, L. B. Couto, and K. A. High**. 1998. Adeno-associated viral vector-mediated gene transfer of human blood coagulation factor IX into mouse liver. Blood **91**:4600-4607.

85. **Nakai, H., Y. Iwaki, M. A. Kay, and L. B. Couto**. 1999. Isolation of recombinant adeno-associated virus vector-cellular DNA junctions from mouse liver. J.Virol. **73**:5438-5447.

86. **Nakai, H., E. Montini, S. Fuess, T. A. Storm, M. Grompe, and M. A. Kay**. 2003. AAV serotype 2 vectors preferentially integrate into active genes in mice. Nat.Genet. **34**:297-302.

87. **Nakai, H., T. A. Storm, and M. A. Kay**. 2000. Recruitment of single-stranded recombinant adeno-associated virus vector genomes and intermolecular

recombination are responsible for stable transduction of liver in vivo. J.Virol. **74**:9451-9463.

88. **Nakai, H., C. E. Thomas, T. A. Storm, S. Fuess, S. Powell, J. F. Wright, and M. A. Kay**. 2002. A limited number of transducible hepatocytes restricts a wide-range linear vector dose response in recombinant adeno-associated virus-mediated liver transduction. J.Virol. **76**:11343-11349.

89. National Institutes of Health. ClinicalTrials.gov, a service of the National Institutes of Health. National Institutes of Health . 2001. 10-1-2003.

90. **Nelson, W. G. and T. T. Sun**. 1983. The 50- and 58-kdalton keratin classes as molecular markers for stratified squamous epithelia: cell culture studies. J.Cell Biol. **97**:244-251.

91. **Nicolino, M. P., J. P. Puech, E. J. Kremer, A. J. Reuser, C. Mbebi, M. Verdiere-Sahuque, A. Kahn, and L. Poenaru**. 1998. Adenovirus-mediated transfer of the acid alpha-glucosidase gene into fibroblasts, myoblasts and myotubes from patients with glycogen storage disease type II leads to high level expression of enzyme and corrects glycogen accumulation. Hum.Mol.Genet. **7**:1695-1702.

92. **Ohtsuka, T., M. Ishibashi, G. Gradwohl, S. Nakanishi, F. Guillemot, and R. Kageyama**. 1999. Hes1 and Hes5 as notch effectors in mammalian neuronal differentiation. EMBO J. **18**:2196-2207.

93. **Owen, R. D.** 1945. Immunogenetic Consequences of Vascular Anastomoses between Bovine Twins. Science **102**:400-401.

94. **Pauly, D. F., T. J. Fraites, C. Toma, H. S. Bayes, M. L. Huie, R. Hirschhorn, P. H. Plotz, N. Raben, P. D. Kessler, and B. J. Byrne**. 2001. Intercellular transfer of the virally derived precursor form of acid alpha-glucosidase corrects the enzyme deficiency in inherited cardioskeletal myopathy Pompe disease. Hum.Gene Ther. **12**:527-538.

95. **Pauly, D. F., D. C. Johns, L. A. Matelis, J. H. Lawrence, B. J. Byrne, and P. D. Kessler**. 1998. Complete correction of acid alpha-glucosidase deficiency in Pompe disease fibroblasts in vitro, and lysosomally targeted expression in neonatal rat cardiac and skeletal muscle. Gene Ther. **5**:473-480.

96. **Pittman, D. D., E. M. Alderman, K. N. Tomkinson, J. H. Wang, A. R. Giles, and R. J. Kaufman**. 1993. Biochemical, immunological, and in vivo functional characterization of B-domain-deleted factor VIII. Blood **81**:2925-2935.

97. **Pompe, J. C.** 1932. Ned Tijdschr Geneeskd **76**:304-312.

98. **Ponce, E., D. P. Witte, R. Hirschhorn, M. L. Huie, and G. A. Grabowski**. 1999. Murine acid alpha-glucosidase: cell-specific mRNA differential expression during development and maturation. Am.J.Pathol. **154**:1089-1096.

99. **Ponder, K.** Personal communication. 2002.

100. **Qing, K., C. Mah, J. Hansen, S. Zhou, V. Dwarki, and A. Srivastava**. 1999. Human fibroblast growth factor receptor 1 is a co-receptor for infection by adeno-associated virus 2 [see comments]. Nat Med **5**:71-77.

101. **Raben, N., M. Danon, A. L. Gilbert, S. Dwivedi, B. Collins, B. L. Thurberg, R. J. Mattaliano, K. Nagaraju, and P. H. Plotz**. 2003. Enzyme replacement therapy in the mouse model of Pompe disease. Mol.Genet.Metab **80**:159-169.

102. **Raben, N., N. Lu, K. Nagaraju, Y. Rivera, A. Lee, B. Yan, B. Byrne, P. J. Meikle, K. Umapathysivam, J. J. Hopwood, and P. H. Plotz**. 2001. Conditional tissue-specific expression of the acid alpha-glucosidase (GAA) gene in the GAA knockout mice: implications for therapy. Hum.Mol.Genet. **10**:2039-2047.

103. **Raben, N., K. Nagaraju, E. Lee, P. Kessler, B. Byrne, L. Lee, M. LaMarca, C. King, J. Ward, B. Sauer, and P. Plotz**. 1998. Targeted disruption of the acid alpha-glucosidase gene in mice causes an illness with critical features of both infantile and adult human glycogen storage disease type II. J.Biol.Chem. **273**:19086-19092.

104. **Raben, N., K. Nagaraju, E. Lee, and P. Plotz**. 2000. Modulation of disease severity in mice with targeted disruption of the acid alpha-glucosidase gene. Neuromuscul.Disord. **10**:283-291.

105. **Raben, N., R. C. Nichols, F. Martiniuk, and P. H. Plotz**. 1996. A model of mRNA splicing in adult lysosomal storage disease (glycogenosis type II). Hum.Mol.Genet. **5**:995-1000.

106. **Raben, N., P. Plotz, and B. J. Byrne**. 2002. Acid alpha-glucosidase deficiency (glycogenosis type II, Pompe disease). Curr.Mol.Med. **2**:145-166.

107. **Raper, S. E., N. Chirmule, F. S. Lee, N. A. Wivel, A. Bagg, G. P. Gao, J. M. Wilson, and M. L. Batshaw**. 2003. Fatal systemic inflammatory response syndrome in a ornithine transcarbamylase deficient patient following adenoviral gene transfer. Mol.Genet.Metab **80**:148-158.

108. **Reitman, M. L. and S. Kornfeld**. 1981. UDP-N-acetylglucosamine:glycoprotein N-acetylglucosamine-1-phosphotransferase. Proposed enzyme for the phosphorylation of the high mannose oligosaccharide units of lysosomal enzymes. J.Biol.Chem. **256**:4275-4281.

109. **Reuser, A. J., M. A. Kroos, M. M. Hermans, A. G. Bijvoet, M. P. Verbeet, O. P. Van Diggelen, W. J. Kleijer, and A. T. Van der Ploeg**. 1995. Glycogenosis type II (acid maltase deficiency). Muscle Nerve **3**:S61-S69.

110. **Reuser, A. J., M. A. Kroos, N. J. Ponne, R. A. Wolterman, M. C. Loonen, H. F. Busch, W. J. Visser, and P. A. Bolhuis**. 1984. Uptake and stability of human and bovine acid alpha-glucosidase in cultured fibroblasts and skeletal muscle cells from glycogenosis type II patients. Exp.Cell Res. **155**:178-189.

111. **Rutledge, E. A., C. L. Halbert, and D. W. Russell**. 1998. Infectious clones and vectors derived from adeno-associated virus (AAV) serotypes other than AAV type 2. J.Virol. **72**:309-319.

112. **Ruttenberg, H. D., R. M. Steidl, L. S. Carey, and J. E. Edwards**. 1964. Glycogen-storage disease of the heart. Hemodynamic and angiocardiographic features in 2 cases. Am.Heart J. **67**:469-480.

113. **Samulski, R. J., A. Srivastava, K. I. Berns, and N. Muzyczka**. 1983. Rescue of adeno-associated virus from recombinant plasmids: gene correction within the terminal repeats of AAV. Cell **33**:135-143.

114. **Samulski, R. J., X. Zhu, X. Xiao, J. D. Brook, D. E. Housman, N. Epstein, and L. A. Hunter**. 1991. Targeted integration of adeno-associated virus (AAV) into human chromosome 19 [published erratum appears in EMBO J 1992 Mar;11(3):1228]. Embo J **10**:3941-3950.

115. **Sarkar, R., W. Xiao, and H. H. Kazazian, Jr.** 2003. A single adeno-associated virus (AAV)-murine factor VIII vector partially corrects the hemophilia A phenotype. J.Thromb.Haemost. **1**:220-226.

116. **Sarukhan, A., S. Camugli, B. Gjata, H. von Boehmer, and K. Jooss**. 2001. Successful interference with cellular immune responses to immunogenic proteins encoded by recombinant viral vectors. J.Virol. **75**:269-277.

117. **Schleissing, M. R.** Biochemical and functional analysis after in utero delivery of recombinant adeno-associated virus to a mouse model of glycogen storage disease type II. University of Florida, Gainesville, Florida . 2002. 11-25-2003.

118. **Seifert, B. L., M. S. Snyder, A. A. Klein, J. E. O'Loughlin, M. S. Magid, and M. A. Engle**. 1992. Development of obstruction to ventricular outflow and impairment of inflow in glycogen storage disease of the heart: serial echocardiographic studies from birth to death at 6 months. Am.Heart J. **123**:239-242.

119. **Slonim, A. E., L. Bulone, S. Ritz, T. Goldberg, A. Chen, and F. Martiniuk**. 2000. Identification of two subtypes of infantile acid maltase deficiency. J.Pediatr. **137**:283-285.

120. **Snyder, R. O., C. Miao, L. Meuse, J. Tubb, B. A. Donahue, H. F. Lin, D. W. Stafford, S. Patel, A. R. Thompson, T. Nichols, M. S. Read, D. A. Bellinger, K. M. Brinkhous, and M. A. Kay**. 1999. Correction of hemophilia B in canine and murine models using recombinant adeno-associated viral vectors. Nat.Med. **5**:64-70.

121. **Snyder, R. O., C. H. Miao, G. A. Patijn, S. K. Spratt, D. Nagy, A. M. Gown, B. Winther, L. Meuse, L. K. Cohen, A. R. Thompson, and M. A. Kay**. 1997. Persistent and therapeutic concentrations of human factor IX in mice after hepatic gene transfer of recombinant AAV vectors. Nat.Genet. **16**:270-276.

122. **Song, S., J. Embury, P. J. Laipis, K. I. Berns, J. M. Crawford, and T. R. Flotte**. 2001. Stable therapeutic serum levels of human alpha-1 antitrypsin (AAT) after portal vein injection of recombinant adeno-associated virus (rAAV) vectors. Gene Ther. **8**:1299-1306.

123. **Sonoda, T., Y. Asada, S. Kurata, and S. Takayasu**. 1999. The mRNA for protease nexin-1 is expressed in human dermal papilla cells and its level is affected by androgen. J.Invest Dermatol. **113**:308-313.

124. **Summerford, C. and R. J. Samulski**. 1998. Membrane-associated heparan sulfate proteoglycan is a receptor for adeno-associated virus type 2 virions. J.Virol. **72**:1438-1445.

125. **Thomas, C. E., T. A. Storm, Z. Huang, and M. A. Kay**. 2004. Rapid uncoating of vector genomes is the key to efficient liver transduction with pseudotyped adeno-associated virus vectors. J.Virol. **78**:3110-3122.

126. **Ulmer, J. B., R. R. Deck, C. M. Dewitt, J. I. Donnhly, and M. A. Liu**. 1996. Generation of MHC class I-restricted cytotoxic T lymphocytes by expression of a viral protein in muscle cells: antigen presentation by non-muscle cells. Immunology **89**:59-67.

127. **Van der Ploeg, A. T., M. A. Kroos, R. Willemsen, N. H. Brons, and A. J. Reuser**. 1991. Intravenous administration of phosphorylated acid alpha-glucosidase leads to uptake of enzyme in heart and skeletal muscle of mice. J.Clin.Invest **87**:513-518.

128. **Van Ginkel, F. W., C. Liu, J. W. Simecka, J. Y. Dong, T. Greenway, R. A. Frizzell, H. Kiyono, J. R. McGhee, and D. W. Pascual**. 1995. Intratracheal gene delivery with adenoviral vector induces elevated systemic IgG and mucosal IgA antibodies to adenovirus and beta-galactosidase. Hum.Gene Ther. **6**:895-903.

129. **Van Hove, J. L., H. W. Yang, J. Y. Wu, R. O. Brady, and Y. T. Chen**. 1996. High-level production of recombinant human lysosomal acid alpha-glucosidase in Chinese hamster ovary cells which targets to heart muscle and corrects glycogen accumulation in fibroblasts from patients with Pompe disease. Proc.Natl.Acad.Sci.U.S.A **93**:65-70.

130. **Vorgerd, M., B. Burwinkel, H. Reichmann, J. P. Malin, and M. W. Kilimann**. 1998. Adult-onset glycogen storage disease type II: phenotypic and allelic heterogeneity in German patients. Neurogenetics. **1**:205-211.

131. **Walvoort, H. C.** 1983. Glycogen storage diseases in animals and their potential value as models of human disease. J.Inherit.Metab Dis. **6**:3-16.

132. **Wisselaar, H. A., M. M. Hermans, W. J. Visser, M. A. Kroos, B. A. Oostra, W. Aspden, B. Harrison, D. J. Hetzel, A. J. Reuser, and R. D. Drinkwater**. 1993. Biochemical genetics of glycogenosis type II in Brahman cattle. Biochem.Biophys.Res.Commun. **190**:941-947.

133. **Xiao, W., S. C. Berta, M. M. Lu, A. D. Moscioni, J. Tazelaar, and J. M. Wilson**. 1998. Adeno-associated virus as a vector for liver-directed gene therapy. J.Virol. **72**:10222-10226.

134. **Xiao, W., N. Chirmule, S. C. Berta, B. McCullough, G. Gao, and J. M. Wilson**. 1999. Gene therapy vectors based on adeno-associated virus type 1. J.Virol. **73**:3994-4003.

135. **Xiao, X., W. deVlaminck, and J. Monahan**. 1993. Adeno-associated virus (AAV) vectors for gene transfer. Advanced Drug Delivery Reviews **12**:201-215.

136. **Xiao, X., J. Li, and R. J. Samulski**. 1998. Production of high-titer recombinant adeno-associated virus vectors in the absence of helper adenovirus. J.Virol. **72**:2224-2232.

137. **Xin, K. Q., M. Urabe, J. Yang, K. Nomiyama, H. Mizukami, K. Hamajima, H. Nomiyama, T. Saito, M. Imai, J. Monahan, K. Okuda, K. Ozawa, and K. Okuda**. 2001. A novel recombinant adeno-associated virus vaccine induces a long-term humoral immune response to human immunodeficiency virus. Hum.Gene Ther. **12**:1047-1061.

138. **Xu, L., T. Daly, C. Gao, T. R. Flotte, S. Song, B. J. Byrne, M. S. Sands, and P. K. Parker**. 2001. CMV-beta-actin promoter directs higher expression from an adeno-associated viral vector in the liver than the cytomegalovirus or elongation factor 1 alpha promoter and results in therapeutic levels of human factor X in mice. Hum.Gene Ther. **12**:563-573.

139. **Yan, B., N. Raben, N. Lu, and P. H. Plotz**. 2001. Identification and characterization of a tissue-specific silencer element in the first intron of the human acid maltase gene. Hum.Genet. **109**:186-190.

140. **Yan, B., N. Raben, and P. Plotz**. 2002. The human acid alpha-glucosidase gene is a novel target of the Notch-1/Hes-1 signaling pathway. J.Biol.Chem. **277**:29760-29764.

141. **Yan, B., N. Raben, and P. H. Plotz**. 2002. Hes-1, a known transcriptional repressor, acts as a transcriptional activator for the human acid alpha-glucosidase gene in human fibroblast cells. Biochem.Biophys.Res.Commun. **291**:582-587.

142. **Yang, Y., H. C. Ertl, and J. M. Wilson**. 1994. MHC class I-restricted cytotoxic T lymphocytes to viral antigens destroy hepatocytes in mice infected with E1-deleted recombinant adenoviruses. Immunity. **1**:433-442.

143. **Yang, Y., S. E. Haecker, Q. Su, and J. M. Wilson**. 1996. Immunology of gene therapy with adenoviral vectors in mouse skeletal muscle. Hum.Mol.Genet. **5**:1703-1712.

144. **Yang, Y., Q. Li, H. C. Ertl, and J. M. Wilson**. 1995. Cellular and humoral immune responses to viral antigens create barriers to lung-directed gene therapy with recombinant adenoviruses. J.Virol. **69**:2004-2015.

145. **Yuan-Tson, C. and A. Burchell**. 2004. Glycogen Storage Diseases, p. 935-956. *In* Scriver.C.R., A. L. Beadet, W. S. Sly, and D. Valle (ed.), Metabolic Basis of Inherited Disease. McGraw Hill, New York.

146. **Zaretsky, J. Z., F. Candotti, C. Boerkoel, E. M. Adams, J. W. Yewdell, R. M. Blaese, and P. H. Plotz**. 1997. Retroviral transfer of acid alpha-glucosidase cDNA to enzyme-deficient myoblasts results in phenotypic spread of the genotypic correction by both secretion and fusion. Hum.Gene Ther. **8**:1555-1563.

147. **Zhang, Y., N. Chirmule, G. Gao, and J. Wilson**. 2000. CD40 ligand-dependent activation of cytotoxic T lymphocytes by adeno-associated virus vectors in vivo: role of immature dendritic cells. J.Virol. **74**:8003-8010.

148. **Ziegler, R. J., S. M. Lonning, D. Armentano, C. Li, D. W. Souza, M. Cherry, C. Ford, C. M. Barbon, R. J. Desnick, G. Gao, J. M. Wilson, R. Peluso, S. Godwin, B. J. Carter, R. J. Gregory, S. C. Wadsworth, and S. H. Cheng**. 2004. AAV2 vector harboring a liver-restricted promoter facilitates sustained expression of therapeutic levels of alpha-galactosidase A and the induction of immune tolerance in Fabry mice. Mol.Ther. **9**:231-240.

149. **Zolotukhin, S., B. J. Byrne, E. Mason, I. Zolotukhin, M. Potter, K. Chesnut, C. Summerford, R. J. Samulski, and N. Muzyczka**. 1999. Recombinant adeno-associated virus purification using novel methods improves infectious titer and yield. Gene Ther. **6**:973-985.

150. **Zolotukhin, S., M. Potter, I. Zolotukhin, Y. Sakai, S. Loiler, T. J. Fraites, Jr., V. A. Chiodo, T. Phillipsberg, N. Muzyczka, W. W. Hauswirth, T. R. Flotte, B. J. Byrne, and R. O. Snyder**. 2002. Production and purification of serotype 1, 2, and 5 recombinant adeno-associated viral vectors. Methods **28**:158-167.

BIOGRAPHICAL SKETCH

Kerry Owens Cresawn was born in Baltimore, Maryland in 1976. She graduated from Hanover High School (Hanover, PA) in 1994 and attended James Madison University in Harrisonburg, VA. In 1998, Kerry graduated *cum laude* with her B.S. in Biology and a minor in Biochemistry. While at James Madison, Kerry trained in the laboratory of Dr. Douglas Dennis where she studied strategies to induce expression of the bacterial polyhydroxyalkanoate (PHA) synthase gene in *Chlamydomanas reinhardtii* as a means to develop an alternative expression system for the plastic-like PHA material.

In August of 1998, Kerry entered the Interdisciplinary Program (IDP) in Biomedical Sciences at the University of Florida where she studied gene therapy approaches for glycogen storage disease type II (GSDII) under the mentorship of Dr. Barry J. Byrne. Kerry's work focused on optimizing liver-directed rAAV-mediated gene delivery in GSDII mice and understanding the consequential immune response. Upon graduation in May of 2004, Kerry plans to pursue her interests in biomedical research as a post-doctoral associate.

I certify that I have read this study and that in my opinion it conforms to acceptable standards of scholarly presentation and is fully adequate, in scope and quality, as a dissertation for the degree of Doctor of Philosophy.

Barry J. Byrne, Chair
Professor of Molecular Genetics and
Microbiology and Pediatrics

I certify that I have read this study and that in my opinion it conforms to acceptable standards of scholarly presentation and is fully adequate, in scope and quality, as a dissertation for the degree of Doctor of Philosophy.

Henry V. Bak

Henry V. Baker, Cochair
Professor of Molecular Genetics and
Microbiology

I certify that I have read this study and that in my opinion it conforms to acceptable standards of scholarly presentation and is fully adequate, in scope and quality, as a dissertation for the degree of Doctor of Philosophy.

William A. Dunn Jr

William A. Dunn, Jr.
Associate Professor of Anatomy and Cell
Biology

I certify that I have read this study and that in my opinion it conforms to acceptable standards of scholarly presentation and is fully adequate, in scope and quality, as a dissertation for the degree of Doctor of Philosophy.

Alfred S. Lewin
Professor of Molecular Genetics and
Microbiology

I certify that I have read this study and that in my opinion it conforms to acceptable standards of scholarly presentation and is fully adequate, in scope and quality, as a dissertation for the degree of Doctor of Philosophy.

Gary A. Visner
Associate Professor of Biochemistry and
Molecular Biology

This dissertation was submitted to the Graduate Faculty of the College of Medicine and to the Graduate School and was accepted as partial fulfillment of the requirements for the degree of Doctor of Philosophy.

May 2004

Wayne J McCormack
Dean, College of Medicine

Winfred M Phillips
Dean, Graduate School

UNIVERSITY OF FLORIDA
3 1262 08554 6033